Stability of Front Solutions of the Bidomain Equation

Yoichiro Mori and Hiroshi Matano

November 17, 2015

Abstract

The bidomain model is the standard model describing electrical activity of the heart. Here we study the stability of planar front solutions of the bidomain equation with a bistable nonlinearity (the bidomain Allen-Cahn equation) in two spatial dimensions. In the bidomain Allen-Cahn equation a Fourier multiplier operator whose symbol is a positive homogeneous rational function of degree two (the bidomain operator) takes the place of the Laplacian in the classical Allen-Cahn equation. Stability of the planar front may depend on the direction of propagation given the anisotropic nature of the bidomain operator. We establish various criteria for stability and instability of the planar front in each direction of propagation. Our analysis reveals that planar fronts can be unstable in the bidomain Allen-Cahn equation in striking contrast to the classical or anisotropic Allen-Cahn equations. We identify two types of instabilities, one with respect to long-wavelength perturbations, the other with respect to medium-wavelength perturbations. Interestingly, whether the front is stable or unstable under long-wavelength perturbations does not depend on the bistable nonlinearity and is fully determined by the convexity properties of a suitably defined Frank diagram. On the other hand, stability under intermediate-wavelength perturbations does depend on the choice of bistable nonlinearity. Intermediate-wavelength instabilities can occur even when the Frank diagram is convex, so long as the bidomain operator does not reduce to the Laplacian. We shall also give a remarkable example in which the planar front is unstable in all directions.

1 Introduction

The bidomain model, introduced in the 1970s [29, 10, 21], is the standard model for cardiac electrophysiology [17, 18, 15, 13]. Cardiac tissue consists of two finely interwoven compartments, the intracellular and extracellular, separated by the cell membrane. In the bidomain model, one takes the homogenized viewpoint so that the intracellular, extracellular and membrane quantities are defined everywhere in space. Let u_{i} and u_{e} be the intracellular and extracellular voltages respectively. These voltages satisfy the bidomain equation, which in

general is given in the following form:

$$C_{\mathrm{m}}\frac{\partial u}{\partial t} - f(u,s) = \nabla\cdot(A_{\mathrm{i}}\nabla u_{\mathrm{i}}) = -\nabla\cdot(A_{\mathrm{e}}\nabla u_{\mathrm{e}}),\ u = u_{\mathrm{i}} - u_{\mathrm{e}}, \tag{1.1}$$

$$\frac{\partial s}{\partial t} = g(u,s). \tag{1.2}$$

The above equations are usually defined on a bounded domain and Neumann boundary conditions are often imposed for u_{i} and u_{e}. The function $u = u_{\mathrm{i}} - u_{\mathrm{e}}$ represents the membrane potential, originally defined on cell membranes but here defined throughout space given our adoption of the homogenized picture. Equation (1.1) expresses current continuity in the intracellular and extracellular spaces. The constant C_{m} is the membrane capacitance, and A_{i} and A_{e} are the conductivity tensors, symmetric positive definite matrices that may be a function of position. The function f expresses the transmembrane current flowing through ion channels and pumps. The quantities s (which take values in $\mathbb{R}^n, n \geq 1$) are known as gating variables and describe the opening and closing of ion channels.

The functions f and g are typically of Hodgkin-Huxley type. State-of-the-art cardiac electrophysiology models incorporate many ion channel types resulting in more than 10 gating variables [25]. It is also common practice to use simplified nonlinearities of FitzHugh-Nagumo type to explore the qualitative behavior of cardiac electrical activity [2, 18].

Suppose A_{i} and A_{e} are related through the relation $A_{\mathrm{e}} = \beta A_{\mathrm{i}}$ where β is a constant. Using the second equality in (1.1), we see that $u_{\mathrm{i}} + \beta u_{\mathrm{e}}$ is equal to a constant (independent of the spatial variable) under suitable conditions on u_{i} and u_{e} on the boundary or at infinity. Equation (1.1) thus reduces to the following simple form:

$$C_{\mathrm{m}}\frac{\partial u}{\partial t} = \nabla\cdot(A_{\mathrm{mono}}\nabla u) + f(u,s),\ A_{\mathrm{mono}} = \frac{\beta}{1+\beta}A_{\mathrm{i}}. \tag{1.3}$$

This is known as the *monodomain reduction*. Equation (1.3) is nothing but a reaction-diffusion equation. It is well-known that the reaction-diffusion equation with the FitzHugh-Nagumo nonlinearity can exhibit propagating fronts, spiral waves and other complicated patterns. Computational investigations show that the bidomain model also produces similar patterns. The monodomain reduction is significantly computationally easier to solve than the bidomain model, and has often been used in place of the bidomain model to study cardiac electrical activity [9, 27, 13]. There are, however, qualitative differences between the two models. An important difference between the bidomain and monodomain models from a physiological standpoint is that the former can explain cardiac defibrillation whereas the latter cannot [18, 15].

Despite its central importance in cardiac electrophysiology, there are few analytical studies of the bidomain model. Among the few such studies are those of [14, 8, 30, 13], in which local-in-time well-posedness on a bounded domain is proved in L^2 based Sobolev spaces. The paper [8] also obtains global

weak solutions for a certain class of nonlinearities. However, well-posedness in L^∞ and global-in-time well-posedness are largely open. In [26], the authors prove that the bidomain model can be derived as a homogenization limit of a microscopic electrophysiology model, providing analytical justification for earlier formal calculations given in [23, 18]. We also mention [4], in which the authors study a variational problem related to the bidomain equation. These results, however, do not reveal the dynamics of solutions of the bidomain equation, and to the best of our knowledge, there are no rigorous results on qualitative properties of the bidomain equation beyond well-posedness such as stability and long-time behavior.

In this paper, we consider the following equation on $\mathbb{R}^2$.

$$\frac{\partial u}{\partial t} - f(u) = \nabla \cdot (A_{\mathrm{i}} \nabla u_{\mathrm{i}}) = -\nabla \cdot (A_{\mathrm{e}} \nabla u_{\mathrm{e}}),\ u = u_{\mathrm{i}} - u_{\mathrm{e}}. \tag{1.4}$$

The nonlinearity $f(u)$ is of bistable type. We suppose that $u = 0$ and $u = 1$ are the two stable zeros of $f(u)$ (i.e., $f'(0) < 0$ and $f'(1) < 0$) and that $u = \alpha_{\mathrm{u}}, 0 < \alpha_{\mathrm{u}} < 1$ is the unique unstable zero of $f(u)$ (i.e., $f'(\alpha_{\mathrm{u}}) > 0$). The conductivities A_{i} and A_{e} are spatially constant 2×2 symmetric positive definite matrices. We shall call equation (1.4) the *bidomain Allen-Cahn equation*.

As we shall see in Section 2, equation (1.4) can be written in the following way.

$$\begin{aligned} &\frac{\partial u}{\partial t} = -\mathcal{L}u + f(u),\ \mathcal{L}u = \mathcal{F}^{-1} Q \mathcal{F} u \\ &Q(\mathbf{k}) = \left(Q_{\mathrm{i}}(\mathbf{k})^{-1} + Q_{\mathrm{e}}(\mathbf{k})^{-1}\right)^{-1},\ Q_{\mathrm{i,e}}(\mathbf{k}) = \mathbf{k}^{\mathrm{T}} A_{\mathrm{i,e}} \mathbf{k}. \end{aligned} \tag{1.5}$$

where $\mathcal{F}$ is the two-dimensional Fourier transform and $\mathbf{k} = (k, l)^{\mathrm{T}}$ is the Fourier coordinate vector. The multiplier symbol Q is a positive homogeneous function of $\mathbf{k}$ of degree 2. If A_{i} is proportional to A_{e}, the symbol Q reduces to a positive definite quadratic polynomial, and the bidomain Allen-Cahn equation above reduces to the classical Allen-Cahn equation.

The bidomain Allen-Cahn equation, similarly to the classical Allen-Cahn equation, possesses planar front solutions in every direction $0 \le \theta < 2\pi$ with velocity given by

$$c = c_* K(\theta),\ K(\theta) = \sqrt{Q(\mathbf{n})},\ \mathbf{n} = (\cos(\theta), \sin(\theta))^{\mathrm{T}}, \tag{1.6}$$

where c_* (the normalized velocity, see (2.11)) is a constant that depends only on the bistable nonlinearity f. The objective of this paper is to study the stability of these planar fronts.

It is of interest to compare the bidomain Allen-Cahn equation with the following *anisotropic Allen-Cahn equation*.

$$\frac{\partial u}{\partial t} = \nabla \cdot (A_{\mathbf{k}}(\nabla u)) + f(u),\ A_{\mathbf{k}} = \left(\frac{\partial A}{\partial k}, \frac{\partial A}{\partial l}\right)^{\mathrm{T}}, \tag{1.7}$$

where A is a convex positive homogeneous function of degree two in $\mathbf{k} = (k, l)^{\mathrm{T}}$. This equation arises in material science and has been studied analytically by a

number of authors [12, 11, 5, 1]. Much like the bidomain Allen-Cahn equation, the anisotropic Allen-Cahn equation reduces to the classical Allen-Cahn equation when A is a positive definite quadratic polynomial. Furthermore, if we set $A = Q/2$ in (1.7), the planar front solutions of the anisotropic and bidomain Allen-Cahn equation will have the same speed and profile in every direction of propagation. These observations lead naturally to the speculation that the behavior of the anisotropic and bidomain Allen-Cahn equation (with $A = Q/2$) should be qualitatively similar. In this connection, we mention the paper [7] which interprets the the operator $-\mathcal{F}^{-1}Q\mathcal{F}$ in (1.5) as the Fourier domain linearization of the anisotropic Laplacian $\nabla \cdot (A_{\mathbf{k}}(\nabla \cdot))$ and uses this to devise a numerical algorithm for anisotropic mean curvature flow.

There are, however, fundamental differences between the bidomain and anisotropic Allen-Cahn equations. First, the anisotropic Allen-Cahn equation is well-posed only if the function $A(\mathbf{k})(= Q(\mathbf{k})/2)$ is convex, while no such restriction is needed for Q in (1.5) in the bidomain Allen-Cahn equation. The symbol Q can indeed be non-convex for a large class of positive symmetric definite matrices A_{i} and A_{e} [5, 6, 3, 13]. Another important difference concerns the maximum principle. More precisely, the maximum principle always holds for the anisotropic Allen-Cahn equation whereas this is not the case for the bidomain Allen-Cahn equation. For the anisotropic Allen-Cahn equation, the maximum principle implies that the planar front solutions are (Lyapunov) stable. The lack of maximum principle in the bidomain Allen-Cahn equation does not allow us to reach this conclusion. As we shall see, planar fronts can be unstable.

In Section 2, we fix notation and establish some elementary facts. We first rewrite the bidomain equation as an equation of u only as in (1.5). We then linearize the bidomain Allen-Cahn model around the planar front solution. Here, we prove a preparatory result which reduces the question of spectral stability to that of determining stability under perturbations of each wavelength. Sections 3, 4 and 5 are devoted to studying the spectral properties of the linearization of the bidomain Allen-Cahn equation around the planar front. In Section 3, we establish a sufficient condition for front stability (Corollary 3.3). So long as A_{i} and A_{e} are close to being proportional (i.e., not too far away from the monodomain model) then the planar fronts are stable. This sufficient condition depends on the nonlinearity f as well as A_{i} and A_{e}. In Section 4, we study stability of the front under long-wavelength perturbations. To state our results, consider the Frank plot [19, 6, 13]:

$$\mathscr{F} = \{(\cos\theta, \sin(\theta))/K(\theta),\ 0 \le 0 < 2\pi\} \tag{1.8}$$

where $K(\theta)$ is as in (1.6) (see also (4.91) and (4.92)). The region enclosed by the Frank plot is the *Frank diagram*. The Frank diagram is a convex set if and only if $Q(\mathbf{k})$ is a convex function. We shall say that the Frank diagram is convex (resp. non-convex) in direction θ if the Frank plot is convex (resp. non-convex) at the point $(\cos\theta, \sin(\theta))/K(\theta)$. We prove that front stability under long-wavelength perturbations is determined by the convexity of Frank diagram (Corollary 4.3 and Proposition 4.4). If the Frank diagram is non-convex in

direction θ, then the planar front propagating in the θ direction is unstable under long-wavelength perturbations. Note here that this stability condition depends only on the properties of the Frank diagram and hence on A_i and A_e and *not* on the nonlinearity f. If the matrices A_i and A_e are sufficiently far from being proportional, the Frank diagram is not convex. There will therefore be a range of θ values for which the planar front is unstable. Recall that, in the anisotropic Allen-Cahn equation, a non-convex Frank diagram (or equivalently a non-convex $A = Q/2$) leads to an ill-posed problem. The bidomain Allen-Cahn equation is well-posed for non-convex Frank diagrams, but this non-convexity leads to planar front instabilities. This result provides a theoretical explanation for numerical simulations shown in [6], in which a curved front of the bidomain Allen-Cahn equation exhibits fine wiggling patterns in directions where the Frank diagram is non-convex. In light of our results, those wiggling patterns may be interpreted as manifestations of such planar front instabilities.

In Section 5, we study front instabilities under perturbations of intermediate wavelength (short-wavelength instabilities are ruled out in Section 2). Intermediate-wavelength instabilities depend on the nonlinearity f. A study of the McKean nonlinearity (5.3) and its regularization (5.2) leads to the following striking result (Corollary 5.8). Suppose that A_i and A_e are not proportional to each other, or equivalently, that the bidomain Allen-Cahn equation does *not* reduce to the classical Allen-Cahn equation. Then there is a smooth bistable nonlinearity f such that a planar front in some direction will be unstable. Planar fronts can thus be unstable even when the Frank diagram (or equivalently the symbol Q) is convex. For certain choices of A_i, A_e and f, it is even possible for fronts propagating in every direction to be unstable (Proposition 5.9). These results are in sharp contrast to the classical or the anisotropic Allen-Cahn case, in which planar fronts in every direction are always stable for any bistable nonlinearity [20].

In Section 6.1, planar front instabilities are observed using numerical simulation. In Section 6.2 we speculate on the asymptotic shape of spreading fronts of the bidomain Allen-Cahn equation in light of our results on stability of planar fronts.

We conclude this introduction with a short discussion on possible physiological implications. A central goal of cardiac electrophysiology is to understand the formation of reentrant cardiac arrhythmias. Such arrhythmias are often initiated by a break-up of propagating planar pulses [18, 32]. Our results suggest that the bidomain operator affords hitherto unrecognized pathways to the destabilization of planar pulses distinct from mechanisms that are present in the monodomain reduction. The intermediate wavelength instability may be of particular interest in this regard. Experimental measurements suggest that the Frank diagram (or the symbol Q) is typically convex with the possible exception of certain pathological situations [4, 13]. Our results show that even when the Frank diagram is convex, planar fronts can become unstable under intermediate-wavelength perturbations. These intermediate-wavelength instabilities result from an interaction between the nonlinearity f and the bidomain operator $\mathcal{L}$. In physiological terms, this means that the composition and current

voltage relationship of ionic channels (reflected in the choice of f) may interact with the bidomain nature of cardiac tissue to destabilize propagating pulses. Finally, we point out that cardiac tissue is not a homogeneous two-dimensional infinite plane. The cardiac wall is a curved three-dimensional slab of tissue in which the fiber direction rotates as one traverses from the epicardial to endocardial surface. Fronts in the presence of three-dimensional anisotropies may exhibit new features. This is beyond the scope of this study and a subject for future investigation.

2 Planar Fronts and Linearization

2.1 Planar Fronts

We begin by rewriting the bidomain Allen-Cahn equation (1.4) as in (1.5). For a function $v(\mathbf{x})$, $\mathbf{x} = (x, y)^{\mathrm{T}} \in \mathbb{R}^2$, consider the Fourier transform:

$$(\mathcal{F}v)(\mathbf{k}) = \widehat{v}(\mathbf{k}) = \int_{\mathbb{R}^2} v(\mathbf{x}) \exp(-i\mathbf{k}\cdot\mathbf{x}) d\mathbf{x},\ \mathbf{k} = (k, l)^{\mathrm{T}} \in \mathbb{R}^2. \tag{2.1}$$

From (1.4), we see that

$$\nabla \cdot (A_{\mathrm{i}} \nabla u_{\mathrm{i}} + A_{\mathrm{e}} \nabla u_{\mathrm{e}}) = 0. \tag{2.2}$$

Take the Fourier transform of the above relation.

$$\begin{aligned} &Q_{\mathrm{i}}(\mathbf{k})\widehat{u}_{\mathrm{i}}(\mathbf{k}) + Q_{\mathrm{e}}(\mathbf{k})\widehat{u}_{\mathrm{e}}(\mathbf{k}) = 0, \\ &Q_{\mathrm{i}}(\mathbf{k}) = \mathbf{k}^{\mathrm{T}} A_{\mathrm{i}} \mathbf{k},\ Q_{\mathrm{e}}(\mathbf{k}) = \mathbf{k}^{\mathrm{T}} A_{\mathrm{e}} \mathbf{k}. \end{aligned} \tag{2.3}$$

Noting that $\widehat{u} = \widehat{u}_{\mathrm{i}} - \widehat{u}_{\mathrm{e}}$, we see that

$$\begin{aligned} &Q_{\mathrm{i}}(\mathbf{k})\widehat{u}_{\mathrm{i}}(\mathbf{k}) = Q(\mathbf{k})\widehat{u}(\mathbf{k}), \\ &Q(\mathbf{k}) = \frac{Q_{\mathrm{i}}(\mathbf{k}) Q_{\mathrm{e}}(\mathbf{k})}{Q_{\mathrm{i}}(\mathbf{k}) + Q_{\mathrm{e}}(\mathbf{k})} = \left(Q_{\mathrm{i}}(\mathbf{k})^{-1} + Q_{\mathrm{e}}(\mathbf{k})^{-1}\right)^{-1}. \end{aligned} \tag{2.4}$$

Hence,

$$\nabla \cdot (A_{\mathrm{i}} \nabla u_{\mathrm{i}}) = -\mathcal{F}^{-1} Q \mathcal{F} u \equiv -\mathcal{L} u, \tag{2.5}$$

where $\mathcal{F}^{-1}$ is the inverse Fourier transform. We shall call $\mathcal{L}$ the *bidomain operator*. The bidomain operator is analogous to the Laplacian in the sense that it is a Fourier multiplier operator whose symbol is a positive homogeneous function of degree two. We may thus rewrite (1.4) as

$$\frac{\partial u}{\partial t} = -\mathcal{L} u + f(u). \tag{2.6}$$

As we remarked earlier, if A_{i} is proportional to A_{e}, the bidomain operator $\mathcal{L}$ reduces to a constant multiple of the Laplacian, and the bidomain Allen-Cahn equation reduces to the classical Allen-Cahn equation.

By performing a suitable linear transformation on the coordinate system, it is possible to transform the conductivity matrices A_i and A_e into the following standard forms

$$A_\mathrm{i} = \begin{pmatrix} 1+b+a & 0 \\ 0 & 1+b-a \end{pmatrix},\ A_\mathrm{e} = \begin{pmatrix} 1-b-a & 0 \\ 0 & 1-b+a \end{pmatrix},\ |a \pm b| < 1. \tag{2.7}$$

When convenient, we may thus assume without loss of generality that A_i and A_e have the above form. The magnitude of a measures the degree of anisotropy in the conductivities. The coefficient b measures the relative size of the conductivities in the intracellular and extracellular spaces. When $a = 0$, A_i and A_e are proportional to each other, and the bidomain operator $\mathcal{L}$ reduces to a multiple of of the Laplacian, or the monodomain operator. The magnitude of a thus measures the deviation of the bidomain operator from the Laplacian.

Consider a planar front $u_\mathrm{f}(\xi) = u_\mathrm{f}(\mathbf{n}\cdot\mathbf{x} - ct)$ propagating in the direction of the unit vector

$$\mathbf{n} = (\cos(\theta), \sin(\theta))^\mathrm{T}. \tag{2.8}$$

We assume that:

$$\lim_{\xi\to-\infty} u_\mathrm{f}(\xi) = 1,\ \lim_{\xi\to\infty} u_\mathrm{f}(\xi) = 0. \tag{2.9}$$

It is easily seen that u_f satisfies the following equation.

$$c\frac{\partial u_\mathrm{f}}{\partial \xi} + Q(\mathbf{n})\frac{\partial^2 u_\mathrm{f}}{\partial \xi^2} + f(u_\mathrm{f}) = 0, \tag{2.10}$$

Let $u_{\mathrm{f}*}$ be the normalized traveling front solution and c_* be the corresponding speed, satisfying the following equation.

$$c_*\frac{\partial u_{\mathrm{f}*}}{\partial \xi} + \frac{\partial^2 u_{\mathrm{f}*}}{\partial \xi^2} + f(u_{\mathrm{f}*}) = 0. \tag{2.11}$$

It is well known that the speed c_* is unique and that $u_{\mathrm{f}*}$ is uniquely determined up to translation. Let us fix one such u_{f^*} Using c_* and $u_{\mathrm{f}*}$, we may express c and u_f as:

$$c = Kc_*,\ u_\mathrm{f}(\xi) = u_{\mathrm{f}*}\left(\xi/K\right),\ K = \sqrt{Q(\mathbf{n})} \tag{2.12}$$

The speed c is expressed as a product of K and c_*. The constant K depends only on the conductivity tensors $A_\mathrm{i}, A_\mathrm{e}$ and the propagation direction $\mathbf{n}$ (and hence on θ). The standard wave speed c_* depends only on the nonlinearity. We note two well-known properties of the front solution $u_\mathrm{f}(\xi)$. First:

$$u_\mathrm{f}(\xi) \text{ is a monotone decreasing function.} \tag{2.13}$$

Second:

$$u_\mathrm{f}(\xi) \text{ decays exponentially as } |\xi| \to \infty. \tag{2.14}$$

We would like to study the stability of these planar front solutions. To do so, we introduce a moving coordinate system $\boldsymbol{\xi} = (\xi, \eta)$ that travels with the front

so that the ξ-axis aligns with the direction of propagation $\mathbf{n} = (\cos(\theta), \sin(\theta))^{\mathrm{T}}$ and the η-axis is parallel to the wave front. The bidomain equation (2.6) in this new coordinate system is

$$\frac{\partial u}{\partial t} = c\frac{\partial u}{\partial \xi} - \mathcal{L}u + f(u), \tag{2.15}$$

where we continue to use $\mathcal{L}$ to denote the transformed operator. The transformed operator $\mathcal{L}$ is given by:

$$\begin{aligned} \mathcal{L}u(\boldsymbol{\xi}) = \mathcal{F}^{-1}Q_\theta \mathcal{F}u(\boldsymbol{\xi}),\ Q_\theta(\mathbf{k}) = \frac{Q^\theta_{\mathrm{i}}(\mathbf{k})Q^\theta_{\mathrm{e}}(\mathbf{k})}{Q^\theta_{\mathrm{i}}(\mathbf{k}) + Q^\theta_{\mathrm{e}}(\mathbf{k})},\ Q^\theta_{\mathrm{i,e}}(\mathbf{k}) = \mathbf{k}^{\mathrm{T}} A^\theta_{\mathrm{i,e}}\mathbf{k}, \\ A^\theta_{\mathrm{i,e}} = R_\theta A_{\mathrm{i,e}} R_{-\theta},\ R_\theta = \begin{pmatrix} \cos(\theta) & -\sin(\theta) \\ \sin(\theta) & \cos(\theta) \end{pmatrix} \end{aligned} \tag{2.16}$$

where $\mathcal{F}$ is the two-dimensional Fourier transform in $\boldsymbol{\xi}$. We continue to use $\mathbf{k} = (k, l)^{\mathrm{T}}$ as the wave vector in the Fourier domain. We shall find it useful to write $Q_\theta(k, l)$ as follows. Note that the multiplier Q_θ is a quotient of a fourth degree and a second degree homogeneous polynomial in (k, l). Setting $l = 1$, and performing polynomial division with remainder, we have

$$\begin{aligned} Q_\theta(k, 1) = p(k) + q(k), \\ p(k) = K^2(k - \alpha_1)^2 + \alpha_0,\ q(k) = \frac{\beta_1(k - \gamma_1) + \beta_0}{(k - \gamma_1)^2 + \gamma_0^2}. \end{aligned} \tag{2.17}$$

We have completed the square in the quadratic polynomials above for future convenience. The denominator of $q(k)$ is a positive quadratic polynomial given that A_{i} and A_{e} are positive definite matrices. We take $\gamma_0 > 0$. The use of K above is consistent with (2.12). It is sometimes useful to view the above coefficients $K, \alpha_i, \beta_i, \gamma_i, i = 0, 1$ as (smooth) functions of θ for fixed A_{i} and A_{e}. Using (2.17), we may write Q_θ as

$$Q_\theta(k, l) = l^2(p(k/l) + q(k/l)). \tag{2.18}$$

With A_{i} and A_{e} in (2.7), Q_θ defined in (2.16) is given by:

$$\begin{aligned} Q(\mathbf{k}) = \frac{Q_{\mathrm{i}}(\mathbf{k})Q_{\mathrm{e}}(\mathbf{k})}{Q_{\mathrm{i}}(\mathbf{k}) + Q_{\mathrm{e}}(\mathbf{k})},\ Q_{\mathrm{i,e}}(\mathbf{k}) = \mathbf{k}^{\mathrm{T}} A^\theta_{\mathrm{i,e}}\mathbf{k}, \\ A^\theta_{\mathrm{i}} = \begin{pmatrix} 1 + b + a\cos(2\theta) & a\sin(2\theta) \\ a\sin(2\theta) & 1 + b - a\cos(2\theta) \end{pmatrix}, \\ A^\theta_{\mathrm{e}} = \begin{pmatrix} 1 - b - a\cos(2\theta) & -a\sin(2\theta) \\ -a\sin(2\theta) & 1 - b + a\cos(2\theta) \end{pmatrix}. \end{aligned} \tag{2.19}$$

We may compute the coefficients in (2.17) as follows.

$$\begin{aligned} K =& \frac{1}{\sqrt{2}}\sqrt{1-(b+a\cos(2\theta))^2},\ \alpha_1 = \frac{2a\sin(2\theta)(b+a\cos(2\theta))}{1-(b+a\cos(2\theta))^2}, \\ \alpha_0 =& \frac{1}{2}+\frac{1}{2}(3a^2\cos^2(2\theta)+2ab\cos(2\theta)-4a^2\sin^2(2\theta)-b^2) \\ & -\frac{2a^2\sin^2(2\theta)(b+a\cos(2\theta))^2}{1-(b+a\cos(2\theta))^2}, \\ \beta_1 =& 2a^2\sin(4\theta),\ \beta_0 = -2a^2\cos(4\theta),\ \gamma_1 = 0,\ \gamma_0 = 1. \end{aligned} \tag{2.20}$$

These expressions will be used later to demonstrate some of our results.

2.2 Linearization at the Front Solution

To study the stability of the planar fronts, we linearize (2.15).

$$\frac{\partial v}{\partial t} = c\frac{\partial v}{\partial \xi} - \mathcal{L}v + f'(u_{\mathrm{f}})v, \tag{2.21}$$

where f' is the derivative of f. Define the operator:

$$\mathcal{P}v = c\frac{\partial v}{\partial \xi} - \mathcal{L}v + f'(u_{\mathrm{f}})v. \tag{2.22}$$

We study the spectrum of the operator $\mathcal{P}$ as an operator on $L^2(\mathbb{R}^2)$. Assuming f is sufficiently smooth, $\mathcal{P}$ is a closed operator with domain $H^2(\mathbb{R}^2) \subset L^2(\mathbb{R}^2)$.

To study the spectrum of $\mathcal{P}$, take the Fourier transform of (2.22) in η.

$$\begin{aligned} \widetilde{\mathcal{P}}\widetilde{v} = \mathcal{P}_l v_l = c\frac{\partial v_l}{\partial \xi} - \mathcal{L}_l v_l + f'(u_{\mathrm{f}})v_l,\ \mathcal{L}_l = \mathcal{F}_\xi^{-1}Q_\theta(k,l)\mathcal{F}_\xi, \\ \widetilde{v}(\xi,l) = v_l(\xi) = \mathcal{F}_\eta v(\xi,\eta) = \int_{-\infty}^{\infty} v(\xi,\eta)\exp(-il\eta)d\eta. \end{aligned} \tag{2.23}$$

where $\mathcal{F}_\eta$ is the Fourier transform in the η variable. The operator $\widetilde{\mathcal{P}}$ is a closed operator on $L^2(\mathbb{R}^2)$ with domain $\mathcal{D}(\widetilde{\mathcal{P}})$ given by:

$$\mathcal{D}(\widetilde{\mathcal{P}}) = \{f(\xi,l) \in L^2(\mathbb{R}^2) | \int_{l\in\mathbb{R}} \|f\|^2_{H^2_\xi(\mathbb{R})}\,(1+l^2)^2 dl < \infty\}. \tag{2.24}$$

where $\|\cdot\|_{H^2_\xi(\mathbb{R})}$ denotes the H^2 norm of the function f in the ξ variable while taking l fixed. Since the Fourier transform is an L^2 isometry, the spectrum of $\mathcal{P}$ and $\widetilde{\mathcal{P}}$ are identical:

$$\Sigma(\widetilde{\mathcal{P}}) = \Sigma(\mathcal{P}), \tag{2.25}$$

where here and henceforth $\Sigma(\cdot)$ refers to the spectrum of an operator. For each $l \in \mathbb{R}$, we view $\mathcal{P}_l$ in (2.23) as a closed oeprator on $L^2(\mathbb{R})$ with domain $H^2(\mathbb{R}) \subset L^2(\mathbb{R})$, and thus consider the spectrum $\Sigma(\mathcal{P}_l)$ for each l. We may view $\mathcal{P}_l$ as the operator governing the growth of perturbations with wavelength $2\pi/l$. This leads us to the following definition of spectral stability.

Definition 2.1 (Spectral Stability of Planar Fronts)**.** *Let $u_{\rm f}(\mathbf{n}\cdot\mathbf{x}-ct)$ be a planar traveling front solution of the bidomain model* (2.6) *where $u_{\rm f}(\xi)$ satisfies* (2.10) *and* (2.9)*. Consider the operator $\mathcal{P}_l$ of* (2.23)*, defined as a closed operator on $L^2(\mathbb{R})$ with domain $H^2(\mathbb{R})\subset L^2(\mathbb{R})$. The planar front is spectrally stable if*

$$\Sigma(\mathcal{P}_l)\subset\{z\in\mathbb{C}|\mathrm{Re}z<0\} \text{ for all } l\neq 0. \tag{2.26}$$

The planar front is spectrally unstable if there exists a value of l such that

$$\Sigma(\mathcal{P}_l)\cap\{z\in\mathbb{C}|\mathrm{Re}z>0\}\neq\emptyset. \tag{2.27}$$

We exclude the case $l=0$ in the above definition since 0 is always in the spectrum of $\mathcal{P}_0$ given the translation invariance of the planar front (see also item 1 of Proposition 3.1). The above definition is justified by the following result.

Proposition 2.2. *Let $\mathcal{P}$ and $\mathcal{P}_l$ be as in* (2.22) *and* (2.23) *respectively. We have*

$$\Sigma(\mathcal{P})=\bigcup_{l\in\mathbb{R}}\Sigma(\mathcal{P}_l). \tag{2.28}$$

When c is equal to 0, $\mathcal{P}$ and $\mathcal{P}_l$ are all self-adjoint and the above assertion is a straightforward consequence of well-known facts about self-adjoint operators. When $c\neq 0$, the authors could not find a general result in the literature that would allow for an immediate proof of the above result. The proof to follow relies on the specific properties of $\mathcal{P}$ and $\mathcal{P}_l$. We note that an interesting detail in (2.28) is that we do not need to take the closure of the set on the right hand side.

We first prove a proposition of independent interest. Define the constants

$$\begin{aligned} f_{\min}=\min_{0\le s\le 1} f'(s),\ f_{\max}=\max_{0\le s\le 1} f'(s),\\ \overline{f}=\frac{f_{\min}+f_{\max}}{2},\ f_\Delta=\frac{f_{\max}-f_{\min}}{2}. \end{aligned} \tag{2.29}$$

Proposition 2.3. *Define the set*

$$\widehat{S}_l=\{z\in\mathbb{C}|ics-Q(s,l)+\overline{f},s\in\mathbb{R}\} \tag{2.30}$$

Then, the spectrum $\Sigma(\mathcal{P}_l)$ satisfies:

$$\Sigma(\mathcal{P}_l)\subset S_l=\{z\in\mathbb{C}|\mathrm{dist}(z,\widehat{S}_l)\le f_\Delta\}, \tag{2.31}$$

where $\mathrm{dist}(z,\widehat{S}_l)$ *is the distance between the point $z\in\mathbb{C}$ and the set $\widehat{S}_l$. If $z\notin S_l$, the resolvent satisfies the estimate*

$$\left\|(z-\mathcal{P}_l)^{-1}\right\|_{\mathcal{L}(L^2(\mathbb{R}))}\le(\mathrm{dist}(z,\widehat{S}_l)-f_\Delta)^{-1} \tag{2.32}$$

where $\|\cdot\|_{\mathcal{L}(L^2(\mathbb{R}))}$ is the operator norm of bounded operators on $L^2(\mathbb{R})$.

Proof. Decompose the operator $\mathcal{P}_l$ as follows:

$$\mathcal{P}_l w = \mathcal{Q}_0 w + \mathcal{Q}_1 w,\ \mathcal{Q}_0 w = c\frac{\partial w}{\partial \xi} - \mathcal{L}_l w + \overline{f} w,\ \mathcal{Q}_1 w = (f'(u_{\rm f}(\xi)) - \overline{f})w. \quad (2.33)$$

Note that

$$\|\mathcal{Q}_1 w\|_{L^2(\mathbb{R})} \le \left\|f'(u_{\rm f}(\xi)) - \overline{f}\right\|_{L^\infty(\mathbb{R})} \|w\|_{L^2(\mathbb{R})} = f_\Delta \|w\|_{L^2(\mathbb{R})} \quad (2.34)$$

where $\|\cdot\|_{L^p(\mathbb{R})}$ for $1 \le p \le \infty$ denotes the L^p norm on the real line. That the above L^∞ norm equals to f_Δ follows from the (2.9) and the monotonicity of $u(\xi)$ (see (2.13)). The spectrum of $\mathcal{Q}_0$ is easily determined by the Fourier transform:

$$\Sigma(\mathcal{Q}_0) = \widehat{S}_l \quad (2.35)$$

where the set $\widehat{S}_l$ was given in (2.30). Since $\mathcal{Q}_0$ is a Fourier multiplier operator, we have the following simple resolvent estimate:

$$\left\|(z - \mathcal{Q}_0)^{-1}\right\|_{\mathcal{L}(L^2(\mathbb{R}))} = (\mathrm{dist}(z, \widehat{S}_l))^{-1},\ z \in \mathbb{C}\backslash\Sigma(\mathcal{Q}_0), \quad (2.36)$$

Take any point $z \in \mathbb{C}$ such that

$$\mathrm{dist}(z, \widehat{S}_l)) > f_\Delta. \quad (2.37)$$

We then have:

$$(z - \mathcal{P}_l)^{-1} = (z - \mathcal{Q}_0 - \mathcal{Q}_1)^{-1} = \left(I + \sum_{k=1}^{\infty}((z - \mathcal{Q}_0)^{-1}\mathcal{Q}_1)^k\right)(z - \mathcal{Q}_0)^{-1}. \quad (2.38)$$

where I is the identity operator. By (2.34), (2.36) and (2.37), we have fu

$$\begin{aligned}\left\|(z - \mathcal{Q}_0)^{-1}\mathcal{Q}_1\right\|_{\mathcal{L}(L^2(\mathbb{R}))} &\le \left\|(z - \mathcal{Q}_0)^{-1}\right\|_{\mathcal{L}(L^2(\mathbb{R}))} \|\mathcal{Q}_1\|_{\mathcal{L}(L^2(\mathbb{R}))} \\ &\le \mathrm{dist}(z, \widehat{S}_l)^{-1} f_\Delta < 1.\end{aligned} \quad (2.39)$$

Therefore, the Neumann series (2.38) converges so long as (2.36) is satisfied. A complex value z satisfying (2.37) is thus in the resolvent set of $\mathcal{P}_l$, and satisfies the resolvent estimate (2.32). □

From the expression for Q_θ in (2.16) and from the fact that $A^\theta_{\rm i,e}$ are symmetric positive definite, we see that $Q_\theta(s, l) \ge 0$ for all $s \in \mathbb{R}$. In fact, it follows from (2.17) that we have the following estimate.

$$Q_\theta(s, l) \ge m_Q l^2,\ m_Q = \min_{s\in\mathbb{R}} Q_\theta(s, 1) = \min_{s\in\mathbb{R}}(p(s) + q(s)). \quad (2.40)$$

Note here that $m_Q > 0$. We see from (2.30) that

$$\widehat{S}_l \subset \{z \in \mathbb{C} | \mathrm{Re} z \le \overline{f} - m_Q l^2\}. \quad (2.41)$$

From this and (2.31), we have

$$\Sigma(\mathcal{P}_l) \subset \{z \in \mathbb{C} | \mathrm{Re} z \leq f_{\max} - m_Q l^2\}. \tag{2.42}$$

This shows that for sufficiently large l, the spectrum of $\mathcal{P}_l$ lies in the left half of the complex plane. In other words, the planar front will always be stable under short wavelength perturbations. We also have the following corollary.

Corollary 2.4. *For any $z \in \mathbb{C}$, there is a $L > 0$ depending on z such that z is in the resolvent set of $\mathcal{P}_l$ for all $|l| > L$ and*

$$\left\|(z - \mathcal{P}_l)^{-1}\right\|_{\mathcal{L}(L^2(\mathbb{R}))} \leq (\mathrm{Re} z - f_{\max} + m_Q l^2)^{-1}. \tag{2.43}$$

Proof. This is an immediate consequence of (2.42) and (2.32). □

We are now ready to prove Proposition 2.2. In the proof to follow, we will make use of the adjoint operators $\mathcal{P}_l^*$ and $\widetilde{\mathcal{P}}^*$, given by

$$\widetilde{\mathcal{P}}^* \widetilde{w} = \mathcal{P}_l^* w_l = c\frac{\partial w_l}{\partial \xi} - \mathcal{L}_l w_l + f'(u_{\mathrm{f}}) w_l,\ \widetilde{w}(\xi, l) = w_l(\xi). \tag{2.44}$$

The domains of these operators are the same as those of $\mathcal{P}_l$ and $\widetilde{\mathcal{P}}$ respectively.

Proof of Proposition 2.2. We prove the forward and reverse implications separately.
Step 1: We prove

$$\Sigma(\widetilde{\mathcal{P}}) \subset \bigcup_{l \in \mathbb{R}} \Sigma(\mathcal{P}_l). \tag{2.45}$$

Suppose

$$z \in \bigcap_{l \in \mathbb{R}} \left(\mathbb{C} \backslash \Sigma(\mathcal{P}_l)\right). \tag{2.46}$$

Given (2.25), we must show that z is in the resolvent set of $\widetilde{\mathcal{P}}$. From (2.23), we immediately see that

$$\left\|(z - \widetilde{\mathcal{P}})^{-1}\right\|_{\mathcal{L}(L^2(\mathbb{R}^2))} \leq \sup_{l \in \mathbb{R}} \left\|(z - \mathcal{P}_l)^{-1}\right\|_{\mathcal{L}(L^2(\mathbb{R}))}. \tag{2.47}$$

It suffices to show that the right hand side is finite. Consider the function

$$g(l) = \left\|(z - \mathcal{P}_l)^{-1}\right\|_{\mathcal{L}(L^2(\mathbb{R}))},\ l \in \mathbb{R}. \tag{2.48}$$

We claim that $g(l)$ is upper semicontinuous. Fix $l = l_0$. For l sufficiently close to l_0, we have

$$(z - \mathcal{P}_l)^{-1} = \left(I + \sum_{k=1}^{\infty} ((z - \mathcal{P}_{l_0})^{-1}(\mathcal{P}_l - \mathcal{P}_{l_0}))^k\right)(z - \mathcal{P}_{l_0})^{-1}. \tag{2.49}$$

Taking the L^2 operator norm on both sides, we have

$$g(l) \le g(l_0)(1 - h(l, l_0))^{-1},\ h(l, l_0) = \left\|(z - \mathcal{P}_{l_0})^{-1}(\mathcal{P}_l - \mathcal{P}_{l_0})\right\|_{\mathcal{L}(L^2(\mathbb{R}))}. \quad (2.50)$$

Let us estimate $h(l, l_0)$.

$$h(l, l_0) \le \left\|(z - \mathcal{P}_{l_0})^{-1}\right\|_{\mathcal{L}(L^2(\mathbb{R});H^1(\mathbb{R}))} \|(\mathcal{P}_l - \mathcal{P}_{l_0})\|_{\mathcal{L}(H^1(\mathbb{R});L^2(\mathbb{R}))} \quad (2.51)$$

where $\|\cdot\|_{\mathcal{L}(X;Y)}$ denotes the operator norm of bounded operators from the function space X to Y. Recall that $(z - \mathcal{P}_{l_0})^{-1}$ is a bounded operator from $L^2(\mathbb{R})$ to $H^2(\mathbb{R})$. The first norm on the right hand side is thus bounded. For the second norm in the above product, we have

$$\mathcal{P}_l - \mathcal{P}_{l_0} = -(\mathcal{L}_l - \mathcal{L}_{l_0}) = \mathcal{F}_\xi^{-1}(Q_\theta(k, l_0) - Q_\theta(k, l))\mathcal{F}_\xi. \quad (2.52)$$

Inspection of the symbol $Q_\theta(k, l)$ shows that

$$\lim_{l \to l_0} \|\mathcal{P}_l - \mathcal{P}_{l_0}\|_{\mathcal{L}(H^1(\mathbb{R});L^2(\mathbb{R}))} = 0. \quad (2.53)$$

Thus,

$$\lim_{l \to l_0} h(l, l_0) = 0. \quad (2.54)$$

This, together with (2.50) shows that the function $g(l)$ is upper semicontinuous.

Take L large enough so that the resolvent estimate of Corollary 2.4 is satisfied for $|l| > L$.

$$g(l) \le K_> = (\mathrm{Re} z - f_{\max} + m_Q L^2)^{-1} \text{ for } |l| > L. \quad (2.55)$$

Since $g(l)$ is upper semicontinuous, it is bounded by some constant $K_<$ on the bounded interval $|l| \le L$. Thus,

$$g(l) \le \max(K_>, K_<),\ l \in \mathbb{R}. \quad (2.56)$$

This shows that the right hand side of (2.47) is finite.

Step 2: We prove

$$\Sigma(\widetilde{\mathcal{P}}) \supset \bigcup_{l \in \mathbb{R}} \Sigma(\mathcal{P}_l). \quad (2.57)$$

Suppose $z \in \Sigma(\mathcal{P}_{l_0})$ for some $l = l_0$. We consider two cases.

Case 1: z is an eigenvalue or the range of $z - \mathcal{P}_{l_0}$ is dense in $L^2(\mathbb{R})$. Then, for each $\epsilon > 0$, there is a function u such that

$$u(\xi) \in H^2(\mathbb{R}),\ \|u\|_{L^2(\mathbb{R})} = 1,\ \|(z - \mathcal{P}_{l_0})u\|_{L^2(\mathbb{R})} \le \epsilon. \quad (2.58)$$

To show that z is in the spectrum of $\widetilde{\mathcal{P}}$, we exhibit a function w such that

$$w(\xi, l) \in \mathcal{D}(\widetilde{\mathcal{P}}),\ \|w\|_{L^2(\mathbb{R}^2)} = 1,\ \left\|(z - \widetilde{\mathcal{P}})w\right\|_{L^2(\mathbb{R})} \le 2\epsilon. \quad (2.59)$$

Note that $\mathcal{D}(\widetilde{\mathcal{P}})$ was given in (2.24). Let $j(x)$ be a positive continuous function compactly supported on the interval $-1 \le x \le 1$ such that

$$\int_{-1}^{1} j^2(x)dx = 1. \tag{2.60}$$

Let

$$w_\delta(\xi, l) = j_\delta(l - l_0)u(\xi),\ j_\delta(x) = \delta^{-1/2} j(x/\delta),\ \delta > 0. \tag{2.61}$$

where $u(\xi)$ satisfies (2.58). We show that, for sufficiently small δ, $w = w_\delta$ satisfies (2.59). It is easily seen that

$$w(\xi, l) \in \mathcal{D}(\widetilde{\mathcal{P}}),\ \|w_\delta\|_{L^2(\mathbb{R}^2)} = 1. \tag{2.62}$$

We verify the last inequality in (2.59). First, note that

$$\begin{aligned} \|(z - \mathcal{P}_l)u\|_{L^2(\mathbb{R})} &\le \|(z - \mathcal{P}_{l_0})u\|_{L^2(\mathbb{R})} + \|(\mathcal{P}_l - \mathcal{P}_{l_0})u\|_{L^2(\mathbb{R})} \\ &\le \epsilon + \|(\mathcal{P}_l - \mathcal{P}_{l_0})u\|_{L^2(\mathbb{R})}. \end{aligned} \tag{2.63}$$

where we used (2.58) in the last inequality. Thus,

$$\begin{aligned} \left\|(z - \widetilde{\mathcal{P}})w_\delta\right\|^2_{L^2(\mathbb{R}^2)} &= \int_{l_0-\delta}^{l_0+\delta} \|(z - \mathcal{P}_l)u\|^2_{L^2(\mathbb{R})}\, j_\delta^2(l - l_0)dl \\ &\le \int_{l_0-\delta}^{l_0+\delta} (\epsilon + \|(\mathcal{P}_l - \mathcal{P}_{l_0})u\|)^2_{L^2(\mathbb{R})} j_\delta^2(l - l_0)dl \end{aligned} \tag{2.64}$$

The operator $\mathcal{P}_l - \mathcal{P}_{l_0}$, as we saw in (2.53), converges to 0 as $l \to l_0$ in the indicated norm. Since $u \in H^2(\mathbb{R}) \subset H^1(\mathbb{R})$,

$$\lim_{l \to l_0} \|(\mathcal{P}_l - \mathcal{P}_{l_0})u\|_{L^2(\mathbb{R})} = 0. \tag{2.65}$$

We may thus take δ small enough so that

$$\|(\mathcal{P}_l - \mathcal{P}_{l_0})u\|_{L^2(\mathbb{R})} \le \epsilon \text{ if } |l - l_0| \le \delta. \tag{2.66}$$

Using this in (2.64), we find that

$$\left\|(z - \widetilde{\mathcal{P}})w_\delta\right\|^2_{L^2(\mathbb{R}^2)} \le \int_{l_0-\delta}^{l_0+\delta} (2\epsilon)^2 j_\delta^2(l - l_0)dl = (2\epsilon)^2, \tag{2.67}$$

where we used (2.60) and (2.61) in the last equality. This was what was to be proved.

Case 2: The range of $z - \mathcal{P}_{l_0}$ is not dense in $L^2(\mathbb{R})$. In this case, $\overline{z}$ (the complex conjugate of z) is an eigenvalue of $\mathcal{P}^*_{l_0}$, the adjoint of $\mathcal{P}_{l_0}$ (see (2.44)). Using the same argument as in Case 1 above, we see that $\overline{z} \in \Sigma(\widetilde{\mathcal{P}}^*)$. This implies that $z \in \Sigma(\widetilde{\mathcal{P}})$. □

3 A Sufficient Condition for Front Stability

We obtain a sufficient condition for front stability, by examining the spectrum of $\mathcal{P}_l$. Proposition 2.3, shows that $\Sigma(\mathcal{P}_l)$ lies in the left half of the complex plane if $|l|$ is large enough. However, this result cannot place $\Sigma(\mathcal{P}_l)$ in the left half of the complex plane for every $l \in \mathbb{R}$ since $f_{\max}$ is positive (recall that $f'(\alpha_{\rm u}) > 0$ where $\alpha_{\rm u}$ is the unstable 0 of f).

For $z \in \mathbb{C}$ consider the following equation for v.

$$(z - \mathcal{P}_l)v = g \tag{3.1}$$

where $g \in L^2(\mathbb{R})$ and $\mathcal{P}_l$ is given in (2.23). It is useful to reformulate this problem. Using (2.17), we may write $\mathcal{L}_l v$ as:

$$\mathcal{L}_l v = K^2 \left(\frac{1}{i} \frac{\partial}{\partial \xi} - \alpha_1 l \right)^2 v + \alpha_0 l^2 v + \mathcal{F}_\xi^{-1}(l^2 q(k/l))\mathcal{F}_\xi v. \tag{3.2}$$

Multiply both sides of (3.1) with $\exp(-i\alpha_1 l\xi)$. After some algebra, we see that

$$\begin{aligned} (\widehat{z} - \mathcal{M}_l)w \equiv (\widehat{z} - (\mathcal{P}_0 - \mathcal{A}_l))w = \widehat{g},\ \widehat{z} = z - i\alpha_1 cl + \alpha_0 l^2, \\ w = v\exp(-i\alpha_1 l\xi),\ \widehat{g} = g\exp(-i\alpha_1 l\xi), \\ \mathcal{A}_l w \equiv \mathcal{F}_\xi^{-1}(l^2 q((k + \alpha_1 l)/l))\mathcal{F}_\xi w. \end{aligned} \tag{3.3}$$

We thus see that

$$z \in \Sigma(\mathcal{P}_l) \text{ if and only if } \widehat{z} \in \Sigma(\mathcal{M}_l). \tag{3.4}$$

The advantage of studying $\mathcal{M}_l$ instead of $\mathcal{P}_l$ is that $\mathcal{M}_l = \mathcal{P}_0 - \mathcal{A}_l$ can be studied as a perturbation to $\mathcal{P}_0$:

$$\mathcal{P}_0 w = c\frac{\partial w}{\partial \xi} + K^2 \frac{\partial^2 v}{\partial \xi^2} + f'(u_{\rm f})w. \tag{3.5}$$

The operator $\mathcal{P}_0$ is nothing other than the linearization of the one-dimensional Allen-Cahn equation around the traveling front solution, and its properties are well-known. We now collect some standard results on $\mathcal{P}_0$. Let $\mathcal{P}_0^*$ be the adjoint of $\mathcal{P}_0$ (in accordance with (2.44)):

$$\mathcal{P}_0^* w = -c\frac{\partial w}{\partial \xi} + K^2 \frac{\partial^2 v}{\partial \xi^2} + f'(u_{\rm f})w. \tag{3.6}$$

Like $\mathcal{P}_0$, $\mathcal{P}_0^*$ is a closed operator on $L^2(\mathbb{R})$ with domain $H^2(\mathbb{R})$.

Proposition 3.1. *The operator $\mathcal{P}_0$ as an operator on $L^2(\mathbb{R})$ with domain $H^2(\mathbb{R})$ satisfies the following properties.*

1. *The right most point of the spectrum of $\mathcal{P}_0$ is 0, and there is a $\nu > 0$ such that*
$$\Sigma(\mathcal{P}_0)\backslash\{0\} \subset \{z \in \mathbb{C} | {\rm Re} z < -\nu\}. \tag{3.7}$$
The spectrum of $\mathcal{P}_0$ is independent of K.

2. *The point* 0 *is a (geometrically and algebraically) simple isolated eigenvalue with eigenvector* $v_0 = -\partial u_{\mathrm{f}}/\partial\xi$. *The function* v_0 *is of positive sign. The function* v_0 *decays exponentially as* $|\xi| \to \infty$.

3. *The null space of* $\mathcal{P}_0^*$ *is one-dimensional and is spanned by*

$$v_0^* = \exp(c\xi/K^2)v_0. \tag{3.8}$$

The function v_0^* *decays exponentially as* $|\xi| \to \infty$.

4. $\mathcal{P}_0$ *satisfies the following resolvent estimate.*

$$\left\|(z-\mathcal{P}_0)^{-1}\right\|_{\mathcal{L}(L^2(\mathbb{R}))} \le \frac{M_f}{|z|} \text{ for } \mathrm{Re} z \ge 0, \tag{3.9}$$

where $M_f \ge 1$ *is a constant that depends only on* f *and not on* K. *If the front speed* $c = 0$ *and* $\mathcal{P}_0$ *is self-adjoint, we may take* $M_f = 1$.

5. *The image* R_0 *of* $\mathcal{P}_0$ *is the orthogonal complement of* v_0^* *(defined in* (3.8)*) in* $L^2(\mathbb{R})$. *The restriction of* $\mathcal{P}_0$ *to* R_0 *is well-defined with domain* $R_0 \cap H^2(\mathbb{R})$. *This restriction* $\mathcal{P}_0|_{R_0}$ *has the following properties.*

$$\begin{aligned} \Sigma(\mathcal{P}_0|_{R_0}) &= \Sigma(\mathcal{P}_0)\backslash\{0\}, \\ \left\|(z-\mathcal{P}_0|_{R_0})^{-1}\right\|_{\mathcal{L}(R_0)} &\le \frac{\widetilde{M_f}}{|z+\nu|}, \ \mathrm{Re} z \ge -\nu, \end{aligned} \tag{3.10}$$

where $\|\cdot\|_{\mathcal{L}(R_0)}$ *is the operator norm on* R_0 *seen as a subspace of* $L^2(\mathbb{R})$ *and* $\widetilde{M_f}$ *is a constant that depends only on* f *and not on* K.

Proof. All of these results are standard and the proofs can be found in many places (see for example [31]). We only discuss dependence on K. Let $\widehat{\mathcal{P}}_0$ be the operator obtained by setting $K = 1$ in $\mathcal{P}_0$:

$$\widehat{\mathcal{P}}_0 w = c_* \frac{\partial w}{\partial \xi} + \frac{\partial^2 w}{\partial \xi^2} + f'(u_{\mathrm{f}*})w. \tag{3.11}$$

We may write $\mathcal{P}_0$ in terms of $\widehat{\mathcal{P}}_0$ as follows.

$$\mathcal{P}_0 w = \mathcal{D}_{1/K}\widehat{\mathcal{P}}_0\mathcal{D}_K w, \ \mathcal{D}_K w(\xi) = w(K\xi). \tag{3.12}$$

This shows that the spectrum of $\mathcal{P}_0$ is the same as the spectrum of $\widehat{\mathcal{P}}_0$ and thus independent of K. Using this, we see that

$$\begin{aligned} &\left\|(z-\mathcal{P}_0)^{-1}\right\|_{\mathcal{L}(L^2(\mathbb{R}))} = \left\|\mathcal{D}_{1/K}(z-\widehat{\mathcal{P}}_0)^{-1}\mathcal{D}_K\right\|_{\mathcal{L}(L^2(\mathbb{R}))} \\ \le &\left\|\mathcal{D}_{1/K}\right\|_{\mathcal{L}(L^2(\mathbb{R}))} \left\|\mathcal{D}_K\right\|_{\mathcal{L}(L^2(\mathbb{R}))} \left\|(z-\widehat{\mathcal{P}}_0)^{-1}\right\|_{\mathcal{L}(L^2(\mathbb{R}))} \\ = &\left\|(z-\widehat{\mathcal{P}}_0)^{-1}\right\|_{\mathcal{L}(L^2(\mathbb{R}))}. \end{aligned} \tag{3.13}$$

We may obtain the reverse inequality in the same way to conclude that

$$\left\|(z-\mathcal{P}_0)^{-1}\right\|_{\mathcal{L}(L^2(\mathbb{R}))} = \left\|(z-\widehat{\mathcal{P}}_0)^{-1}\right\|_{\mathcal{L}(L^2(\mathbb{R}))}. \tag{3.14}$$

This shows that the constant M_f in (3.9) can be taken independent of K. The independence of $\widetilde{M}_f$ in (3.10) can be proved in a similar fashion. □

To state our sufficient condition, we define the following.

$$\begin{aligned} q_{\inf} = \inf_{k\in\mathbb{R}} q(k),\ q_{\sup} = \sup_{k\in\mathbb{R}} q(k), \\ \overline{q} = \frac{q_{\inf}+q_{\sup}}{2},\ q_\Delta = \frac{q_{\sup}-q_{\inf}}{2}. \end{aligned} \tag{3.15}$$

We have the following result.

Theorem 3.2. *The spectrum of $\mathcal{P}_l$, $\Sigma(\mathcal{P}_l)$ satisfies:*

$$\Sigma(\mathcal{P}_l) \subset \{z\in\mathbb{C} | \mathrm{Re} z \le -(\alpha_0 + \overline{q} - M_f q_\Delta) l^2\}. \tag{3.16}$$

where $M_f \ge 1$ is the constant in the resolvent estimate (3.9).

Proof. Rewrite equation (3.3) as follows:

$$(\widetilde{z} - (\mathcal{P}_0 + \mathcal{B}_l))w = \widehat{g},\ \widetilde{z} = \widehat{z} + \overline{q}l^2,\ \mathcal{B}_l w = (-\mathcal{A}_l + \overline{q}l^2)w. \tag{3.17}$$

It can be seen from the definition of $\mathcal{A}_l$ in (3.3) that

$$\|\mathcal{B}_l\|_{L^2(\mathbb{R})} = \max_{k\in\mathbb{R}} l^2\,|q((k+al)/l) - \overline{q}| = q_\Delta l^2. \tag{3.18}$$

We have

$$(\widetilde{z} - (\mathcal{P}_0 + \mathcal{B}_l))^{-1} = \left(I + \sum_{k=1}^{\infty} ((\widetilde{z}-\mathcal{P}_0)^{-1}\mathcal{B}_l)^k\right)(\widetilde{z}-\mathcal{P}_0)^{-1}. \tag{3.19}$$

Using (3.9), we see that the above Neumann series converges if

$$M_f q_\Delta l^2 < |\widetilde{z}| \ \text{ and } \mathrm{Re}\widetilde{z} \ge 0. \tag{3.20}$$

Given (3.3) and (3.4), we see that z is in the resolvent set of $\mathcal{P}_l$ if

$$M_f q_\Delta l^2 < \left|z - i\alpha_1 cl + (\alpha_0+\overline{q})l^2\right| \ \text{ and } \mathrm{Re} z + (\alpha_0+\overline{q})l^2 \ge 0. \tag{3.21}$$

Both of the above conditions are satisfied if

$$\mathrm{Re} z + (\alpha_0+\overline{q})l^2 > M_f q_\Delta l^2. \tag{3.22}$$

This was the result to be proved. □

We have the following immediate corollary.

Corollary 3.3. *The planar front is spectrally stable if*

$$\alpha_0 > M_f q_\Delta - \overline{q}. \tag{3.23}$$

Proof. When $l \neq 0$, we see from (3.16) that

$$\Sigma(\mathcal{P}_l) \subset \{z \in \mathbb{C} | \mathrm{Re} z < 0\}. \tag{3.24}$$

This is nothing other than (2.26) in Definition 2.1. □

The right hand side of (3.23) is always non-negative. To see this, note that

$$M_f q_\Delta - \overline{q} \geq -q_{\inf} = -\inf_{s\in\mathbb{R}} q(s) \geq -\lim_{|s|\to\infty} q(s) = 0. \tag{3.25}$$

where we used $M_f \geq 1$ and (3.15) in the first inequality, (3.15) in the first equality and the expression for q in (2.17) in the last equality.

When $c = 0$, the stability criterion (3.23) assumes a simpler form. Given that $\mathcal{P}_0$ is self-adjoint, M_f may be taken equal to 1 (see item 4 of Proposition 3.1). Therefore, (3.23) reduces to:

$$\alpha_0 > -q_{\inf}. \tag{3.26}$$

When $c = 0$, we have a stability criterion that is independent of f. When $c \neq 0$, our criterion (3.23) depends on f through the constant M_f.

Let us demonstrate the above stability result when the conductivity matrices are given by (2.7). In this case, we may compute $\overline{q}$ and q_Δ in (3.15) using expressions (2.20) as follows:

$$\overline{q} = -a^2 \cos(4\theta),\ q_\Delta = a^2. \tag{3.27}$$

Proposition 3.4. *Suppose the conductivity matrices A_i and A_e are given by* (2.7)*. The planar front in the θ direction is spectrally stable if*

$$\alpha_0(a, b, \theta) > M_f q_\Delta(a) - \overline{q}(a, \theta) \tag{3.28}$$

where α_0, q_Δ and $\overline{q}$ are given in (2.20) *and* (3.27)*. When $b = 0$, this condition reduces to*

$$|a| < \frac{1}{\sqrt{2(M_f+1)}} \ \text{ or } \ |\cos(2\theta)| > \sqrt{-\frac{1}{a^2} - (M_f - 1) + \sqrt{\frac{4M_f}{a^2} + (M_f-1)^2}}. \tag{3.29}$$

Proof. Equation (3.29) can be derived by using criterion (3.23), substituting the expressions for $\alpha_0, \overline{q}, q_\Delta$ in (2.20) and (3.27). After some algebraic manipulations, we obtain the condition

$$h(\rho) = \rho^2 + 2(a^{-2} + (M_f - 1))\rho + a^{-4} - 2(M_f + 1)a^{-2} > 0,\ \rho = \cos^2(2\theta). \tag{3.30}$$

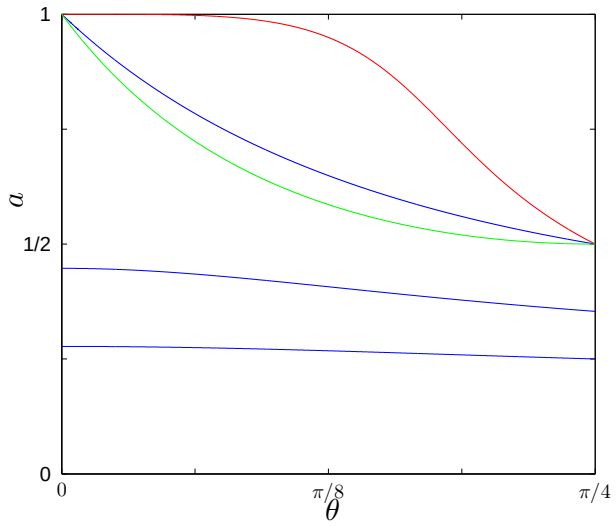

Figure 1: Plot of stable/unstable regions in the (θ, a) parameter plane when $b = 0$. In the region above the red line, $\alpha_0 < 0$, and the front is unstable. The three blue lines correspond to stability criteria for $M_f = 1, 3, 7$ respectively from the top. If $M_f = 1$, the front is stable below the $M_f = 1$ line (and likewise for other values of M_f). The region above the green line lies inside the convex hull of the Frank diagram (see (4.91) in Section 4 and the discussion in Section 6.2).

Thus,

$$\rho < \varrho_- \text{ or } \rho > \varrho_+, \ \varrho_\pm = -\frac{1}{a^2} - (M_f - 1) \pm \sqrt{\frac{4M_f}{a^2} + (M_f - 1)^2}. \tag{3.31}$$

Since $M_f > 1$, the above roots are both real, and $\varrho_- < 0$. Noting that $0 \leq \rho \leq 1$, we must have $\rho > \varrho_+$. The larger root ϱ_+ is negative if and only if $|a| < 1/\sqrt{2(M_f + 1)}$ and we obtain (3.29). □

In figure 1, we have plotted the stability regions demarcated by our stability criteria when $b = 0$. According to 3.29, planar fronts in all propagation directions are stable if $|a| < 1/\sqrt{2(M_f + 1)}$. When

$$|a| > \frac{1}{\sqrt{2M_f - 1}} \tag{3.32}$$

the right hand side of the cosine inequality in (3.29) is greater than 1. For values of a above $1/\sqrt{2M_f - 1}$, therefore, our stability criteria cannot rule out instabilities in any direction. There is a large parameter region in which we cannot guarantee front stability. In the next Section, we shall see that the front can indeed become unstable.

4 Front Stability under Long-Wavelength Perturbations

We now study the spectral properties of $\mathcal{P}_l$ when $|l|$ is small or equivalently at long wavelengths. In this case, it is possible to obtain detailed information on the spectrum of $\mathcal{P}_l$. Our results here will help us show that the planar front can be unstable.

Before we proceed, we collect some results on the operator $\mathcal{A}_l$ defined in (3.3). It is useful to note that $\mathcal{A}_l$ can be written as a convolution integral.

$$\begin{aligned}(\mathcal{A}_l w)(\xi) = (K_l \star w)(\xi) = \int_{\mathbb{R}} K_l(\xi - \xi') w(\xi') d\xi',\ K_l(\xi) = |l|^3 K_1(l\xi),\\ K_1(\xi) = \frac{1}{2}\left(\frac{\beta_0}{\gamma_0} + i\beta_1 \mathrm{sign}(\xi)\right) \exp(-\gamma_0 |\xi| + i(\gamma_1 - \alpha_1)\xi),\end{aligned} \tag{4.1}$$

where $\mathrm{sign}(\xi)$ is the sign of ξ (1 if ξ is positive, -1 if negative). In what follows, we let

$$\langle v, w\rangle = \int_{\mathbb{R}} v(\xi)\overline{w(\xi)} d\xi, \tag{4.2}$$

(where $\bar{\cdot}$ is the complex conjugate) whenever the above integral is well-defined.

Lemma 4.1. *The operator $\mathcal{A}_l$ is a bounded operator on $L^2(\mathbb{R})$ that has a C^1 dependence on l for $l \in \mathbb{R}$ and is smooth on $l \in \mathbb{R}\backslash\{0\}$. Let $\partial_l \mathcal{A}_l$ and $\partial_l^2 \mathcal{A}_l$ be the first and second derivatives of $\mathcal{A}_l$, where the latter is defined for $l \neq 0$. We have*

$$\|\partial_l^m \mathcal{A}_l\|_{\mathcal{L}(L^2(\mathbb{R}))} \leq C_{\mathcal{A}}^1 |l|^{2-m},\ m = 0, 1, 2, \tag{4.3}$$

where $m_{\mathcal{A}}$ is a positive constant that does not depend on l. Let $v, w \in L^1(\mathbb{R}) \cap L^2(\mathbb{R})$. We have

$$\|\mathcal{A}_l v\|_{L^2(\mathbb{R})} \leq C_{\mathcal{A}}^2 \|v\|_{L^1(\mathbb{R})} |l|^{5/2-m},\ m = 0, 1, 2, \tag{4.4}$$

$$|\langle \partial_l^m \mathcal{A}_l v, w\rangle| \leq C_{\mathcal{A}}^\infty \|v\|_{L^1(\mathbb{R})} \|w\|_{L^1(\mathbb{R})} |l|^{3-m},\ m = 0, 1, 2, \tag{4.5}$$

where $C_{\mathcal{A}}^2$ and $C_{\mathcal{A}}^\infty$ are constants that do not depend on l.

Proof. From expression (4.1), it is immediate that $\partial_l^m K_l(\xi)$ (the m-th partial derivative of K_l with respect to l) is integrable for any m so long as $l \neq 0$. For $v \in L^2(\mathbb{R})$, we have

$$\|\partial_l^m (\mathcal{A}_l v)\|_{L^2(\mathbb{R})} = \|(\partial_l^m K_l) \star v\|_{L^2(\mathbb{R})} \leq \|\partial_l^m K_l\|_{L^1(\mathbb{R})} \|v\|_{L^2(\mathbb{R})}, \tag{4.6}$$

where we used Young's inequality in the inequality above. This implies that $\mathcal{A}_l$ has smooth dependence on l as an operator on $L^2(\mathbb{R})$ for $l \neq 0$.

To prove (4.3), note from (4.1) that

$$\|\partial_l^m K_l\|_{L^1(\mathbb{R})} \leq C_{\mathcal{A}}^1 |l|^{2-m},\ m = 0, 1, 2, \tag{4.7}$$

where C_K^1 is a constant independent of l. From this and (4.6), (4.3) is immediate. Setting $m = 1$ in (4.3), we see that $\mathcal{A}_l$ has C^1 dependence on l for $l \in \mathbb{R}$.

For (4.4), note that

$$\|\partial_l^m K_l\|_{L^2(\mathbb{R})} \le C_{\mathcal{A}}^1 |l|^{5/2-m}, \ m = 0, 1, 2. \tag{4.8}$$

Proceeding as in (4.6), we have:

$$\|(\partial_l^m \mathcal{A}_l)v\|_{L^2(\mathbb{R})} \le \|\partial_l^m K_l\|_{L^2(\mathbb{R})} \|v\|_{L^1(\mathbb{R})} \le C_{\mathcal{A}}^2 |l|^{5/2-m} \|v\|_{L^1(\mathbb{R})}, \tag{4.9}$$

where we used Young's inequality in the first inequality above and (4.8) in the last inequality.

We now turn to (4.5). From (4.1) we see that

$$|\partial_l^m K_l(\xi)| \le C_{\mathcal{A}}^\infty |l|^{3-m}, m = 0, 1, 2, \tag{4.10}$$

where $\partial_l^m K_l$ is the m-th partial derivative of K_l with respect to l and $C_{\mathcal{A}}^\infty$ is a constant independent of l. Thus, we have:

$$\begin{aligned} &|\langle \partial_l^m \mathcal{A}_l v, w\rangle| = |\langle \partial_l^m K_l \star v, w\rangle| \\ &\le \|\partial_l^m K_l(\xi)\|_{L^\infty(\mathbb{R})} \|v\|_{L^1(\mathbb{R})} \|w\|_{L^1(\mathbb{R})} \le C_{\mathcal{A}}^\infty |l|^{3-m} \|v\|_{L^1(\mathbb{R})} \|w\|_{L^1(\mathbb{R})}. \end{aligned} \tag{4.11}$$

□

We consider the following eigenvalue perturbation problem for l close to 0:

$$\mathcal{P}_l v_l = \lambda_l v_l, \ \lambda_0 = 0, \ v_0 = -\frac{\partial u_{\mathrm{f}}}{\partial \xi}. \tag{4.12}$$

We normalize v_l as follows:

$$v_l(0) = v_0(0). \tag{4.13}$$

To study this problem, multiply both sides of the first equation in (4.12) by $\exp(-i\alpha_1 l\xi)$ (as in (3.3)). We see that (4.12) is equivalent to solving the following problem.

$$\begin{aligned} \mathcal{M}_l w_l \equiv \mathcal{P}_0 w_l - \mathcal{A}_l w_l = \mu_l w_l, \\ \mu_0 = 0, \ w_0 = v_0 = -\frac{\partial u_{\mathrm{f}}}{\partial \xi}, \end{aligned} \tag{4.14}$$

where $\mathcal{M}_l$ and $\mathcal{A}_l$ were defined in (3.3). It is convenient to normalize w_l as follows:

$$\langle w_l, v_0^*\rangle = \langle v_0, v_0^*\rangle, \ v_0^* = -\frac{\partial u_{\mathrm{f}}}{\partial \xi} \exp(c\xi). \tag{4.15}$$

Once a (w_l, μ_l) satisfying (4.14) and (4.15) is obtained, we may find (v_l, λ_l) satisfying (4.12) and (4.13) by letting

$$v_l = \frac{v_0(0)}{w_l(0)} w_l \exp(i\alpha_1 l\xi), \ \lambda_l = \mu_l + i\alpha_1 cl - \alpha_0 l^2, \tag{4.16}$$

provided $w_l(0) \neq 0$.

Before we state our results on problem (4.14) and hence (4.12), let us perform a short calculation to see what to expect. Let w_l^* be the solution to the adjoint problem of (4.14) (equation (4.31)). Taking the inner product of the first equation in (4.14) with respect to w_l^*, we obtain:

$$\mu_l = \frac{\langle (\mathcal{P}_0 - \mathcal{A}_l) w_l, w_l^* \rangle}{\langle w_l, w_l^* \rangle} \approx -\frac{\langle \mathcal{A}_l v_0, v_0^* \rangle}{\langle v_0, v_0^* \rangle}. \tag{4.17}$$

We may use expression (4.1) to compute the last quotient explicitly to obtain an expression of order $|l|^3$. This, together with (4.16), gives us an expansion of λ_l up to order three in l. The above heuristic calculation is justified in the following theorem.

Theorem 4.2. *There is a $\delta > 0$ such that for $|l| < \delta$ there is an eigenvector-eigenvalue pair $(v_l, \lambda_l) \in H^2(\mathbb{R}) \times \mathbb{C}$ satisfying (4.12) and (4.13) with the following properties.*

1. *The pair (v_l, λ_l) is a continuous function of l with values in $H^2(\mathbb{R}) \times \mathbb{C}$. The eigenvalue λ_l is simple, and is the principal eigenvalue of $\mathcal{P}_l$ in the following sense: there is a positive constant ν_δ independent of l such that*

$$\Sigma(\mathcal{P}_l) \backslash \{\lambda_l\} \subset \{z \in \mathbb{C} | \mathrm{Re} z < -\nu_\delta\}. \tag{4.18}$$

2. *The eigenvalue λ_l is a C^2 function of l and has the following expansion near $l = 0$:*

$$\begin{aligned} &\lambda_l = i\alpha_1 c l - \alpha_0 l^2 - \rho_{\mathrm{r}} |l|^3 - i\rho_{\mathrm{i}} l^3 + \mathcal{O}(l^4), \\ &\rho_{\mathrm{r}} = \frac{\beta_0 K}{2\gamma_0} \frac{\|\widehat{v}_0\|_{L^1(\mathbb{R})} \|\widehat{v}_0^*\|_{L^1(\mathbb{R})}}{\langle \widehat{v}_0, \widehat{v}_0^* \rangle},\ \rho_{\mathrm{i}} = \beta_1 K \frac{\langle \mathrm{sign} \star \widehat{v}_0, \widehat{v}_0^* \rangle}{\langle \widehat{v}_0, \widehat{v}_0^* \rangle}, \end{aligned} \tag{4.19}$$

   where $\widehat{v}_0$ and $\widehat{v}_0^*$ are the normalized versions of v_0 and v_0^*:

$$\widehat{v}_0 = -\frac{\partial u_{\mathrm{f}*}}{\partial \xi},\ \widehat{v}_0^* = \widehat{v}_0 \exp(c_* \xi). \tag{4.20}$$

3. *The function v_l satisfies the following estimate*

$$\|v_l - v_0 \exp(i\alpha_1 l \xi)\|_{H^2(\mathbb{R})} \leq C_v |l|^{5/2},\ v_0 = -\frac{\partial u_{\mathrm{f}}}{\partial \xi}, \tag{4.21}$$

   where C_v is a constant that does not depend on l. Moreover, the function $v_l \exp(-i\alpha_1 l \xi)$ is a C^2 function of l with values in $H^2(\mathbb{R})$.

Proof. As discused above, solving (4.12) is equivalent to solving (4.14) (with the normalization condition (4.15)). The proof is somewhat long, and we divide it into several steps.

Step 1. To solve (4.14) and (4.15) for small l, we apply the implicit function theorem. Consider the map $\mathcal{T}_l$ mapping $H^2(\mathbb{R}) \times \mathbb{C}$ to $L^2(\mathbb{R}) \times \mathbb{C}$:

$$\mathcal{T}_l(w, \mu) = (\mathcal{M}_l w - \mu w, \langle w, v_0^* \rangle). \tag{4.22}$$

By Lemma 4.1, $\mathcal{A}_l$ has C^1 dependence on l as an operator on $L^2(\mathbb{R})$. From this, it follows that $\mathcal{T}_l$ has C^1 dependence on l as an operator from $H^2(\mathbb{R}) \times \mathbb{C}$ to $L^2(\mathbb{R}) \times \mathbb{C}$. To apply the implicit function theorem, we must examine the invertibility of the linearization of $\mathcal{T}_l$ at $l = 0$ and $(w, \mu) = (v_0, \mu_0)$. This linearization, which we call $\mathcal{S}_0$, is given by

$$\mathcal{S}_0(w, \mu) = (\mathcal{P}_0 w - \mu v_0, \langle w, v_0^* \rangle), \tag{4.23}$$

We used the fact that the derivative of $\mathcal{A}_l$ with respect to l at $l = 0$ vanishes (set $m = 1$ in (4.3) of Lemma 4.1). We show that the kernel of $\mathcal{S}_0$ is trivial. Consider:

$$\mathcal{P}_0 w = \mu v_0, \ \langle w, v_0^* \rangle = 0. \tag{4.24}$$

Since v_0 is an algebraically simple eigenvector of $\mathcal{P}_0$, $\mu = 0$ or else there is no solution. The function w must then be an eigenvector of $\mathcal{P}_0$ with eigenvalue 0, and is therefore a scalar multiple of v_0. Since w is orthogonal to v_0^* and $\langle v_0, v_0^* \rangle \neq 0$, w must be 0. To see that $\mathcal{S}_0$ is onto, note that $\mathcal{P}_0$ maps $H^2(\mathbb{R})$ onto the orthogonal complement of v_0^* (by item 3 of Proposition 3.1 and the closed range theorem). Since $\langle v_0, v_0^* \rangle \neq 0$, we see that $\mathcal{P}_0 v - \mu v_0$ maps $H^2(\mathbb{R}) \times \mathbb{C}$ onto $L^2(\mathbb{R})$. From this, we conclude that $\mathcal{S}_0$ is onto. The operator $\mathcal{S}_0$ is thus a bijection, and by the implicit function theorem, we have the existence of a C^1 family (w_l, μ_l) that satisfies (4.14) for $|l| < \delta$ for some $\delta > 0$. Note also that this family is smooth for $l \neq 0$, given the smoothness of $\mathcal{A}_l$ when $l \neq 0$ (see Lemma 4.1). That w_l is continuous in l with values in $H^2(\mathbb{R})$ implies the same for v_l given (4.16). We have used the fact that $w_l(0)$ depends continuously on l by Sobolev embedding and that $w_0(0) \neq 0$ (note that the C^1 dependence of w_l on l may not in general imply the same for $v_l = w_l \exp(i\alpha_1 l\xi)$, viewed as functions of l with values in $H^2(\mathbb{R})$; the derivative of $\exp(i\alpha_1 l\xi)$ with respect to l grows linearly in ξ as $|\xi| \to \infty$). We have thus proved the first line of item 1.
Step 2. Consider the operator:

$$\widehat{\mathcal{M}}_l w = \mathcal{M}_l w - \mu_l w. \tag{4.25}$$

Note that $\widehat{\mathcal{M}}_0 = \mathcal{P}_0$, and therefore, $\widehat{\mathcal{M}}_l$ is a bounded perturbation of $\mathcal{P}_0$. Since $\mathcal{P}_0$ is a Fredholm operator with index 0 by Proposition 3.1, $\widehat{\mathcal{M}}_l$ is also a Fredholm operator with index 0 for sufficiently small l. Since μ_l is an eigenvalue of $\mathcal{M}_l$, the nullspace of $\widehat{\mathcal{M}}_l$, which we denote by N_l, is at least one-dimensional:

$$\dim(N_l) = \operatorname{codim}(R_l) \geq 1. \tag{4.26}$$

where R_l is the range of $\widehat{\mathcal{M}}_l$ and $\dim(\cdot), \operatorname{codim}(\cdot)$ refer to the dimension and codimension respectively. Consider the linear map

$$\widehat{\mathcal{T}}_l(w, \mu) = (\widehat{\mathcal{M}}_l w - \mu v_0, \langle w, v_0^* \rangle) \tag{4.27}$$

mapping $H^2(\mathbb{R}) \times \mathbb{C}$ to $L^2(\mathbb{R}) \times \mathbb{C}$. At $l = 0$, $\widehat{\mathcal{T}}_l$ is the same as S_0 of (4.23), and therefore, $\widehat{\mathcal{T}}_l$ is a bijection. Thus, $\widehat{\mathcal{T}}_l$ is a bijection for sufficiently small l. In particular, the range of $\widehat{\mathcal{M}}_l$, together with v_0 spans $L^2(\mathbb{R})$. This shows that the codimension of R_l is at most one dimensional. Combining this with (4.26), we see that

$$\dim(N_l) = \operatorname{codim}(R_l) = 1. \tag{4.28}$$

The nullspace N_l is thus spanned by w_l. Now, let

$$w_l^* \in R_l^\perp,\ \langle w_l^*, v_0 \rangle = \langle v_0^*, v_0 \rangle, \tag{4.29}$$

where $R_l^\perp$ is the orthogonal complement of R_l in $L^2(\mathbb{R})$. The above conditions determine w_l^* uniquely since $R_l^\perp$ is one-dimensional and $v_0 \notin R_l$. By the closed range theorem, w_l^* is in the nullspace of

$$\widehat{\mathcal{M}}_l^* = \mathcal{M}_l^* - \overline{\mu_l},\ \mathcal{M}_l^* = \mathcal{P}_0^* - \mathcal{A}_l, \tag{4.30}$$

where $\bar{\cdot}$ denotes the complex conjugate and $\mathcal{P}_0^*$ was defined in (3.6). Therefore, w_l^* satisfies:

$$(\mathcal{P}_0^* - \mathcal{A}_l) w_l^* = \overline{\mu_l} w_l^*,\ \langle w_l^*, v_0 \rangle = \langle v_0^*, v_0 \rangle. \tag{4.31}$$

Note that $w_0^* = v_0^*$ where v_0^* was defined in (4.14) or item 3 of Proposition 3.1. The above is just a linear equation in w_l^* and is uniquely solvable for l small since the linear system varies continuously on l and is uniquely solvable when $l = 0$. Since λ_l and $\mathcal{A}_l$ have C^1 dependence on l, $w_l^* \in H^2(\mathbb{R})$ has C^1 dependence on l. A simple consequence of this is that μ_l is a simple eigenvalue of $\mathcal{M}_l$. To see this, note that

$$\langle w_l, w_l^* \rangle \neq 0 \tag{4.32}$$

for l small, since the above is a continuous (in fact, a C^1) function of l and $\langle v_0, v_0^* \rangle \neq 0$. Thus, $w_l \notin R_l$, and thus μ_l is an algebraically simple eigenvalue, and so is λ_l.

Step 3. Let us now examine $\Sigma(\mathcal{M}_l) \backslash \{\mu_l\}$. This is the part of the spectrum of $\mathcal{M}_l$ associated with its action on R_l. Consider the linear operator:

$$\Pi_l w = \frac{\langle w, w_l^* \rangle}{\langle w_l, w_l^* \rangle} w_l. \tag{4.33}$$

This is just the spectral projection of $\mathcal{M}_l$ onto N_l. Now, define the operator:

$$\widetilde{\mathcal{M}}_l = \mathcal{M}_l - 2\nu \Pi_l \tag{4.34}$$

where ν is the spectral gap constant that appears in (3.7). The restriction of $\widetilde{\mathcal{M}}_l$ and $\mathcal{M}_l$ to R_l are exactly the same. If we let $\mathcal{M}_l|_{R_l}$ be the restriction of $\mathcal{M}_l$ to R_l, we have:

$$(\Sigma(\mathcal{M}_l) \backslash \{\mu_l\}) = \Sigma\left(\mathcal{M}_l|_{R_l}\right) \subset \Sigma\left(\widetilde{\mathcal{M}}_l\right). \tag{4.35}$$

Let us now study the spectrum of $\widetilde{\mathcal{M}}_l$. When $l = 0$, we have:

$$\widetilde{\mathcal{M}}_0 = \mathcal{P}_0 - 2\nu\Pi_0. \tag{4.36}$$

The spectrum of $\widetilde{\mathcal{M}}_0$ consists of:

$$\Sigma\left(\widetilde{\mathcal{M}}_0\right) = ((\Sigma(\mathcal{P}_0)\backslash\{0\}) \cup \{-2\nu\}) \subset \{z \in \mathbb{C} | \mathrm{Re} z < -\nu\}, \tag{4.37}$$

where we used (3.7) of Proposition 3.1. Let $z \in \mathbb{C}$ be such that $\mathrm{Re} z \geq -\nu$, and therefore, in the resolvent set of $\widetilde{\mathcal{M}_0}$. Note that:

$$(z - \widetilde{\mathcal{M}}_0)^{-1} = (z - \mathcal{P}_0|_{R_0})^{-1}(I - \Pi_0) + (z + 2\nu)^{-1}\Pi_0, \tag{4.38}$$

where I is the identity operator. Using (3.10), we have

$$\left\|(z - \widetilde{\mathcal{M}}_0)^{-1}\right\|_{\mathcal{L}(L^2(\mathbb{R}))} \leq \frac{C_{\mathcal{M}}}{|z + \nu|} \tag{4.39}$$

where $C_{\mathcal{M}}$ is a constant that does not depend on z. Now,

$$\widetilde{\mathcal{M}}_l - \widetilde{\mathcal{M}}_0 = -\mathcal{A}_l - 2\nu(\Pi_l - \Pi_0). \tag{4.40}$$

From Lemma 4.1 and the expression of Π_l in (4.33), we know that the right hand side of (4.40) has C^1 dependence on l. Therefore, for sufficiently small l, the difference $\widetilde{\mathcal{M}}_l - \widetilde{\mathcal{M}}_0$ is small, and by a Neumann series argument similar to the one used in the proof of Proposition 2.3, we see that

$$\Sigma\left(\widetilde{\mathcal{M}}_l\right) \subset \{z \in \mathbb{C} | \mathrm{Re} z < -3\nu/4\}. \tag{4.41}$$

Together with (4.35), this implies that

$$(\Sigma(\mathcal{M}_l)\backslash\{\mu_l\}) \subset \{z \in \mathbb{C} | \mathrm{Re} z < -3\nu/4\}. \tag{4.42}$$

By (3.4),

$$(\Sigma(\mathcal{P}_l)\backslash\{\lambda_l\}) \subset \{z \in \mathbb{C} | \mathrm{Re} z < -\nu/2\}, \tag{4.43}$$

for sufficiently small l. Taking l even smaller if necessary, we can make λ_l be the right-most point of the spectrum of $\mathcal{P}_l$. This completes the proof of item 1.

Step 4. Let us now compute the derivative of μ_l and w_l with respect to l at $l = 0$. We may take the derivative of (4.14) in l and let $l = 0$ to find:

$$\mathcal{P}_0\left(\partial_l w_l\right)|_{l=0} = \partial_l \mu_l|_{l=0}\, v_0,\ \langle \partial_l w_l|_{l=0}, v_0^* \rangle = 0, \tag{4.44}$$

where ∂_l denotes derivatives in l. This equation (not surprisingly) is identical to (4.24), and therefore,

$$\partial_l \mu_l|_{l=0} = 0,\ \partial_l w_l|_{l=0} = 0. \tag{4.45}$$

We now show that the second derivatives of μ_l and w_l exist at $l = 0$. To do so, take the derivative of (4.14) with respect to l.

$$\mathcal{P}_0 \partial_l w_l - \partial_l \mathcal{A}_l w_l - \mathcal{A}_l \partial_l w_l = \partial_l \mu_l w_l + \mu_l \partial_l w_l, \ \langle \partial_l w_l, v_0^* \rangle = 0. \tag{4.46}$$

Take the inner product of the above operator equation with v_0^*. Noting that the range of $\mathcal{P}_0$ is orthogonal to v_0^* and the above orthogonality relation, we have:

$$-\langle \partial_l \mathcal{A}_l w_l + \mathcal{A}_l \partial_l w_l, v_0^* \rangle = \partial_l \mu_l \langle v_0, v_0^* \rangle . \tag{4.47}$$

where we used (4.14). Let us estimate the magnitude of the left hand side of the above. First, note that

$$\begin{aligned} &\langle \partial_l \mathcal{A}_l w_l + \mathcal{A}_l \partial_l w_l, v_0^* \rangle \\ =& \langle \partial_l \mathcal{A}_l (w_l - v_0), v_0^* \rangle + \langle \partial_l \mathcal{A}_l v_0, v_0^* \rangle + \langle \mathcal{A}_l \partial_l w_l, v_0^* \rangle \end{aligned} \tag{4.48}$$

We estimate each term in turn. For the first term, we have:

$$\begin{aligned} &|\langle \partial_l \mathcal{A}_l (w_l - v_0), v_0^* \rangle| \leq \|\partial_l \mathcal{A}_l\|_{\mathcal{L}(L^2(\mathbb{R}))} \|w_l - v_0\|_{L^2(\mathbb{R})} \|v_0^*\|_{L^2(\mathbb{R})} \\ \leq& C_{\mathcal{A}}^1 |l| \|w_l - v_0\|_{L^2(\mathbb{R})} \|v_0^*\|_{L^2(\mathbb{R})} \leq C_1 |l|^2 \end{aligned} \tag{4.49}$$

where C_1 is a constant that does not depend on l. In the above, we used (4.3) of Lemma 4.1 in the second inequality and the fact that w_l is C^1 in the last inequality. For the second term in (4.48), we have

$$|\langle \partial_l \mathcal{A}_l v_0, v_0^* \rangle| \leq C_{\mathcal{A}}^{\infty} \|v_0\|_{L^1(\mathbb{R})} \|v_0^*\|_{L^1(\mathbb{R})} l^2 \tag{4.50}$$

where we used (4.5) with $m = 1$ and the fact that v_0 and v_0^* are in $L^1(\mathbb{R}) \cap L^2(\mathbb{R})$. For the last term in (4.48), we have

$$\begin{aligned} &|\langle \mathcal{A}_l \partial w_l, v_0^* \rangle| \leq \|\mathcal{A}_l\|_{L^2(\mathbb{R})} \|\partial_l w_l\|_{L^2(\mathbb{R})} \|v_0^*\|_{L^2(\mathbb{R})} \\ \leq& C_{\mathcal{A}}^1 l^2 \|\partial_l w_l\|_{L^2(\mathbb{R})} \|v_0^*\|_{L^2(\mathbb{R})} \leq C_2 |l|^2 \end{aligned} \tag{4.51}$$

where C_2 is a constant that does not depend on l. In the above, we used (4.3) with $m = 0$ in Lemma 4.1 in the second inequality and the fact that w_l is C^1 in the third equality. Combining (4.49), (4.50), (4.51), (4.48) together with (4.47), we have:

$$|\partial_l \mu_l| \leq C_\mu |l|^2 \tag{4.52}$$

where C_μ is a constant that does not depend on l. Let us compute the second derivative of μ_l at $l = 0$.

$$\lim_{l \to 0} l^{-1} (\partial_l \mu_l - \partial_l \mu_l|_{l=0}) = \lim_{l \to 0} l^{-1} \partial_l \mu_l = 0 \tag{4.53}$$

where we used (4.45) in the first equality and (4.52) in the second equality. The second derivative thus exists at $l = 0$ and it evaluates to 0. We also conclude from (4.52) and the fact that $\mu_0 = 0$ that

$$|\mu_l| \leq \frac{C_\mu}{3} |l|^3 . \tag{4.54}$$

Combining this with (4.16), we obtain (4.19) of item 2 without the $\mathcal{O}(|l|^3)$ correction.

Step 5. To prove that the second derivative of w_l exists, we return to (4.46):

$$\mathcal{P}_0\partial_l w_l = \partial_l \mathcal{A}_l w_l + \mathcal{A}_l \partial_l w_l + \partial_l \mu_l w_l + \mu_l \partial_l w_l,\ \langle \partial_l w_l, v_0^* \rangle = 0. \tag{4.55}$$

Let us estimate the right hand side of the first equality. We have

$$\begin{aligned} &\|\partial_l \mathcal{A}_l w_l + \mathcal{A}_l \partial_l w_l\|_{L^2(\mathbb{R})} \\ \leq &\|\partial_l \mathcal{A}_l v_0\|_{L^2(\mathbb{R})} + \|\partial A_l (w_l - v_0)\|_{L^2(\mathbb{R})} + \|\mathcal{A}_l \partial_l w_l\|_{L^2(\mathbb{R})} \\ \leq &C_{\mathcal{A}}^2 \|v_0\|_{L^1(\mathbb{R})} |l|^{3/2} + C_{\mathcal{A}}^1 \|w_l - v_0\|_{L^2(\mathbb{R})} |l| + C_{\mathcal{A}}^1 \|\partial_l w_l\|_{L^2(\mathbb{R})} l^2 \\ \leq &C_3 |l|^{3/2} \end{aligned} \tag{4.56}$$

where C_3 is a constant independent of l. We used (4.4) and (4.3) of Lemma 4.1 in the second inequality and the C^1 dependence of w_l with respect to l in the last inequality. We also have

$$\begin{aligned} &\|\partial_l \mu_l w_l + \mu_l \partial_l w_l\|_{L^2(\mathbb{R})} \leq \|\partial_l \mu_l w_l\|_{L^2(\mathbb{R})} + \|\mu_l \partial_l w_l\|_{L^2(\mathbb{R})} \\ \leq &C_\mu l^2 \|w_l\|_{L^2(\mathbb{R})} + \frac{C_\mu}{3} |l|^3 \|\partial_l w_l\|_{L^2(\mathbb{R})} \leq C_4 |l|^2 \end{aligned} \tag{4.57}$$

where C_4 is a constant independent of l, and we used (4.52) and (4.54) in the second inequality, and the fact that w_l is C^1 with respect to l in the last inequality. With these estimates, we see that (4.55) is of the form:

$$\mathcal{P}_0\partial_l w_l = r_l,\ \|r_l\|_{L^2(\mathbb{R})} \leq C_r |l|^{3/2},\ \langle \partial_l w_l, v_0^* \rangle = 0. \tag{4.58}$$

Now, apply the projection operator Π_0 (see (4.33)) on both sides of the above, noting that $\partial_l w_l \in R_0$. We have

$$\mathcal{P}_0|_{R_0}\, \partial_l w_l = \Pi_0 r_l. \tag{4.59}$$

The operator $\mathcal{P}_0|_{R_0}$ is invertible as an operator from $H^2(\mathbb{R}) \cap R_0$ to R_0. We thus obtain the following estimate:

$$\|\partial_l w_l\|_{H^2(\mathbb{R})} \leq \frac{5}{2} C_v |l|^{3/2} \tag{4.60}$$

where C_v is a constant independent of l. From this, we see that

$$\lim_{l\to 0} \left\| l^{-1} \left(\partial_l w_l - \partial_l w_l|_{l=0}\right) \right\|_{H^2(\mathbb{R})} = \lim_{l\to 0} l^{-1} \|\partial_l w_l\|_{H^2(\mathbb{R})} = 0. \tag{4.61}$$

The second derivative of w_l at $l = 0$ therefore exists and:

$$\partial_l^2 w_l = 0. \tag{4.62}$$

Furthermore, using (4.60) and noting that $w_0 = v_0$, we have

$$\|w_l - v_0\|_{H^2(\mathbb{R})} \leq C_v |l|^{5/2}. \tag{4.63}$$

This, together with (4.16), implies (4.21) in item 3.
Step 6. To show that μ_l and w_l are C^2, we have only to show that the second derivative is continuous at $l = 0$. Indeed, as we remarked toward the end of Step 1 of this proof, μ_l and w_l depend smoothly on l for $l \neq 0$. Let us take two derivatives of (4.14) with respect to l for $l \neq 0$.

$$\widehat{\mathcal{M}}_l \partial_l^2 w_l = 2\partial_l(\mathcal{A}_l + \mu_l)\partial_l w_l + \partial_l^2(\mathcal{A}_l + \mu_l)w_l,\ \left\langle \partial_l^2 w_l, v_0^* \right\rangle = 0. \tag{4.64}$$

Taking the inner product of both sides with respect to w_l^* and noting that w_l^* is in N_l, the null space of $\widehat{\mathcal{M}}_l^*$, we have

$$\langle w_l, w_l^* \rangle\, \partial_l^2 \mu_l = -2\left\langle \partial_l(\mathcal{A}_l + \mu_l)\partial_l w_l, w_l^* \right\rangle - \left\langle \partial_l^2 \mathcal{A}_l w_l, w_l^* \right\rangle. \tag{4.65}$$

Much in the same fashion as before, we may estimate the right hand side of the above using Lemma 4.1 and the C^1 dependence of w_l and w_l^* with respect to l. We see that

$$2\left|\langle \partial_l(\mathcal{A}_l + \mu_l)\partial_l w_l, w_l^* \rangle\right| + \left|\left\langle \partial_l^2 \mathcal{A}_l w_l, w_l^* \right\rangle\right| \leq C_3 |l| \tag{4.66}$$

where C_3 is independent of l. Noting that $\langle w_l, w_l^* \rangle$ is continuous in l and positive at $l = 0$, we conclude that:

$$\left|\partial_l^2 \mu_l\right| \leq C_4 |l|,\ l \neq 0 \tag{4.67}$$

for a constant independent of l. Given (4.62), we see that μ_l and hence λ_l is a C^2 function of l. This is the first assertion in item 2.
Step 7. Now, we show that w_l is a C^2 function of l. To do so, we return to (4.64). Let us first estimate the $L^2(\mathbb{R})$ norm of the right hand side of (4.64). Proceeding as before, using the estimates of Lemma 4.1 and our estimates for the derivatives of μ_l, (4.52) and (4.67), we have

$$\left\|2\partial_l(\mathcal{A}_l + \mu_l)\partial_l w_l + \partial_l^2(\mathcal{A}_l + \mu_l)w_l\right\|_{L^2(\mathbb{R})} \leq C_5 |l|^{1/2} \tag{4.68}$$

for a constant C_5 independent of l. Now, let us apply the projection operator $I - \Pi_l$ to both sides of (4.64). We have

$$\widehat{\mathcal{M}}_l\Big|_{R_l}((I - \Pi_l)\partial_l^2 w_l) = (I - \Pi_l)r_l,\ \|r_l\|_{L^2(\mathbb{R})} \leq C_5 |l|^{1/2}. \tag{4.69}$$

As we saw in the discussion following equation (4.34), the action of $\widehat{\mathcal{M}}_l$ on R_l is the same as $\widetilde{M}_l - \mu_l$ on R_l. We thus have

$$(\widetilde{\mathcal{M}}_l - \mu_l)((I - \Pi_l)\partial_l^2 w_l) = (I - \Pi_l)r_l. \tag{4.70}$$

Using the resolvent estimate (4.39) and the fact that $\widetilde{\mathcal{M}}_0$ maps $H^2(\mathbb{R})$ onto $L^2(\mathbb{R})$, we may use a Neumann series argument to conclude that

$$\left\|(I - \Pi_l)\partial_l^2 w_l\right\|_{H^2(\mathbb{R})} \leq C_6 \|(I - \Pi_l)r_l\| \leq C_7 |l|^{1/2} \tag{4.71}$$

for sufficiently small l, where C_6 and C_7 are constants independent of l. In the second inequality, we used the estimate of r_l in (4.69) and the fact that Π_l is a bounded operator on $L^2(\mathbb{R})$. Now, note by (4.64) that $\partial_l^2 w_l \in R_0$. The restriction of $I - \Pi_l$ to R_0 is invertible as an operator from R_0 to R_l. To see this, introduce the operator:

$$\widetilde{\Pi}_l w = \frac{\langle w, v_0^* \rangle}{\langle w_l, v_0^* \rangle} w_l. \tag{4.72}$$

Note that this operator is well defined so long as l is close to 0 since $\langle v_0, v_0^* \rangle \neq 0$ and w_l is continuous in l. It is easily seen that:

$$(I - \Pi_l)|_{R_0} = \mathcal{B}_l|_{R_0}\,,\ \mathcal{B}_l = I - \Pi_l(\Pi_l - \widetilde{\Pi}_l). \tag{4.73}$$

The operator $\mathcal{B}_l$ is clearly invertible for l small on $L^2(\mathbb{R})$, given continuity of $\mathcal{B}_l$ with respect to l and the fact that $\mathcal{B}_0 = I$. Furthermore, for small enough l, the norm of the inverse of $\mathcal{B}_l$ is bounded independent of l. Combining this with (4.71), we have:

$$\left\|\partial_l^2 w_l\right\|_{L^2(\mathbb{R})} \leq C_8 \left|l\right|^{1/2}. \tag{4.74}$$

Note here that the above bound $\partial_l^2 w_l$ on in the $L^2(\mathbb{R})$ norm and not in the $H^2(\mathbb{R})$ norm, since we only used the boundedness $\mathcal{B}_l^{-1}$ as an operator on $L^2(\mathbb{R})$. To obtain a similar bound in $H^2(\mathbb{R})$, we use the decomposition:

$$\partial_l^2 w_l = (I - \Pi_l)\partial_l^2 w_l + \Pi_l \partial_l^2 w_l. \tag{4.75}$$

Note that

$$\left\|\Pi_l \partial_l^2 w_l\right\|_{H^2(\mathbb{R})} = \frac{\left|\langle \partial_l^2 w_l, w_l^* \rangle\right|}{\langle w_l, w_l^* \rangle} \left\|w_l\right\|_{H^2(\mathbb{R})} \leq C_9 \left|l\right|^{1/2} \tag{4.76}$$

where C_9 is a constant independent of l. In the above, we used the L^2 estimate in (4.74) and the continuity of w_l and w_l^* with respect to l. Using (4.75), (4.71) and (4.76), we have:

$$\left\|\partial_l^2 w_l\right\|_{H^2(\mathbb{R})} \leq (C_7 + C_9)\left|l\right|^{1/2} = C_{10}\left|l\right|^{1/2}. \tag{4.77}$$

With (4.62), this shows that w_l is C^2 for l small. The C^2 dependence of w_l with respect to l, together with (4.16) implies the same for the function $v_l \exp(-i\alpha_1 l\xi)$. This is the last assertion in item 3. Together with the result from Step 5, this concludes the proof of item 3.

Step 8. We finally turn to the determination of the $\mathcal{O}(l^3)$ terms in the expansion of λ_l in (4.19). Take the inner product of (4.14) with respect to v_0^*. We have:

$$\mu_l = -\frac{\langle \mathcal{A}_l w_l, v_0^* \rangle}{\langle w_l, v_0^* \rangle}. \tag{4.78}$$

It is easily seen, from the estimates of Lemma 4.1 and the foregoing estimates on w_l that

$$\mu_l = -\frac{\langle \mathcal{A}_l v_0, v_0^* \rangle}{\langle v_0, v_0^* \rangle} + \mathcal{O}(l^5). \tag{4.79}$$

Consider:

$$|l|^{-3}\,\frac{\langle \mathcal{A}_l v_0, v_0^*\rangle}{\langle v_0, v_0^*\rangle} = -\frac{\langle K_1(l\xi)\star v_0, v_0^*\rangle}{\langle v_0, v_0^*\rangle}. \tag{4.80}$$

Now,

$$\langle K_1(l\xi)\star v_0, v_0^*\rangle = \int_{\mathbb{R}}\int_{\mathbb{R}} K_1(l(\xi-\xi'))v_0(\xi')v_0^*(\xi)d\xi' d\xi. \tag{4.81}$$

Since

$$|K_1(l(\xi-\xi'))v_0(\xi')v_0^*(\xi)| \le \frac{1}{2}\left(\frac{|\beta_0|}{\gamma_0}+|\beta_1|\right)|v_0(\xi')|\,|v_0^*(\xi)| \tag{4.82}$$

and v_0 and v_0^* are integrable, by the Lebesgues dominated convergence theorem, we have:

$$\lim_{l\to 0\pm}\langle K_1(l\xi)\star v_0, v_0^*\rangle = \left\langle K_0^{\pm}\star v_0, v_0^*\right\rangle,\ K_0^{\pm}(\xi) = \frac{1}{2}\left(\frac{\beta_0}{\gamma_0}\pm i\beta_1 \mathrm{sign}(\xi)\right). \tag{4.83}$$

The above, together with (4.80), yields the $\mathcal{O}(l^3)$ expressions in (4.19) of item 2 by noting that:

$$v_0(\xi) = \frac{1}{K}\widehat{v}_0\left(\frac{\xi}{K}\right). \tag{4.84}$$

To show that the error terms are $\mathcal{O}(l^4)$, we consider the difference:

$$\frac{\langle \mathcal{A}_l v_0, v_0^*\rangle - |l|^3\left\langle K_0^{\pm}\star v_0, v_0^*\right\rangle}{\langle v_0, v_0^*\rangle}. \tag{4.85}$$

For $l>0$, we have:

$$|l|^{-3}\langle \mathcal{A}_l v_0, v_0^*\rangle - \left\langle K_0^{+}\star v_0, v_0^*\right\rangle = \left\langle (K_1(l\xi)-K_0^{+}(\xi))\star v_0, v_0^*\right\rangle. \tag{4.86}$$

It is easily seen that:

$$\left|K_1(l\xi)-K_0^{+}(\xi)\right| \le C_{11}\,|l\xi| \tag{4.87}$$

where C_{11} is a constant that depends only on the constants that appear in the definition of K_1 in (4.1). We thus have:

$$\left|\left\langle (K_1(l\xi)-K_0^{+}(\xi))\star v_0, v_0^*\right\rangle\right| \le C_{11}\,|l|\int_{\mathbb{R}}\int_{\mathbb{R}}|\xi-\xi'|\,|v_0(\xi)|\,|v_0^*(\xi')|\,d\xi' d\xi. \tag{4.88}$$

The above integral is convergent, given the exponential decay of v_0 and v_0^* as $|\xi|\to\infty$ (see items 2 and 3 of Proposition 3.1). This shows that the error term is $\mathcal{O}(l^4)$ when $l>0$. The proof for $l<0$ can be obtained by replacing K_0^+ in the above with K_0^-. This concludes the proof of item 2. □

The interest in writing the third order term in (4.19) using $\widehat{v}_0$ and $\widehat{v}_0^*$ (instead of v_0 and v_0^*) is that $\widehat{v}_0$ and $\widehat{v}_0^*$ depend on f only. The third order coefficients $\rho_{\mathrm{r,i}}$ are thus written as a product of coefficients that come from the electrical conductivities and a constant that depends only on the nonlinearity f.

A salient feature of the above result is that front stability at long wavelengths is almost completely determined by the sign of α_0 and does not depend on the choice of bistable nonlinearity f.

Corollary 4.3. *The planar front is spectrally unstable if*

$$\alpha_0 < 0. \tag{4.89}$$

When $\alpha_0 > 0$, the planar front is spectrally stable under long-wavelength perturbations in the following sense: $\Sigma(\mathcal{P}_l), l \neq 0$ lies entirely in the left half of the complex plane for sufficiently small $|l|$.

Proof. The instability result is immediate from the above theorem and the definition of spectral instability in Definition 2.1. The long-wavelength stability result follows directly from (4.18) of the above Theorem. □

Note that the the above long-wavelength stability result is consistent with (3.23), a sufficient condition for front stability. Given that the right hand side of (3.23) is non-negative (see (3.25)), (3.23) implies $\alpha_0 > 0$ and hence stability at long wavelengths. It is possible to handle the borderline case of $\alpha_0 = 0$ by noting that the sign of β_0 would then determine stability at long wavelengths.

When $\alpha_0 < 0$, expression (4.21) gives us the approximate shape of the growing perturbation:

$$-\frac{\partial u_{\mathrm{f}}}{\partial \xi} \exp(il(\alpha_1(\xi + ct) + \eta) - \alpha_0 l^2 t). \tag{4.90}$$

It has the form of a traveling wave (if $\alpha_1 c \neq 0$), localized near the front, growing at a rate of $-\alpha_0 l^2$ with time.

The sign of α_0 has the following graphical interpretation. Another closely related interpretation, based on energy, is discussed in Appendix A. Define the *Frank plot* as follows [19, 6]:

$$\mathscr{F} = \{(\cos\theta, \sin(\theta))/K(\theta),\ 0 \leq 0 < 2\pi\} \tag{4.91}$$

where $K(\theta) = \sqrt{Q(\mathbf{n})}$ as defined in (2.12). The quantity $K(\theta)$ has a dual interpretation as the speed of the planar front (see (2.12)) and as the energy associated with the front [19]. This latter point of view and its relation to the stability condition (4.89) is given in Appendix A. An equivalent definition of the Frank plot is

$$\mathscr{F} = \{(k, l) \in \mathbb{R}^2 | Q(k, l) = 1\}. \tag{4.92}$$

Examples of Frank plots when A_{i} and A_{e} are as in (2.7) are shown in Figure 2. The region enclosed by the Frank plot is called the *Frank diagram*. We say that the Frank plot $\mathscr{F}$ is convex if its corresponding Frank diagram is convex. The following relates the sign of α_0 to the shape of the Frank plot.

Proposition 4.4. *Let P_θ be the point $(\cos\theta, \sin(\theta))/K(\theta)$ on $\mathscr{F}$. The curvature of $\mathscr{F}_K$ at P_θ is given by:*

$$\kappa(\theta) = \frac{\alpha_0}{K(1 + \alpha_1^2)^{3/2}}. \tag{4.93}$$

In particular, the sign of κ and α_0 coincide.

In the definition of curvature κ above, we have taken the unit circle $(\cos\theta, \sin\theta)$ to have positive curvature. The above result states that the sign of α_0 is equivalent to a local convexity condition. If α_0, and hence κ, is positive everywhere, the Frank diagram is convex. If α_0 is negative somewhere, the Frank diagram is non-convex.

Proof of Proposition 4.4. Rotate the curve $\mathscr{F}$ by $-\theta$ degrees about the origin to obtain the curve $\mathscr{F}_\theta$:

$$\mathscr{F}_\theta = \{(k,l) \in \mathbb{R}^2 | Q_\theta(k,l) = 1\} \tag{4.94}$$

We have only to compute the curvature of $\mathscr{F}_\theta$ at the intersection point of $\mathscr{F}_\theta$ with the positive $k-$axis. Near this point, the curve C_θ may be expressed as $k = g(l)$. Plugging this into (4.94), we obtain:

$$Q_\theta(g(l), l) = 1, \ g(0) = \frac{1}{K}. \tag{4.95}$$

We may compute the first and second derivatives of g with respect to l.

$$\left.\frac{dg}{dl}\right|_{l=0} = -\left(\frac{\partial Q_\theta}{\partial k}\right)^{-1}\left(\frac{\partial Q_\theta}{\partial l}\right)\Bigg|_{k=1/K, l=0} = \alpha_1. \tag{4.96}$$

where we used (2.17).

$$\begin{aligned}\left.\frac{d^2 g}{dl^2}\right|_{l=0} &= -\left(\frac{\partial Q_\theta}{\partial k}\right)^{-1}\left(\frac{\partial^2 Q_\theta}{\partial k^2}\left(\frac{dg}{dl}\right)^2 + 2\frac{\partial^2 Q_\theta}{\partial k \partial l}\frac{dg}{dl} + \frac{\partial^2 Q_\theta}{\partial l^2}\right)\Bigg|_{k=1/K, l=0} \\ &= -\frac{1}{K}p(\alpha_1) = -\frac{\alpha_0}{K},\end{aligned} \tag{4.97}$$

where we used (2.17) and (4.96) in the first equality and (2.17) in the second. Equation (4.93) follows from (4.97), (4.96) and the well-known formula for the curvature of a graph. □

Let us now apply the above criterion to when the conductivity matrices are given by (2.7).

Proposition 4.5. *The planar front is spectrally unstable if*

$$\alpha_0(a, b, \theta) < 0 \tag{4.98}$$

where α_0 is given in (2.20)*. When $b = 0$, this condition reduces to*

$$|a| > \frac{1}{2} \text{ and } |\cos(2\theta)| < \frac{1}{|a|}\sqrt{1 - \frac{2}{\sqrt{3}}\sqrt{1-a^2}}. \tag{4.99}$$

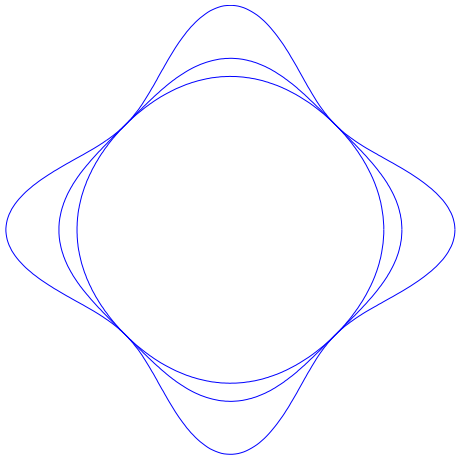

Figure 2: The Frank diagrams when A_i and A_e are as in (2.7) and $b = 0$, $a = 0.7, 0.5$ and 0.3. The outer-most curve corresponds to $a = 0.7$, and the inner-most curve to $a = 0.3$. $a = 0.5$ is the threshold value below which the Frank diagram is convex. The directions for which the Frank diagram is non-convex correspond to the directions $\alpha_0 < 0$.

Proof. By (4.89) of Corollary 4.3, $\alpha_0 < 0$ implies instability. Using the expression for α_0 in (2.20) with $b = 0$, we obtain the condition:

$$g(\rho) = 3a^4\rho^2 - 6a^2\rho + 4a^2 - 1 > 0, \ \rho = \cos^2(2\theta). \tag{4.100}$$

Thus,

$$\rho < \rho_- \text{ or } \rho > \rho_+, \text{ where } \rho_\pm = \frac{1}{a^2}\left(1 \pm \frac{2}{\sqrt{3}}\sqrt{1-a^2}\right). \tag{4.101}$$

Note that, given $|a| < 1$, the roots $\rho_\pm$ are real and $\rho_+ > 1$. Combining the above with $0 \le \rho = \left|\cos^2(2\theta)\right| \le 1$, we obtain the condition $0 \le \rho < \rho_-$. The root ρ_- is positive if and only if $|a| > 1/2$, and we obtain (4.99). □

In addition to (4.99), we can obtain an instability condition in the borderline case of $\alpha_0 = 0$ by looking at the sign of β_0. This follows from the remark immediately following the proof of Corollary 4.3.

Let $b = 0$. Condition (4.99) says that there always is an unstable direction if $|a| > 1/2$ (see Figure 1). As we saw in Proposition 4.4, the sign condition on α_0 is equivalent to local convexity of the Frank plot. The Frank plot becomes non-convex when $a > 1/2$, and planar fronts traveling in a direction in which the Frank plot is non-convex are unstable (see Figure 2). It is not difficult to see that the right hand side of (4.99) is a an increasing function of $|a|$ and that it reaches 1 as $|a| \nearrow 1$. Thus as $|a|$ increases, the unstable directions span an ever greater sector, and as $|a|$ approaches 1, directions close to $\theta = 0$ (or $\pi/2$) are the only angles that are not unstable under long wavelength perturbations.

Let us combine the above instability results with the stability results of Proposition 3.4. When the planar front speed c is equal to 0, then $M_f = 1$. In this case, expression (3.29) takes a particularly simple form:

$$|a| < \frac{1}{2} \text{ or } |\cos(2\theta)| > \frac{1}{|a|}\sqrt{2\,|a| - 1}. \tag{4.102}$$

The right hand side of the above cosine inequality never attains 1 and therefore, the planar front in the $\theta = 0$ direction is always stable. The above states that if $|a| < 1/2$, waves in all directions are stable. We know from (4.99) that, for $|a| > 1/2$, there is an unstable direction. Thus, for $c = 0$, $|a| = 1/2$ is the threshold value below which planar waves in all directions are stable. When $c \neq 0$, we can only say that this threshold value lies between $|a| = 1/\sqrt{2(M_f + 1)}$ and $|a| = 1/2$.

5 Stability at Intermediate Wavelengths

Let us summarize what we have found so far about the stability of planar fronts. By (3.23), if $\alpha_0 > M_f q_\Delta - \overline{q}$, the front is spectrally stable. If $\alpha_0 < 0$, the front is spectrally unstable. When

$$0 \le \alpha_0 \le M_f q_\Delta - \overline{q} \tag{5.1}$$

front stability cannot be determined with our estimates (note that $M_f q_\Delta - \overline{q} \geq 0$, as we saw in (3.25)). When the conductivity matrices are given by (2.7) and $b = 0$, the parameter region satisfying this condition can be seen graphically in Figure 1. Equation (2.42) and Corollary 4.3 shows that instabilities cannot arise at short or long wavelengths when α_0 is in the range (5.1). We cannot, however, rule out the possibility of an instability at intermediate wavelengths. We shall now see that this is indeed possible.

Unlike the case of long-wavelength perturbations studied in the previous section, instabilities in the intermediate-wavelength regime depends on the nonlinearity f. This is already suggested by the expression for $\mathrm{Re}\lambda_l$ in (4.19). Indeed, the leading order term $\alpha_0 l^2$ does not depend on f, but the next term, $-\rho_{\mathrm{r}} |l|^3$ depends on $\widehat{v_0}$ and $\widehat{v_0}^*$ which in turn depend on the nonlinearity f. Here we focus on a particular class of bistable nonlinearities.

Consider the following family of nonlinearities:

$$\begin{aligned} &f_\epsilon(u) = -u + H_\epsilon(u - \alpha),\ 0 < \alpha \leq 1/2, \\ &H_\epsilon(x) = \int_{-\infty}^{x} j_\epsilon(s)ds,\ j_\epsilon(x) = \epsilon^{-1} j_1(x/\epsilon),\ 0 < \epsilon < \alpha, \end{aligned} \tag{5.2}$$

where $j_1(x)$ is a smooth positive function, supported on $|x| \leq 1$ with integral equal to 1. It is easily checked that f_ϵ satisfies the properties of the nonlinearity f listed below (1.4). The above should be seen as a regularization of the following McKean model [22]:

$$f_0(u) = \begin{cases} -u & \text{if } u < \alpha, \\ 1 - u & \text{if } \alpha \leq u. \end{cases} \tag{5.3}$$

We may obtain (5.3) above by taking $\epsilon \to 0$ in (5.2).

Let $u_{\mathrm{f}}(\xi, \epsilon, \theta)$ and $c(\epsilon, \theta)$ be the front solution and its speed satisfying:

$$\begin{aligned} &c\frac{\partial u_{\mathrm{f}}^\epsilon}{\partial \xi} + K^2 \frac{\partial^2 u_{\mathrm{f}}^\epsilon}{\partial \xi^2} + f_\epsilon(u_{\mathrm{f}}^\epsilon) = 0, \\ &\lim_{\xi \to \infty} u_{\mathrm{f}}^\epsilon(\xi) = 0,\ \lim_{\xi \to -\infty} u_{\mathrm{f}}^\epsilon(\xi) = 1,\ u_{\mathrm{f}}^\epsilon(0) = \alpha, \end{aligned} \tag{5.4}$$

where $0 \leq \epsilon < \alpha$. We let $u_{\mathrm{f}*}^\epsilon(\xi)$ and $c_*(\epsilon)$ be the front solution and speed when K is set to 1 in the above. We thus have:

$$u_{\mathrm{f}}(\xi, \epsilon, \theta) = u_{\mathrm{f}*}^\epsilon(\xi/K),\ c(\epsilon, \theta) = K c_*(\epsilon). \tag{5.5}$$

It is well-known that, for each ϵ, $c_*(\epsilon)$ and $u_{\mathrm{f}*}^\epsilon$ are uniquely determined.

Our goal is to prove the following result. First, recall that the coefficients $K, \alpha_i, \beta_i, \gamma_i, i = 0, 1$ in (2.17) are periodic smooth functions of $\theta \in \mathbb{S}^1 = \mathbb{R}/(2\pi\mathbb{Z})$ for fixed A_{i} and A_{e}. Given any bistable nonlinearity, there is a planar front solution in each direction $\theta \in \mathbb{S}^1$.

Theorem 5.1. *For fixed A_{i} and A_{e}, consider all planar front solutions (labeled by $\theta \in \mathbb{S}^1$) with nonlinearity f_ϵ given in* (5.2)*. Take any $\nu > 0$ and take $\alpha > 0$*

sufficiently small in (5.2). *Then, for sufficiently small* $\epsilon > 0$, *planar fronts in all directions* θ *satisfying*

$$\beta_0(\theta) < -\nu \tag{5.6}$$

are spectrally unstable. The function β_0 *was given in* (2.17).

An immediate corollary is that, for any direction satisfying $\beta_0(\theta) < 0$, the front can be destabilized by taking a suitable bistable nonlinearity of the form (5.2).

As a first step toward proving this result, we examine the stability of front solutions to the McKean model (5.3). For (5.3), the traveling front solution $u_{\rm f}$ and its speed c can be computed explicitly and are given by:

$$\begin{aligned} &c = c_*(0)K,\ c_*(0) = \frac{1-2\alpha}{\sqrt{\alpha(1-\alpha)}}, \\ &u_{\rm f} = u^0_{{\rm f}*}(\xi/K),\ u^0_{{\rm f}*}(\xi) = \begin{cases} 1-(1-\alpha)\exp\left(\sqrt{\frac{\alpha}{1-\alpha}}\xi\right) & \text{if } \xi < 0 \\ \alpha\exp\left(-\sqrt{\frac{1-\alpha}{\alpha}}\xi\right) & \text{if } \xi \geq 0 \end{cases}. \end{aligned} \tag{5.7}$$

The linearization of the bidomain equation around this traveling front solution is given by:

$$\frac{\partial v}{\partial t} = c\frac{\partial v}{\partial \xi} - \mathcal{L}v - v + \frac{Kv(0)}{\sqrt{\alpha(1-\alpha)}}\delta(\xi), \tag{5.8}$$

where δ is the Dirac delta function in the ξ direction only (but not in the η direction). The Fourier decomposition of the above linear operator, as in (2.23), is given by:

$$\mathcal{P}_l v = c\frac{\partial v}{\partial \xi} - \mathcal{L}_l v - v + \frac{Kv(0)}{\sqrt{\alpha(1-\alpha)}}\delta(\xi). \tag{5.9}$$

Let us view $\mathcal{P}_l$ as a closed operator defined on $H^{-1}(\mathbb{R})$. We define the $H^{-1}(\mathbb{R})$ norm to be

$$\|u\|^2_{H^{-1}(\mathbb{R})} = \int_{\mathbb{R}} |\widehat{u}(k)|^2 (1+k^2)^{-1} dk \tag{5.10}$$

where $\widehat{u}$ is the Fourier transform of u. It is easily checked that the domain of $\mathcal{P}_l$ is $H^1(\mathbb{R})$. Suppose $\lambda \in \mathbb{C}$ belong to the point spectrum of $\mathcal{P}_l$. Then,

$$\lambda v = c\frac{\partial v}{\partial \xi} - \mathcal{L}_l v - v + \frac{Kv(0)}{\sqrt{\alpha(1-\alpha)}}\delta(\xi). \tag{5.11}$$

Taking the Fourier transform on both sides, we have:

$$\lambda\widehat{v}(k) = (ick - Q_\theta(k,l) - 1)\widehat{v}(k) + \frac{K}{2\pi\sqrt{\alpha(1-\alpha)}}\int_{\mathbb{R}} \widehat{v}(k')dk'. \tag{5.12}$$

where $\widehat{v}$ is the Fourier transform of v. The condition $v \in H^1(\mathbb{R})$ is equivalent to the condition that $\widehat{v}(k)$ be in $\mathcal{H}^1$ where

$$\mathcal{H}^1 = \{\widehat{v} \in L^1_{\rm loc}(\mathbb{R}) |\ \|\widehat{v}\|^2_{\mathcal{H}^1} = \int_{\mathbb{R}} |\widehat{v}(k)|^2 (1+|k|^2)dk < \infty\}, \tag{5.13}$$

where $L^1_{\mathrm{loc}}(\mathbb{R})$ is the space of locally integrable functions. Note that $\widehat{v} \in \mathcal{H}^1$ implies that $\widehat{v}$ is integrable and the integral in (5.12) well-defined. Suppose the integral in (5.12) is 0. Then, $\widehat{v}(k)$ is equal to 0 almost everywhere, and given that $\widehat{v} \in \mathcal{H}^1$, $\widehat{v}(k) = 0$. Since we are interested in non-zero functions satisfying (5.12), we have

$$\int_{\mathbb{R}} \widehat{v}(k)dk \neq 0. \tag{5.14}$$

This is equivalent to the condition that $v(0) \neq 0$. Let us normalize v (and hence $\widehat{v}$) so that

$$v(0) = 1, \text{ or equivalently, } \frac{1}{2\pi}\int_{\mathbb{R}} \widehat{v}(k)dk = 1. \tag{5.15}$$

Solving (5.12) for $\widehat{v}$, we have:

$$\widehat{v}(k) = \frac{K}{\sqrt{\alpha(1-\alpha)}(\lambda + 1 - ic_0k + Q_\theta(k,l))} \tag{5.16}$$

The right hand side of the above equality belongs to $\mathcal{H}^1$ if and only if the denominator never vanishes for $k \in \mathbb{R}$. Integrating both sides of (5.16) with respect to k and using (5.15), we obtain the following compatibility condition:

$$I(\lambda, \alpha, l, \theta) \equiv \frac{K}{\sqrt{\alpha(1-\alpha)}}\int_{\mathbb{R}} \frac{dk}{\lambda + 1 - ick + Q_\theta(k,l)} - 2\pi = 0, \tag{5.17}$$

This is the equation satisfied by the eigenvalue λ. Conversely it is clear that any λ satisfying the above equation is an eigenvalue with the corresponding eigenfunction given by (5.16).

Before we study (5.17), let us apply expression (4.19) to the McKean model to compute the real part of the principal eigenvalue to order l^3 (the careful reader will notice that (4.19) cannot be applied to the McKean model since the linearization does not satisfy the hypotheses of Theorem 4.2; this will be of no consequence to us since we will only be using the resulting expression as a guide). Using (5.7), we may compute the coefficients ρ_{r} in (4.19) to find:

$$\mathrm{Re}\lambda_l = -\alpha_0 l^2 - \frac{\beta_0 K}{4\gamma_0}(\alpha(1-\alpha))^{-3/2}\,|l|^3 + \mathcal{O}(l^4). \tag{5.18}$$

Suppose $\alpha_0 > 0$. This implies that, for small values of l, $\mathrm{Re}\lambda_l$ is negative. Suppose in addition that $\beta_0 < 0$. The third order term is then positive, and the coefficient of this term can be made arbitrarily large by taking α small. It may therefore be possible for $\mathrm{Re}\lambda_l$ to be positive for small enough α. We now show that this is indeed the case.

Proposition 5.2. *Let*

$$\widehat{I}_\rho(\lambda, \alpha, \theta) = \frac{1}{\alpha} I\left(\lambda, \alpha, \frac{\rho}{K}\sqrt{\alpha(1-\alpha)}, \theta\right). \tag{5.19}$$

For $|\rho|$ sufficiently small and $\rho \neq 0$, there is a function $\lambda_\rho(\alpha, \theta)$ with the following properties.

1. *The function λ_ρ satisfies the following:*

$$\widehat{I}_\rho(\lambda_\rho, \alpha, \theta) = 0,\ \frac{\partial \widehat{I}_\rho}{\partial \lambda}(\lambda_\rho, \alpha, \theta) \neq 0 \text{ for } (\alpha, \theta) \in (0, \alpha_{\rm c}] \times \mathbb{S}^1. \tag{5.20}$$

   where $\alpha_{\rm c}$ is a positive number that depends on ρ. Furthermore, $\lambda_\rho(\alpha, \theta)$ is a continuous function of (α, θ) defined on $[0, \alpha_{\rm c}] \times \mathbb{S}^1$ (that is, continuous up to $\alpha = 0$).

2. *At $\alpha = 0$, λ_ρ satisfies the following estimate:*

$$\left| \lambda_\rho(0, \theta) - \left(i\alpha_1 \rho - \frac{i\beta_1 \gamma_0 \rho^3 + \beta_0 |\rho|^3}{4\gamma_0 K^2} \right) \right| \leq \widehat{C} \rho^4 \tag{5.21}$$

   where the above constant $\widehat{C}$ does not depend on ρ or θ.

Proof. We first obtain a suitable integral expression for $\widehat{I}_\rho$ defined in (5.19). Substitute $l = \rho\sqrt{\alpha(1-\alpha)}/K$ into the expression for I in (5.17), and make the following change of variables.

$$s = \frac{Kk}{\sqrt{\alpha(1-\alpha)}} - \alpha_1 \rho. \tag{5.22}$$

After some calculation, we obtain:

$$\begin{aligned} \widehat{I}_\rho(\lambda, \alpha, \theta) &= \frac{1}{\alpha} \left(\int_{\mathbb{R}} \frac{ds}{A + \alpha(1-\alpha)B} - 2\pi \right), \\ A(\lambda, \alpha, \rho, s, \theta) &= \lambda + 1 - i(1-2\alpha)(s + \alpha_1 \rho) + \alpha(1-\alpha)s^2, \\ B(\rho, s, \theta) &= \frac{\alpha_0 \rho^2}{K^2} + \frac{\rho^2}{K^2} q \left(\frac{s}{\rho} + \alpha_1 \right). \end{aligned} \tag{5.23}$$

We now evaluate $\widehat{I}_\rho$ when $\mathrm{Re}\lambda > -1$. We split $\widehat{I}_\rho$ into two pieces and evaluate them separately.

$$\widehat{I}_\rho = J_1 - J_2,\ J_1 = \frac{1}{\alpha} \left(\int_{\mathbb{R}} \frac{ds}{A} - 2\pi \right),\ J_2 = \int_{\mathbb{R}} \frac{(1-\alpha)B ds}{A(A + \alpha(1-\alpha)B)}. \tag{5.24}$$

Let us first compute J_1. We have:

$$\begin{aligned} \int_{\mathbb{R}} \frac{ds}{A} &= \int_{\mathbb{R}} \frac{ds}{\alpha(1-\alpha)(s-\mu_+)(s-\mu_-)}, \\ \mu_\pm &= i \frac{(1-2\alpha) \pm \sqrt{1 + 4\alpha(1-\alpha)(\lambda - i(1-2\alpha)\alpha_1 \rho)}}{2\alpha(1-\alpha)}, \end{aligned} \tag{5.25}$$

where we choose the branch of the square root so that positive numbers yield positive square roots. Note that this determines the value of the above square

root unambiguously given $\mathrm{Re}\lambda > -1$ and $0 < \alpha \leq 1/2$. It is also easily seen that $\mathrm{Im}\mu_+ > 0$ and $\mathrm{Im}\mu_- < 0$. Using the calculus of residues, we see that

$$J_1(\lambda, \alpha, \theta) = \frac{2\pi}{\alpha}\left(\frac{1}{\sqrt{1 + 4\alpha(1-\alpha)(\lambda - i(1-2\alpha)\alpha_1\rho)}} - 1\right). \tag{5.26}$$

Taking the limit $\alpha \to 0$ in the above expression, we see that J_1 is well defined as a smooth function up to $\alpha = 0$.

We use contour integration to evaluate J_2. Integrate the integrand in J_2 along a semicircle of radius R in the lower half of the complex plane.

$$\int_{\mathcal{C}_R^-} \frac{(1-\alpha)Bds}{A(A + \alpha(1-\alpha)B)}, \;\; \mathcal{C}_R^- = \{R\exp(-i\varphi) | 0 \leq \varphi \leq \pi\}. \tag{5.27}$$

Let us evaluate the magnitude of A on $\mathcal{C}_R^-$. Note first that

$$A = \lambda - i(1-2\alpha)\alpha_1\rho + (\alpha s - i)((1-\alpha)s + i) \tag{5.28}$$

On $\mathcal{C}_R^-$, we have

$$|(\alpha s - i)((1-\alpha)s + i)| \geq |(1-\alpha)s + i| \geq \frac{1}{2}R - 1, \tag{5.29}$$

where we used the fact that $\mathrm{Im}(\alpha s) \leq 0$ in the first inequality and $|s| = R$ and $\alpha \leq 1/2$ in the second inequality. Using this fact, we have

$$|A| \geq \frac{1}{2}R - 1 - |\lambda| - |\alpha_1\rho| \tag{5.30}$$

where we used the fact that $0 < \alpha \leq 1/2$ in the above inequality. From (5.23) and (2.17) it is clear that B can be bounded as follows.

$$|B(\rho, s)| \leq C_B(\rho) \text{ for } R \geq R_B(\rho) \tag{5.31}$$

where C_B and R_B are constants that depend only on ρ. Using (5.30) and (5.31) we have

$$|A + \alpha(1-\alpha)B| \geq \frac{1}{2}R - 1 - |\lambda| - |\alpha_1\rho| - \frac{1}{4}C_B \tag{5.32}$$

for $R \geq R_B(\rho)$. Suppose $|\lambda| \leq 1/2$, and choose R_0 (depending on ρ but *not* on α) so that

$$\frac{1}{2}R_0 - 1 - \frac{1}{2} - |\alpha_1\rho| - \frac{1}{4}C_B \geq 1 \text{ and } R_0 \geq R_B(\rho). \tag{5.33}$$

The integral (5.27) is then well-defined for all $R \geq R_0$ and clearly tends to 0 as $R \to \infty$ since

$$\frac{(1-\alpha)B}{A(A + \alpha(1-\alpha)B)} = \mathcal{O}(R^{-2}). \tag{5.34}$$

by (5.30) (5.31) and (5.32). Thus,

$$J_2(\lambda,\alpha,\theta) = \int_{-R_0}^{R_0} + \int_{\mathcal{C}^-_{R_0}} \frac{(1-\alpha)B ds}{A(A+\alpha(1-\alpha)B)} \tag{5.35}$$

Note that the integrand remains bounded along the integration contour up to $\alpha = 0$. Now, J_2 is an integral of a smooth function of λ, α and θ over a fixed piecewise smooth contour of finite length (recall that R_0 does not depend on α or λ so long as $|\lambda| \le \lambda_0$). J_2 as defined in (5.35) is thus a smooth function in the following range with derivatives continuous up to the boundary:

$$|\lambda| \le \frac{1}{2},\ 0 \le \alpha \le 1/2 \text{ and } \theta \in \mathbb{S}^1. \tag{5.36}$$

Combining this fact with the observation following (5.26), we see that $\widehat{I}_\rho = J_1 - J_2$ is a smooth function (up to the boundary) defined in the same range.

Let us evaluate $\widehat{I}_\rho = J_1 - J_2$ at $\alpha = 0$. From (5.26), we obtain

$$J_1(\lambda, 0, \theta) = -4\pi(\lambda - i\alpha_1\rho). \tag{5.37}$$

We now turn to J_2.

$$J_2(\lambda, 0, \theta) = \int_{-R}^{R} + \int_{\mathcal{C}^-_R} \frac{B}{A^2} ds. \tag{5.38}$$

where $R \ge R_0$. Taking $R \to \infty$,

$$J_2(\lambda, 0, \theta) = \int_{-\infty}^{\infty} \frac{B}{A^2} ds. \tag{5.39}$$

The integrand B/A^2 has a simple pole and a double pole in the lower half plane, and a simple pole σ in the upper half plane:

$$\sigma = -(\alpha_1 - \gamma_1)\rho + i\gamma_0 |\rho|. \tag{5.40}$$

It is thus easier to apply the calculus of residues using the pole in the upper half plane. We have

$$J_2(\lambda, 0, \theta) = 2\pi i \lim_{s\to\sigma} \frac{(s-\sigma)B}{A^2} = \frac{\pi(i\beta_1\gamma_0\rho^3 + \beta_0 |\rho|^3)}{\gamma_0 K^2(\lambda + 1 + \gamma_0|\rho| - i\gamma_1\rho)^2}. \tag{5.41}$$

Consider the equation

$$\begin{aligned} \widehat{I}_\rho(\lambda, 0, \rho) &= J_1(\lambda, 0, \rho) - J_2(\lambda, 0, \rho) \\ &= -4\pi(\lambda - i\alpha_1\rho) - \frac{\pi(i\beta_1\gamma_0\rho^3 + \beta_0|\rho|^3)}{\gamma_0 K^2(\lambda + 1 + \gamma_0|\rho| - i\gamma_1\rho)^2} = 0, \end{aligned} \tag{5.42}$$

where we used (5.37) and (5.41). Let us now view the above as an equation for λ for small ρ. When $\rho = 0$, $\lambda = 0$ is a solution to the above equation. We may

now use the implicit function theorem at $\rho = \lambda = 0$ for fixed θ to find a solution λ^0_ρ with the following property:

$$\left| \lambda^0_\rho(\theta) - \left(i\alpha_1 \rho - \frac{i\beta_1\gamma_0\rho^3 + \beta_0 |\rho|^3}{4\gamma_0 K^2} \right) \right| \leq C\rho^4 \tag{5.43}$$

where the above constant C does not depend on ρ or θ. Furthermore, we have:

$$\frac{\partial \widehat{I}_\rho}{\partial \lambda}(\lambda^0_\rho, 0, \rho) \neq 0. \tag{5.44}$$

Recall that $\widehat{I}_\rho$ was a smooth in the region (5.36). Consider the equation:

$$\widehat{I}_\rho(\lambda, \alpha, \theta) = 0. \tag{5.45}$$

Given the non-degeneracy condition (5.44), for each $\theta' \in \mathbb{S}^1$ we may use the implicit function theorem at $(\lambda, \alpha, \theta) = (\lambda^0_\rho(\theta'), 0, \theta')$ to obtain:

$$\widehat{I}_\rho(\lambda_{\rho,\theta'}(\alpha,\theta)), \alpha, \theta) = 0,\ \frac{\partial \widehat{I}_\rho}{\partial \lambda}(\lambda_{\rho,\theta'}(\alpha,\theta)), \alpha, \theta) \neq 0,\ \lambda_{\rho,\theta'}(0,\theta) = \lambda^0_\rho(\theta). \tag{5.46}$$

The solution $\lambda_{\rho,\theta'}(\alpha,\theta)$ is the unique solution to $\widehat{I}_\rho = 0$ in a neighborhood

$$\mathcal{N}_{\theta'} = \{ \left|\lambda - \lambda^0_\rho(\theta')\right| < r'_\theta,\ 0 \leq \alpha < r'_\theta,\ |\theta - \theta'| < r'_\theta \} \tag{5.47}$$

where r'_θ is some positive number depending on θ'. Any two functions λ_{ρ,θ_1} and λ_{ρ,θ_2} must thus coincide on the intersection $\mathcal{N}_{\rho,\theta_1} \cap \mathcal{N}_{\rho,\theta_2}$. The collection $(\lambda_{\rho,\theta'}), \theta' \in \mathbb{S}^1$ thus defines a single continuous function $\lambda_\rho(\alpha,\theta)$ uniquely solving $\widehat{I}_\rho = 0$ on the union of the sets $\mathcal{N}_{\theta'}, \theta' \in \mathbb{S}^1$. Since the set:

$$\mathcal{S} = \{ (\lambda^0_\rho(\theta), 0, \theta), \theta \in \mathbb{S}^1 \} \tag{5.48}$$

is compact, and since $\mathcal{N}_{\theta'}$ form an open cover of $\mathcal{S}$, we may obtain a finite subcover $\mathcal{N}_{\theta_1}, \cdot, \mathcal{N}_{\theta_n}$. If we let

$$\alpha_{\mathrm{c}} = \min_{k=1,\cdots,n} r_{\theta_k} \tag{5.49}$$

we see that $\lambda_\rho(\alpha,\theta)$ is defined on $[0, \alpha_{\mathrm{c}}] \times \mathbb{S}^1$. □

Recall the normalized traveling front solutions $u^\epsilon_{\mathrm{f}*}$ and $c_*(\epsilon)$ discussed in (5.4) and (5.5). We now study the dependence $u^\epsilon_{\mathrm{f}*}$ and $c_*(\epsilon)$ as a function of ϵ. Consider the following system of differential equations.

$$\begin{aligned} \frac{du}{d\xi} &= -w, \\ \frac{dw}{d\xi} &= -\gamma w + f_\epsilon(u). \end{aligned} \tag{5.50}$$

Finding $u^\epsilon_{\mathrm{f}*}$ and $c_*(\epsilon)$ corresponds to finding a value of $\gamma(=c_*(\epsilon))$ such that there is a heteroclinic orbit connecting the fixed point $(u,w)=(1,0)$ and $(0,0)$. The stable manifold of $(0,0)$ can be computed explicitly:

$$w = W^0_{\epsilon,\gamma}(u) = \mu_0 u,\ \mu_0 = \frac{\gamma+\sqrt{\gamma^2+4}}{2},\ u \le \alpha-\epsilon. \tag{5.51}$$

Likewise, the unstable manifold of $(1,0)$ is given by:

$$w = W^1_{\epsilon,\gamma}(u) = -\mu_1(u-1),\ \mu_1 = \frac{-\gamma+\sqrt{\gamma^2+4}}{2},\ u \ge \alpha+\epsilon. \tag{5.52}$$

We now show that the stable and unstable manifolds above can be extended to $u=\alpha$ provided ϵ is sufficiently small.

Proposition 5.3. *There is a continuous positive function $h(\gamma), \gamma \in \mathbb{R}$ with the following properties. Suppose $0 \le \epsilon < h(\gamma)$. Then, the stable manifold at $(u,w)=(0,0)$ of the system* (5.50) *can be expressed as a graph:*

$$w = W^0_{\epsilon,\gamma}(u),\ 0 \le u \le \alpha, \tag{5.53}$$

which satisfies (5.51) *and the bound*

$$\frac{\mu_0\alpha}{4} \le W^0_{\epsilon,\gamma} \le \frac{5\mu_0\alpha}{4} \text{ for } \alpha-\epsilon \le u \le \alpha, \tag{5.54}$$

where μ_0 is given in (5.51)*. Likewise, the unstable manifold at $(u,w)=(1,0)$ of the system* (5.50) *can be expressed as a graph:*

$$w = W^1_{\epsilon,\gamma}(u),\ \alpha \le u \le 1, \tag{5.55}$$

which satisfies (5.52) *and the bound*

$$\frac{\mu_1(1-\alpha)}{4} \le W^1_{\epsilon,\gamma} \le \frac{5\mu_1(1-\alpha)}{4} \text{ for } \alpha \le u \le \alpha+\epsilon. \tag{5.56}$$

where μ_1 is given in (5.52)*.*

Proof. We first prove the above assertion for the stable manifold at $(0,0)$. In (5.51), we have already seen that the stable manifold can be expressed as a graph up to $u \le \alpha-\epsilon$. There is nothing to prove when $\epsilon=0$ so we assume $\epsilon>0$. If we can solve the following initial value problem, we can extend this stable manifold as a graph $W^0_{\epsilon,\gamma}(u)$ up to $u=\alpha$:

$$\frac{dW^0_{\epsilon,\gamma}}{du} = -\gamma - \frac{f_\epsilon(u)}{W^0_{\epsilon,\gamma}},\ \alpha-\epsilon \le u \le \alpha,\ W^0_{\epsilon,\gamma}(\alpha-\epsilon) = \mu_0(\alpha-\epsilon). \tag{5.57}$$

Let us solve this differential equation. Define

$$V(s) = W^0_{\epsilon,\gamma}(\alpha-\epsilon+s) - \mu_0(\alpha-\epsilon). \tag{5.58}$$

We seek a solution to the integral equation:

$$V(s) = (\mathcal{T}V)(s) \equiv -\gamma s - \int_0^s \frac{f_\epsilon(s+\alpha-\epsilon)}{\mu_0(\alpha-\epsilon)+V}. \tag{5.59}$$

We consider $\mathcal{T}$ as a map on the set:

$$\mathcal{V} = \{V \in C([0,\epsilon]) |\, \|V\|_{C([0,\epsilon])} \le \mu_0\alpha/4\}, \tag{5.60}$$

where $C([0,\epsilon])$ is the space of continuous functions on the closed interval $0 \le s \le \epsilon$. Let us check the conditions under which $\mathcal{T}$ is a contraction mapping on $\mathcal{V}$. First, in order for $\mathcal{T}$ to map $\mathcal{V}$ to itself, we need:

$$\|\mathcal{T}V\|_{C([0,\epsilon])} \le |\gamma|\,\epsilon + \int_0^\epsilon \frac{|f_\epsilon(s+\alpha-\epsilon)|}{|\mu_0(\alpha-\epsilon)+V|} ds \tag{5.61}$$

Note that

$$|f_\epsilon(u)| \le 1 \text{ for } 0 \le u \le 1. \tag{5.62}$$

Furthermore, assume $\epsilon \le \alpha/2$, in which case

$$|\mu_0(\alpha-\epsilon)+V(s)| \ge \frac{\mu_0\alpha}{2} - |V(s)| \ge \frac{\mu_0\alpha}{4} \text{ for } V \in \mathcal{V} \tag{5.63}$$

where we used the fact that $V \in \mathcal{V}$ in the last inequality. Combining (5.61) with (5.62) and (5.63) we have

$$\|\mathcal{T}V\|_{C([0,\epsilon])} \le \left(|\gamma| + \frac{4}{\mu_0\alpha}\right)\epsilon. \tag{5.64}$$

Therefore, provided

$$0 < \epsilon \le h_0(\gamma),\ h_0(\gamma) = \min\left(\frac{(\mu_0\alpha)^2}{4(\mu_0\alpha\,|\gamma|+4)}, \frac{\alpha}{2}\right) \tag{5.65}$$

$\mathcal{T}$ maps $\mathcal{V}$ to itself. Let us now check the condition on ϵ under which $\mathcal{T}$ is a contraction mapping. Take $V, V' \in \mathcal{V}$. We have

$$\|\mathcal{T}(V-V')\|_{C([0,\epsilon])} \le \int_0^\epsilon \frac{|f_\epsilon(s+\alpha-\epsilon)|\,|V-V'|}{|\mu_0(\alpha-\epsilon)+V|\,|\mu_0(\alpha-\epsilon)+V'|} ds. \tag{5.66}$$

Assuming $\epsilon \le \alpha/2$ and using (5.62) and (5.63), we see that

$$\|\mathcal{T}(V-V')\|_{C([0,\epsilon])} \le \frac{16\epsilon}{(\mu_0\alpha)^2}\,\|V-V'\|_{C([0,\epsilon])}\,. \tag{5.67}$$

Thus, $\mathcal{T}$ is a contraction mapping on $\mathcal{V}$ if (5.65) holds together with

$$0 < \epsilon < \widetilde{h}_0(\gamma),\ \widetilde{h}_0(\gamma) = \min\left(\frac{(\mu_0\alpha)^2}{16}, \frac{\alpha}{2}\right). \tag{5.68}$$

Noting that $\widetilde{h}_0(\gamma) \geq h_0(\gamma)$, we see that if

$$0 < \epsilon < h_0(\gamma), \tag{5.69}$$

$\mathcal{T}$ is a contraction mapping. By the contraction mapping principle, $\mathcal{T}$ has a unique fixed point in $\mathcal{V}$, and this provides the desired extension of the stable manifold $W^0_{\epsilon,\gamma}(u)$ up to $u = \alpha$. Note here that $h_0(\gamma)$ is a positive continuous function of ϵ. Furthermore, since

$$W^0_{\epsilon,\gamma}(\alpha - \epsilon + s) = \mu_0(\alpha - \epsilon) + V(s),\ |V(s)| \leq \frac{\mu_0 \alpha}{4} \text{ for } 0 \leq s \leq \epsilon \tag{5.70}$$

and $\epsilon < h_0(\gamma) \leq \alpha/2$ we see that $W^0_{\epsilon,\gamma}$ satisfies (5.54).

Likewise, the unstable manifold at $(0, 1)$ can be expressed as a graph $w = W^1_{\epsilon,\gamma}(u)$ for $\alpha \leq u \leq 1$ provided

$$0 < \epsilon < h_1(\gamma) \leq (1 - \alpha)/2, \tag{5.71}$$

where $h_1(\gamma)$ is a positive continuous function for $\gamma \in \mathbb{R}$. Furthermore, $W^1_{\epsilon,\gamma}$ satisfies (5.56). We obtain the desired result by letting

$$h(\gamma) = \min(h_0(\gamma), h_1(\gamma)). \tag{5.72}$$

□

Given that the stable manifold $W^0_{\epsilon,\gamma}$ and the unstable manifold $W^1_{\epsilon,\gamma}$ are now extended to $u = \alpha$, the desired heteroclinic orbit can be found by solving the following equation for γ for fixed ϵ:

$$g(\gamma, \epsilon) = g_0(\gamma, \epsilon) - g_1(\gamma, \epsilon) = 0,\ g_0(\gamma, \epsilon) \equiv W^0_{\epsilon,\gamma}(\alpha),\ g_1(\gamma, \epsilon) \equiv W^1_{\epsilon,\gamma}(\alpha). \tag{5.73}$$

Once the solution to $g(\gamma, \epsilon) = 0$ for each fixed ϵ yields the normalized front speed $c_*(\epsilon)$

Proposition 5.4. *There is a positive constant $\epsilon_0 > 0$ such that (5.73) is uniquely solvable for $0 \leq \epsilon \leq \epsilon_0$. This solution is equal to $\gamma = c_*(\epsilon)$. The function $c_*(\epsilon)$ is a continuous function of ϵ up to $\epsilon = 0$. Furthermore,*

$$W^0_{\epsilon,c_*(\epsilon)}(\alpha) = W^1_{\epsilon,c_*(\epsilon)}(\alpha) \tag{5.74}$$

is a continuous function of ϵ up to $\epsilon = 0$.

Proof. We first show that $g(\gamma, \epsilon)$ is a continuous function of γ and ϵ where defined. When $\epsilon > 0$, the continuity of g_0 follows directly from the continuous dependence of solutions of (5.57) to (γ, ϵ). The same is true for g_1. We have thus only to consider continuity at $\epsilon = 0$.

$$|g_0(\gamma, \epsilon) - g_0(\gamma', 0)| = |g_0(\gamma, \epsilon) - g_0(\gamma, 0)| + |g_0(\gamma, 0) - g_0(\gamma', 0)| \tag{5.75}$$

Let us estimate the first term.

$$\begin{aligned} |g_0(\gamma,\epsilon)-g_0(\gamma,0)| &= \left|-\mu_0\epsilon-\gamma_\epsilon-\int_{\alpha-\epsilon}^{\alpha}\frac{f_\epsilon}{W^0_{\epsilon,\gamma}}du\right| \\ &\le \left((\mu_0+|\gamma|)+\frac{4}{\alpha\mu_0}\right)\epsilon, \end{aligned} \tag{5.76}$$

where we used (5.57) in the equality and (5.62) and (5.54) in the inequality. We also have

$$|g_0(\gamma,0)-g_0(\gamma',0)| = |\mu_0(\gamma)-\mu_0(\gamma')|\,\alpha. \tag{5.77}$$

Since $\mu_0(\gamma)$ is a smooth function of γ, (5.76) and (5.77) establishes continuity of g_0 at $\epsilon=0$. Likewise, we may prove the continuity of g_1 at $\epsilon=0$.

Note that the equation $g(\gamma,0)=0$ is a monotone increasing function of γ with a single zero at the value $\gamma=c_*(0)$ where $c_*(0)$ is given in (5.7). Take two values $\gamma_+ > c_*(0)$ and $\gamma_- < c_*(0)$. Choose $\epsilon_0>0$ so that $g(\gamma,\epsilon)$ is defined for $(\gamma,\epsilon)\in[\gamma_-,\gamma_+]\times[0,\epsilon_0]$. This is possible thanks to Proposition 5.3; $g(\gamma,\epsilon)$ is defined for $0\le\epsilon<h(\gamma)$ where $h(\gamma)$ is a positive continuous function. Given the continuity of g, we may take $\epsilon_0>0$ smaller if necessary so that $g(\gamma_+,\epsilon)\ge 0\ge g(\gamma_-,\epsilon)$. By the intermediate value theorem, for each $0\le\epsilon\le\epsilon_0$ there is at least one zero of $g(\gamma,\epsilon)=0$ in the interval $\gamma_-\le\gamma\le\gamma_+$. By the known uniqueness of the front speed, this γ must be unique, and is equal to $c_*(\epsilon)$. We claim that $c_*(\epsilon)$ is a continuous function of ϵ for $0\le\epsilon\le\epsilon_0$. Indeed, suppose $\epsilon_k, k=1,2,\cdots$ converges to ϵ_∞. Take any subsequence of $c_*(\epsilon_k)$. This subsequence contains a subsequence that is convergent since $\gamma_-\le c_*(\epsilon_k)\le\gamma_+$. Let us still call this subsequence $c_*(\epsilon_k)$ and its limit γ_∞. By continuity of $g(\gamma,\epsilon)$, we have

$$\lim_{k\to\infty} g(c_*(\epsilon_k),\epsilon_k) = g(\gamma_\infty,\epsilon_\infty) = 0. \tag{5.78}$$

Since $c_*(\epsilon_\infty)$ is the unique solution of $g(\gamma,\epsilon_\infty)=0$, we see that $c_*(\epsilon_\infty)=\gamma_\infty$. This concludes the proof that $c_*(\epsilon)$ is a continuous function for $0\le\epsilon\le\epsilon_0$. The continuity of (5.74) follows from the fact that $W^0_{\epsilon,c_*(\epsilon)}(\alpha)=g_0(c_*(\epsilon),\epsilon)$ and the continuity of g_0 and c_*. □

We will need some properties of the front solution $u^\epsilon_{\rm f}$. The traveling front solution corresponds to the above heteroclinic orbit in the (u,w) phase plane. Therefore, $u^\epsilon_{\rm f*}$ satisfies the following. Define

$$W_\epsilon(u) = \begin{cases} W^0_{\epsilon,c_*(\epsilon)}(u) \text{ if } 0\le u\le\alpha, \\ W^1_{\epsilon,c_*(\epsilon)}(u) \text{ if } \alpha\le u\le 1, \end{cases} \tag{5.79}$$

The graph $w=W_\epsilon(u)$ is the graph of the heteroclinic orbit. Using the first equation in (5.50), we see that:

$$\frac{\partial u^\epsilon_{\rm f*}}{\partial\xi} = -W_\epsilon(u^\epsilon_{\rm f*}),\ u^\epsilon_{\rm f*}(0)=\alpha. \tag{5.80}$$

The last condition is the normalization condition in (5.4). Similarly, using the second equation in (5.50), we have:

$$\frac{\partial^2 u^\epsilon_{\mathrm{f}*}}{\partial \xi^2} = c_*(\epsilon) W_\epsilon(u^\epsilon_{\mathrm{f}*}) - f_\epsilon(u^\epsilon_{\mathrm{f}*}),\ \frac{\partial u^\epsilon_{\mathrm{f}*}}{\partial \xi}(0) = -W_\epsilon(\alpha). \tag{5.81}$$

Note that $W_\epsilon(\alpha)$ is continuous at $\epsilon = 0$ given (5.79) and Proposition 5.4.

Proposition 5.5. *The front solution $u^\epsilon_{\mathrm{f}*}$ satisfying* (5.4) *satisfies the following properties.*

1. *For sufficiently small ϵ, there is a constant L_0 independent of ϵ such that if $|\xi| \geq L_0\epsilon$, then,*
$$|u^\epsilon_{\mathrm{f}*}(\xi) - \alpha| \geq \epsilon. \tag{5.82}$$
2. *For any $y \in \mathbb{R}$,*
$$\lim_{\epsilon\to 0} \frac{1}{\epsilon}(u^\epsilon_{\mathrm{f}*}(\epsilon y) - \alpha) = \frac{\partial u^0_{\mathrm{f}*}}{\partial \xi}(0) y, \tag{5.83}$$
where $u^0_{\mathrm{f}*}$ is given in (5.7).

Proof. We first prove item 1. Note that $u = u^\epsilon_{\mathrm{f}*}(\xi)$ is a monotone decreasing function of ξ. Therefore, we may consider the inverse $\xi = (u^\epsilon_{\mathrm{f}*})^{-1}(u)$. Using (5.80), we have:

$$\xi = (u^\epsilon_{\mathrm{f}*})^{-1}(u) = -\int_\alpha^u \frac{ds}{W_\epsilon(s)},\ u = u^\epsilon_{\mathrm{f}*}(\xi). \tag{5.84}$$

Setting $u = \alpha - \epsilon$ in the above, we have:

$$\xi = (u^\epsilon_{\mathrm{f}*})^{-1}(\alpha - \epsilon) \geq \frac{4\epsilon}{\alpha\mu_0(c_*(\epsilon))} \tag{5.85}$$

where we used (5.79), (5.54) and $\gamma = c_*(\epsilon)$. Using the fact that $u^\epsilon_{\mathrm{f}*}$ is monotone decreasing, we see that

$$u^\epsilon_{\mathrm{f}*}(\xi) \leq \alpha - \epsilon \text{ if } \xi \geq \frac{4\epsilon}{\alpha\mu_0(c_*(\epsilon))}. \tag{5.86}$$

In a similar fashion, we find

$$u^\epsilon_{\mathrm{f}*}(\xi) \geq \alpha + \epsilon \text{ if } \xi \leq \frac{4\epsilon}{(1-\alpha)\mu_1(c_*(\epsilon))} \tag{5.87}$$

Item 1 follows from the two inequalities above noting the continuity of $c_*(\epsilon)$ at $\epsilon = 0$.

We turn to item 2. There is nothing to prove for $y = 0$. We henceforth assume that $y > 0$. The case $y < 0$ is similar. Note that

$$\begin{aligned} &\frac{1}{\epsilon}(u^\epsilon_{\mathrm{f}*}(\epsilon y) - \alpha) - \frac{\partial u^0_{\mathrm{f}*}}{\partial \xi}(0) y \\ &= \left(\frac{1}{\epsilon}(u^\epsilon_{\mathrm{f}*}(\epsilon y) - \alpha) - \frac{\partial u^\epsilon_{\mathrm{f}*}}{\partial \xi}(0) y\right) + \left(\frac{\partial u^\epsilon_{\mathrm{f}*}}{\partial \xi}(0) - \frac{\partial u^0_{\mathrm{f}*}}{\partial \xi}(0)\right) y \end{aligned} \tag{5.88}$$

Note that

$$\lim_{\epsilon\to 0}\left(\frac{\partial u^\epsilon_{\mathrm{f}*}}{\partial\xi}(0)-\frac{\partial u^0_{\mathrm{f}*}}{\partial\xi}(0)\right)=-\left(\lim_{\epsilon\to 0}W_\epsilon(\alpha)-W_0(\alpha)\right)=0 \tag{5.89}$$

where we used the second relation in (5.81) and the continuity of $W_\epsilon(\alpha)$ at $\epsilon=0$ (see remark below equation (5.81)). Let us now consider the first half of the last line in (5.88).

$$\frac{1}{\epsilon}(u^\epsilon_{\mathrm{f}*}(\epsilon y)-\alpha)-\frac{\partial u^\epsilon_{\mathrm{f}*}}{\partial\xi}(0)y=\frac{1}{\epsilon}\int_0^{\epsilon y}\left(\frac{\partial u^\epsilon_{\mathrm{f}*}}{\partial\xi}-\frac{\partial u^\epsilon_{\mathrm{f}*}}{\partial\xi}(0)\right)d\xi. \tag{5.90}$$

Using (5.81), we have

$$\frac{\partial u^\epsilon_{\mathrm{f}*}}{\partial\xi}(s)-\frac{\partial u^\epsilon_{\mathrm{f}*}}{\partial\xi}(0)=\int_0^s\frac{\partial^2 u^\epsilon_{\mathrm{f}*}}{\partial\xi^2}d\xi=\int_0^s(c_*(\epsilon)W_\epsilon(u^\epsilon_{\mathrm{f}*})-f_\epsilon(u^\epsilon_{\mathrm{f}*}))d\xi. \tag{5.91}$$

For $s>0$, we may bound the above integrand as follows for sufficiently small values of ϵ:

$$|c_*(\epsilon)W_\epsilon(u^\epsilon_{\mathrm{f}*})-f_\epsilon(u^\epsilon_{\mathrm{f}*})|\le\frac{5}{4}c_*(\epsilon)\mu_0(c_*(\epsilon))\alpha+1\le C_0 \tag{5.92}$$

where C_0 is a constant independent of ϵ. In the first inequality, we used (5.79), (5.51), (5.54) and (5.62), and in the second inequality we used the continuity of $c_*(\epsilon)$ at $\epsilon=0$. Combining the above with (5.91), we have, for sufficiently small ϵ,

$$\left|\frac{\partial u^\epsilon_{\mathrm{f}*}}{\partial\xi}(s)-\frac{\partial u^\epsilon_{\mathrm{f}*}}{\partial\xi}(0)\right|\le C_0 s. \tag{5.93}$$

Using this estimate in (5.90), we have

$$\left|\frac{1}{\epsilon}(u^\epsilon_{\mathrm{f}*}(\epsilon y)-\alpha)-\frac{\partial u^\epsilon_{\mathrm{f}*}}{\partial\xi}(0)y\right|\le\frac{1}{\epsilon}\int_0^{\epsilon y}C_0\xi d\xi=\frac{C_0y^2}{2}\epsilon. \tag{5.94}$$

Equation (5.88), together with (5.89) and (5.94) gives us the desired result. □

We need one last result. Define $\mathcal{T}_{\epsilon,\theta}$ to be the operator

$$(\mathcal{T}_{\epsilon,\theta}w)(\xi)=\begin{cases}j_\epsilon(u^\epsilon_{\mathrm{f}*}(\xi/K)-\alpha)w(\xi) & \text{for } \epsilon>0,\\ (\alpha(1-\alpha))^{-1/2}K\delta(\xi)w(0), & \text{for } \epsilon=0,\end{cases} \tag{5.95}$$

where j_ϵ was given in (5.2). We view $\mathcal{T}_{\epsilon,\theta}$ as an operator from $H^1(\mathbb{R})$ to $H^{-1}(\mathbb{R})$.

Proposition 5.6. *Consider the family of operators $\mathcal{T}_{\epsilon,\theta}$ defined above, where $(\epsilon,\theta)\in[0,\epsilon_0]\times\mathbb{S}^1$ and ϵ_0 was given in Proposition 5.4. Then, $\mathcal{T}_{\epsilon,\theta}$ depends continuously on (ϵ,θ) as an operator from $H^1(\mathbb{R})$ to $H^{-1}(\mathbb{R})$.*

Proof. Continuity is clear for $\epsilon > 0$. We have therefore only to establish continuity at $\epsilon = 0$. For notational convenience, let:

$$\sigma = \frac{\partial u^0_{\mathrm{f}*}}{\partial \xi}(0) = -\sqrt{\alpha(1-\alpha)}. \tag{5.96}$$

The second equality follows from (5.7) by direct computation. We estimate the difference $(\mathcal{T}_{\epsilon,\theta} - T_{0,\theta'})w$ as follows.

$$\begin{aligned}
(\mathcal{T}_{\epsilon,\theta} - \mathcal{T}_{0,\theta'})w &= J_1 + J_2 + J_3 + J_4, \\
J_1 &= (j_\epsilon(u^\epsilon_{\mathrm{f}*}(\xi/K(\theta)) - \alpha) - j_\epsilon(\sigma\xi/K(\theta)))w(\xi), \\
J_2 &= j_\epsilon(\sigma\xi/K(\theta))(w(\xi) - w(0)), \\
J_3 &= (j_\epsilon(\sigma\xi/K(\theta)) - |\sigma|^{-1} K(\theta)\delta(\xi))w(0), \\
J_4 &= (K(\theta) - K(\theta'))\,|\sigma|^{-1}\,\delta(\xi)w(0).
\end{aligned} \tag{5.97}$$

Let us estimate J_1.

$$\begin{aligned}
\|J_1\|_{L^1(\mathbb{R})} &= \int_{\mathbb{R}} |j_\epsilon(u^\epsilon_{\mathrm{f}*}(\xi/K(\theta)) - \alpha) - j_\epsilon(\sigma\xi/K(\theta))|\,|w(\xi)|\,d\xi \\
&\le K(\theta)\,\|w\|_{L^\infty(\mathbb{R})} \int_{\mathbb{R}} |j_1((u^\epsilon_{\mathrm{f}*}(\epsilon y) - \alpha)/\epsilon) - j_1(\sigma y)|\,dy
\end{aligned} \tag{5.98}$$

By item 1 of Proposition 5.5, we see that the above integrand is 0 when

$$|y| \ge \widetilde{L}_0,\ \widetilde{L}_0 = \max(L_0, 1/|\sigma|). \tag{5.99}$$

Thus, the above integral may be restricted to the interval $|y| \le \widetilde{L}_0$, and in this interval, we have:

$$|j_1((u^\epsilon_{\mathrm{f}}(\epsilon y) - \alpha)/\epsilon) - j_1(\sigma y)| \le \max_{|x|\le 1} 2j_1(x) < \infty. \tag{5.100}$$

Furthermore, by item 2 of Proposition 5.5,

$$\lim_{\epsilon\to 0} |j_1((u^\epsilon_{\mathrm{f}*}(\epsilon y) - \alpha)/\epsilon) - j_1(\sigma y)| = 0 \tag{5.101}$$

for every y. Thus, by the Lebesgues dominated convergence theorem, we have

$$\|J_1\|_{L^1(\mathbb{R})} \le K(\theta)E_1(\epsilon)\,\|w\|_{L^\infty(\mathbb{R})} \le K_1 E_1(\epsilon)\,\|w\|_{L^\infty(\mathbb{R})}\,,\ \lim_{\epsilon\to 0} E_1(\epsilon) = 0, \tag{5.102}$$

where K_1 is a constant independent of θ and ϵ. In the last inequality, we used the fact that $K(\theta)$ is bounded for $\theta \in \mathbb{S}^1$

We turn to J_2. We have:

$$\|J_2\|_{L^1(\mathbb{R})} \le \int_{\mathbb{R}} j_\epsilon(\sigma\xi/K(\theta))\,|w(\xi) - w(0)|\,d\xi \le \frac{K(\theta)}{|\sigma|} \max_{|\xi|\le \epsilon K(\theta)/|\sigma|} |w(\xi) - w(0)|\,. \tag{5.103}$$

For smooth w, we have:

$$|w(\xi) - w(0)| = \left| \int_0^\xi \frac{\partial w}{\partial \xi} d\xi \right| \leq \sqrt{\xi} \, \|w\|_{H^1(\mathbb{R})} \tag{5.104}$$

where we used the Cauchy-Schwartz inequality in the above inequality. Since smooth compactly supported functions are dense in $H^1(\mathbb{R})$, the above inequality holds for $w \in H^1(\mathbb{R})$. Thus, (5.103) with (5.104) yields

$$\|J_2\|_{L^1(\mathbb{R})} \leq \left(\frac{K(\theta)}{|\sigma|} \right)^{3/2} \sqrt{\epsilon} \, \|w\|_{H^1(\mathbb{R})} \leq K_2 \sqrt{\epsilon} \, \|w\|_{H^1(\mathbb{R})} \,, \tag{5.105}$$

where K_2 is a constant independent of θ or ϵ.

Let us turn to J_3.

$$\|J_3\|^2_{H^{-1}(\mathbb{R})} = \int_{\mathbb{R}} \left| (\mathcal{F}_\xi(j_\epsilon(\sigma\xi/K(\theta)) - |\sigma|^{-1} K(\theta)\delta))(k) \right|^2 \frac{dk}{1+k^2} \, |w(0)|^2 \tag{5.106}$$

where $\mathcal{F}_\xi$ is the Fourier transform with respect to ξ (see (5.10)). An easy computation shows that

$$\mathcal{F}_\xi(j_\epsilon(\sigma\xi/K(\theta)) - |\sigma|^{-1} K(\theta)\delta) = \frac{K(\theta)}{|\sigma|} \left(\widehat{j}_1 \left(\frac{kK(\theta)\epsilon}{\sigma} \right) - 1 \right) \tag{5.107}$$

where $\widehat{j}_1 = \mathcal{F}_\xi j_1$. Thus,

$$\begin{aligned} \|J_3\|^2_{H^{-1}(\mathbb{R})} &\leq \int_{\mathbb{R}} \left| \widehat{j}_1(\epsilon y) - 1 \right|^2 \frac{dy}{1 + (K(\theta)\sigma^{-1})^2 y^2} \, |w(0)|^2 \\ &\leq \int_{\mathbb{R}} \left| \widehat{j}_1(\epsilon y) - 1 \right|^2 \frac{dy}{1 + K_4 y^2} \, |w(0)|^2 \end{aligned} \tag{5.108}$$

where $K_4 > 0$ is a is a constant independent of θ. In the last inequality, we used the fact that $K(\theta)$ is bounded from below by a positive constant. Since the integral of j_1 is equal to 1, $\widehat{j}_1(0) = 1$. Therefore,

$$\lim_{\epsilon \to 0} \left(\widehat{j}_1 \left(\epsilon y \right) - 1 \right) = 0 \tag{5.109}$$

for every $y \in \mathbb{R}$. Furthermore,

$$\left| \widehat{j}_1(\epsilon y) - 1 \right| \leq 1 + \left\| \widehat{j}_1 \right\|_{L^\infty(\mathbb{R})} . \tag{5.110}$$

Note that $\widehat{j}_1$ is bounded since j_1 is a compactly supported smooth function (and hence $j_1 \in L^1(\mathbb{R})$). Therefore, we may use the Lebesgues dominated convergence theorem to conclude that:

$$\|J_3\|_{H^{-1}(\mathbb{R})} \leq E_3(\epsilon) \, |w(0)| \leq E_3(\epsilon) \, \|w\|_{L^\infty(\mathbb{R})} \,, \; \lim_{\epsilon \to 0} E_3(\epsilon) = 0. \tag{5.111}$$

Finally, we estimate J_4.

$$\begin{aligned}\|J_4\|_{\|H\|^{-1}(\mathbb{R})} &= |\sigma|^{-1} |K(\theta) - K(\theta')| \, \|\delta\|_{H^{-1}(\mathbb{R})} \, |w(0)| \\ &\leq |\sigma|^{-1} \sqrt{\pi} \, |K(\theta) - K(\theta')| \, \|w\|_{L^\infty(\mathbb{R})} \, .\end{aligned} \tag{5.112}$$

Noting the fact that $H^1(\mathbb{R})$ embeds continuously into $L^\infty(\mathbb{R})$ and $L^1(\mathbb{R})$ into $H^{-1}(\mathbb{R})$, we may conclude from (5.102), (5.105), (5.111), (5.112) together with (5.97) that

$$\|(\mathcal{T}_{\epsilon,\theta} - \mathcal{T}_{0,\theta'})w\|_{H^{-1}(\mathbb{R})} \leq (E(\epsilon) + K_5(K(\theta) - K(\theta'))) \, \|w\|_{H^1(\mathbb{R})} \, , \ \lim_{\epsilon \to 0} E(\epsilon) = 0, \tag{5.113}$$

where K_5 is a constant independent of θ or ϵ. This shows that $T_{\epsilon,\theta}$ is continuous in (ϵ, θ) at $(0, \theta)$. □

We are now ready to prove Theorem 5.1.

Proof of Theorem 5.1. Pick an arbitrary $\nu > 0$. Fix $\rho > 0$ and $\alpha > 0$ in Proposition 5.2 so that

$$\max_{\theta \in \mathbb{S}^1} (4\gamma_0 K^2) \widehat{C} \, |\rho| \leq \frac{\nu}{4}, \ |\lambda_\rho(\alpha, \theta) - \lambda_\rho(0, \theta)| \leq \widehat{C} \, |\rho|^4 \, . \tag{5.114}$$

The first inequality is possible given the boundedness of γ_0 and K as functions of $\theta \in \mathbb{S}^1$. The second is possible given the continuity of λ_ρ with respect to $(\alpha, \theta) \in [0, \alpha_c] \times \mathbb{S}^1$.

Consider the following family of eigenvalue problems parametrized by $\epsilon > 0$ and $\theta \in \mathbb{S}^1$:

$$\lambda v = K c_*(\epsilon) \frac{\partial v}{\partial \xi} - \widehat{\mathcal{L}}_\rho v + f'_\epsilon(u^\epsilon_{\mathrm{f}*}(\xi/K)) v, \ v(0) = 1. \tag{5.115}$$

where

$$\widehat{\mathcal{L}}_\rho v = \mathcal{L}_{l_\rho} v, \ l_\rho = \frac{\rho}{K} \sqrt{\alpha(1-\alpha)}. \tag{5.116}$$

For $\epsilon = 0$, we set:

$$\lambda v = K c_*(0) \frac{\partial v}{\partial \xi} - \widehat{\mathcal{L}}_\rho v - v + \frac{K v(0)}{\sqrt{\alpha(1-\alpha)}} \delta, \ v(0) = 1. \tag{5.117}$$

Equation (5.115) is eigenvalue problem for $\mathcal{P}_l$ specialized to the nonlinearity (5.2) and $l = l_\rho$, and whereas equation (5.117) is problem (5.11) with $l = l_\rho$.

Introduce the following operator $\mathcal{S}_{\epsilon,\theta}$ mapping $H^1(\mathbb{R}) \times \mathbb{C}$ to $H^{-1}(\mathbb{R}) \times \mathbb{C}$:

$$\mathcal{S}_{\epsilon,\theta}(v, \lambda) = \left((\lambda + 1) v - K c_*(\epsilon) \frac{\partial v}{\partial \xi} + \widehat{\mathcal{L}}_\rho v - \mathcal{T}_{\epsilon,\theta} v, v(0) - 1 \right) \tag{5.118}$$

where $\mathcal{T}_{\epsilon,\theta}$ was defined in (5.95). Problems (5.115) and (5.117) can then be written as $S_{\epsilon,\theta}(v, \lambda) = 0$. By Propositions 5.4 and 5.6, $\mathcal{S}_{\epsilon,\theta}$ is continuous with

respect to $(\epsilon, \theta) \in [0, \epsilon_0] \times \mathbb{S}^1$. The derivative of the above operator with respect to (v, λ) is given by:

$$DS_{\epsilon,\theta}(w, \mu) = \left(\mu v + (\lambda + 1)w - Kc_*(\epsilon)\frac{\partial w}{\partial \xi} + \widehat{\mathcal{L}}_\rho w - \mathcal{T}_{\epsilon,\theta} w, w(0) \right). \quad (5.119)$$

The operator $DS_{\epsilon,\theta}$ is clearly a continuous with respect to (v, λ) and is also continuous with respect to (ϵ, θ) for $(\epsilon, \theta) \in [0, \epsilon_0] \times \mathbb{S}^1$, thanks to Propositions 5.4 and 5.6.

By Proposition 5.2, we know that $S_{0,\theta}(v, \lambda) = 0$ has the following solution for each value of $\theta \in \mathbb{S}^1$ given by:

$$\begin{aligned} &\lambda = \lambda_0^\theta = \lambda_\rho(\alpha, \theta), \\ &v = v_0^\theta,\ \widehat{v}_0^\theta(k) = \frac{K}{\sqrt{\alpha(1-\alpha)}(\lambda_0^\theta + 1 - ic_0 k + Q_\theta(k, l_\rho))}, \end{aligned} \quad (5.120)$$

where $\widehat{\cdot}$ denotes the Fourier transform. The expression for $\widehat{v}_0^\theta(k)$ was given in (5.16). We now use the implicit function theorem to extend this family of solutions to nonzero values of ϵ. Suppose we can show that $DS_{0,\theta}$ is invertible at every $\theta' \in \mathbb{S}^1$. Then, we may obtain a family of solutions, each defined in a small neighborhood for each $\theta' \in \mathbb{S}^1$. These solutions may be pasted together to obtain the desired solution $(v_{\rho,\alpha}(\xi, \epsilon, \theta), \lambda_{\rho,\alpha}(\epsilon, \theta))$:

$$\begin{aligned} S_{\epsilon,\theta}(v_{\rho,\alpha}, \lambda_{\rho,\alpha}) = 0,\ \lambda_{\rho,\alpha}(0, \theta) = \lambda_0^\theta,\ v_{\rho,\alpha}(\xi, 0, \theta) = v_0^\theta(\xi), \\ (\epsilon, \theta) \in [0, \epsilon_1] \times \mathbb{S}^1, \epsilon_1 > 0. \end{aligned} \quad (5.121)$$

In particular, $\lambda_{\rho,\alpha}$ is a continuous function up to $\epsilon = 0$. Recall that a similar pasting procedure was performed in the proof of Proposition 5.2, (see equation (5.45) to end of the proof). The pasting procedure here can be carried out in a similar fashion.

We now check the invertibility of $DS_{0,\theta}$ at $(v, \lambda) = (v_0^\theta, \lambda_0^\theta)$. Given $(f, \zeta) \in H^{-1}(\mathbb{R}) \times \mathbb{C}$, we solve the following linear equation for $(w, \mu) \in H^1(\mathbb{R}) \times \mathbb{C}$:

$$\mu v_0^\theta + (\lambda_0^\theta + 1)w - Kc_*(0)\frac{\partial w}{\partial \xi} + \widehat{\mathcal{L}}_\rho w - \frac{Kw(0)}{\sqrt{\alpha(1-\alpha)}}\delta = f,\ w(0) = \zeta. \quad (5.122)$$

Solving the above is equivalent to solving the equation after applying the Fourier transform.

$$\begin{aligned} &\mu \widehat{v}_0^\theta + (\lambda_0^\theta + 1 - iKc_*(0)k + Q_\theta(k, l_\rho))\widehat{w} - \frac{K}{2\pi\sqrt{\alpha(1-\alpha)}} \int_{\mathbb{R}} \widehat{w} dk = \widehat{f}, \\ &\frac{1}{2\pi} \int_{\mathbb{R}} \widehat{w}(k) dk = \zeta, \end{aligned} \quad (5.123)$$

where $\widehat{\cdot}$ denotes the Fourier transform. We seek a solution $(\widehat{w}, \mu) \in \mathcal{H}^1 \times \mathbb{C}$ where $(\widehat{f}, \zeta) \in \mathcal{H}^{-1} \times \mathbb{C}$ and

$$\mathcal{H}^{-1} = \{\widehat{v} \in L^1_{\mathrm{loc}}(\mathbb{R}) |\ \|\widehat{v}\|^2_{\mathcal{H}^{-1}} = \int_{\mathbb{R}} |\widehat{v}(k)|^2 (1 + k^2)^{-1} dk < \infty\}. \quad (5.124)$$

We can solve the first equation in (5.123) for $\widehat{w}$. We have

$$\widehat{w} = \frac{-\mu\widehat{v_0^\theta} + \zeta K(\alpha(1-\alpha))^{-1/2} + \widehat{f}}{\lambda_0^\theta + 1 - iKc_*(0)k + Q_\theta(k, l_\rho)}. \tag{5.125}$$

It is easily checked that $\widehat{w}$ is in $\mathcal{H}^1$. Substituting this expression into the second equation in (5.123), we obtain the following equation for μ:

$$\frac{1}{2\pi}\int_{\mathbb{R}} \frac{-\mu\widehat{v_0^\theta} + \zeta K(\alpha(1-\alpha))^{-1/2} + \widehat{f}}{\lambda_0^\theta + 1 - iKc_*(0)k + Q_\theta(k, l_\rho)} dk = \zeta. \tag{5.126}$$

This is just a linear equation in μ and is uniquely solvable if the coefficient multiplying μ is not zero. We thus see that DS_0 is invertible if and only if:

$$\int_{\mathbb{R}} \frac{\widehat{v_0^\theta} dk}{\lambda_0^\theta + 1 - iKc_*(0)k + Q_\theta(k, l_\rho)} \neq 0. \tag{5.127}$$

Substituting (5.120) for $\widehat{v_0^\theta}$, we have:

$$\begin{aligned} &\int_{\mathbb{R}} \frac{\widehat{v_0^\theta} dk}{\lambda_0^\theta + 1 - iKc_*(0)k + Q_\theta(k, l_\rho)} \\ =&\frac{K}{\sqrt{\alpha(1-\alpha)}} \int_{\mathbb{R}} \frac{dk}{(\lambda_0^\theta + 1 - iKc_*(0)k + Q_\theta(k, l_\rho))^2} = -\alpha \frac{\partial \widehat{I}_\rho}{\partial \lambda}(\lambda_0^\theta, \alpha, \theta), \end{aligned} \tag{5.128}$$

where we used (5.17) and (5.19). Since $\alpha \neq 0$, the above is nonzero thanks to (5.20) of Proposition 5.2.

Now, let us choose $\epsilon > 0$ so that

$$|\lambda_{\rho,\alpha}(\epsilon, \theta) - \lambda_\rho(\alpha, \theta)| \leq 2\widehat{C} |\rho|^4 \tag{5.129}$$

This is possible given the continuity of $\lambda_{\rho,\alpha}$ and the fact that $\lambda_{\rho,\alpha}(0, \theta) = \lambda_\rho(\alpha, \theta)$. Combining the above with (5.21) and (5.114), we have:

$$\left| \mathrm{Re}\lambda_{\rho,\alpha}(\epsilon, \theta) + \frac{\beta_0 |\rho|^3}{4\gamma_0 K^2} \right| \leq 4\widehat{C} |\rho|^4 . \tag{5.130}$$

Thus,

$$\mathrm{Re}\lambda_{\rho,\alpha}(\epsilon, \theta) \geq \frac{-\beta_0 |\rho|^3}{4\gamma_0 K^2} - 4\widehat{C} |\rho|^4 \geq -\frac{(\beta_0 + \nu) |\rho|^3}{4\gamma_0 K^2}, \tag{5.131}$$

where we used (5.114) in the second inequality. Since $|\rho| > 0$, if $-(\beta_0 + \nu) > 0$, $\mathrm{Re}\lambda_\rho(\epsilon, \theta) > 0$. There is thus a point in the spectrum of $\mathcal{P}_{l_\rho}$ (where l_ρ was defined in (5.116)) that lies in the right half complex plane. Given Definition 2.1, the front in this direction is spectrally unstable.

Recall that, in defining the spectrum of $\mathcal{P}_l$, we viewed $\mathcal{P}_l$ as a closed operator on $L^2(\mathbb{R})$ with domain $H^2(\mathbb{R})$. We must thus check that $v_\epsilon = v_{\rho,\alpha}(\cdot, \epsilon, \theta), \epsilon > 0$

is in fact in $H^2(\mathbb{R})$. This is a simple consequence of elliptic regularity. Indeed, we have:

$$\begin{aligned}\mathcal{G}v_\epsilon &\equiv (\lambda_0+1)v_\epsilon - Kc_*(0)\frac{\partial v_\epsilon}{\partial \xi} + \widehat{\mathcal{L}}_\rho v_\epsilon \\ &= (\lambda_0-\lambda_\epsilon)v_\epsilon + K(c_*(\epsilon)-c_*(0))\frac{\partial v_\epsilon}{\partial \xi} + \mathcal{T}_{\epsilon,\theta}v_\epsilon \equiv r\end{aligned} \tag{5.132}$$

where $\lambda_\epsilon = \lambda_{\rho,\alpha}(\epsilon,\theta)$. Since $u^\epsilon_{\mathrm{f}*}$ is smooth for $\epsilon > 0$ and j_ϵ is compactly supported, $\mathcal{T}_{\epsilon,\theta}v_\epsilon$ belongs to $H^1(\mathbb{R})$. Since $\partial v_\epsilon/\partial\xi$ belongs to $L^2(\mathbb{R})$, we see that $r \in L^2(\mathbb{R})$. It is easily seen, by taking the Fourier transform, that $\mathcal{G}$ is a bijection from $H^2(\mathbb{R})$ to $L^2(\mathbb{R})$, and therefore, $v_\epsilon = \mathcal{G}^{-1}r \in H^2(\mathbb{R})$. □

Let us now apply the above results to the case when A_{i} and A_{e} are given by (2.7).

Proposition 5.7. *Suppose $a \neq 0$ and pick any $\nu > 0$. Then, there is a smooth bistable nonlinearity f so that the planar fronts in all directions satisfying $\cos(4\theta) > \nu$ are spectrally unstable.*

Proof. This is a direct consequence of Theorem 5.1 and the expression for β_0 in (2.20). □

This implies the following result.

Corollary 5.8. *Suppose that the conductivities A_{i} and A_{e} are not proportional to each other, so that the bidomain Allen-Cahn equation does not reduce to the classical Allen-Cahn equation. Then, there is a smooth nonlinearity f such that the planar front in some direction is spectrally unstable.*

Proof. There is no loss of generality in assuming that A_{i} and A_{e} are of the form given in (2.7) since A_{i} and A_{e} can always be transformed into this standard form by a suitable linear transformation. Suppose A_{i} and A_{e} are not proportional to each other. Then, $a \neq 0$ in (2.7). The claim follows from Proposition 5.7. □

This corollary shows, in particular, that the front can be unstable even when the Frank diagram is convex.

We may combine Proposition 5.7 and Proposition 4.5 to obtain the following striking result.

Proposition 5.9. *Suppose a and b satisfy*

$$\alpha_0(a,b,\theta) < 0 \text{ when } \cos(4\theta) \leq 0. \tag{5.133}$$

Then, there is a smooth bistable nonlinearity f for which planar fronts in all directions are spectrally unstable. When $b = 0$, this condition is satisfied if $a > \sqrt{2/3}$.

Proof. Since the function $\alpha_0(a, b, \theta)$ is a continuous function of θ, we may take $\nu > 0$ sufficiently small so that

$$\alpha_0(a, b, \theta) < 0 \text{ when } \cos(4\theta) \le \nu. \tag{5.134}$$

By Proposition 4.5, all front directions satisfying $\cos(4\theta) \le \nu$ are spectrally unstable for any nonlinearity f. By Proposition 5.7, we may choose a nonlinearity f so that all front directions satisfying $\cos(4\theta) > \nu$ are spectrally unstable. Fronts in all directions will thus be spectrally unstable. That condition (5.133) reduces to $a > \sqrt{2/3}$ when $b = 0$ follows easily from (4.99). □

In the case of the McKean model (5.3), we can numerically compute the leading eigenvalue using (5.17). In Figure 3, we plot λ_l as a function of l for $\theta = 0, a = 0.4, b = 0$ and different values of α. For $\alpha = 0.01$ and 0.02, the eigenvalue λ_l is positive for a range of values of l, and thus the front is unstable. In Figure 4, we plot, as a function of a, the critical value of α below which the front becomes unstable in the $\theta = 0$ direction. We see that the critical α value is small when a is close to 0 or 1. This is consistent with (5.18). Indeed, when $\theta = 0$ and $b = 0$, (5.18) reduces to

$$\mathrm{Re}\lambda_l = -\frac{1}{2}\left(3a^2 + 1\right) l^2 + \frac{1}{2\sqrt{2}} a^2 \sqrt{1 - a^2} (\alpha(1 - \alpha))^{-3/2} |l|^3 + \mathcal{O}(l^4). \tag{5.135}$$

The third order term in l is proportional to $a^2\sqrt{1 - a^2}$, and we would thus expect that α needs to be made smaller to have an instability when a is close to 0 or 1.

6 Computational Demonstration and Asymptotic Behavior

In this section, we show some numerical examples of planar front instabilities and discuss the asymptotic behavior of spreading fronts.

6.1 Planar Fronts

To test the instability results obtained above, we performed numerical simulations of the bidomain model. For A_i and A_e we use (2.7). We then rotate the coordinate system by an angle of $-\theta$ so that the θ direction in the original coordinate system aligns with the x axis. The bidomain model thus rotated is simulated on a rectangular domain of size $L_x \times L_y$ that is periodic in the y direction with Neumann boundary conditions at $x = 0$ and $x = L_x$. We initiate the simulation with a planar wave front near $x = 0$ (parallel to the y axis) modulated with small perturbations. If the width of the planar front is sufficiently thin compared with the length L_x of the domain, boundary effects should be minimal, and the simulated propagating front front should be a good approximation to the planar fronts studied in this paper. If the planar front

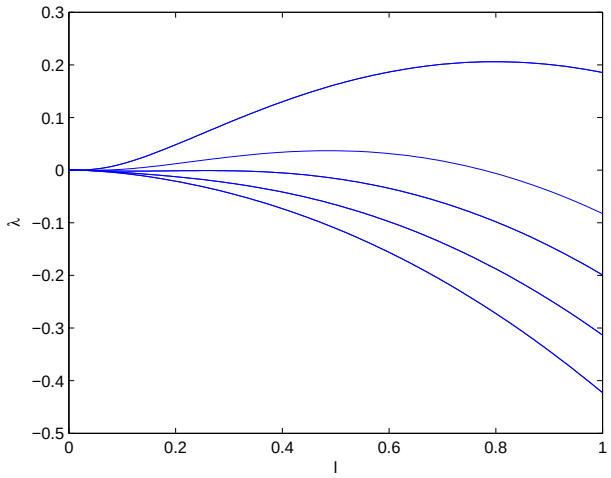

Figure 3: Plot of λ_l as a function of l, with $\theta = 0, a = 0.4$ and $\alpha = 0.01, 0.02, 0.03, 0.05, 0.1$ from the top. Note that, for $\alpha = 0.01$ and 0.02, there is a region of l for which λ_l is positive.

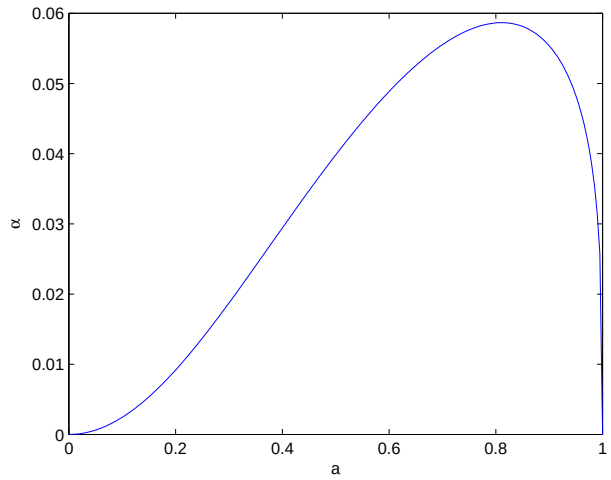

Figure 4: Critical value of α below which the front in the $\theta = 0$ direction becomes unstable, as a function of a.

is unstable under perturbations with wave numbers $k = 2\pi n/L_x, n \in \mathbb{N}$, then disturbances to the propagating front should grow over time. The details of the numerical scheme is discussed in Appendix B.

In the computations shown in Figure 5, we set

$$\begin{aligned} &a = 0.9,\ b = 0,\ \text{in (2.7)},\ \theta = \pi/4, 3\pi/16, \\ &f = -u(u-1)(u-0.4),\ L_x = 200,\ L_y = 100. \end{aligned} \tag{6.1}$$

The parameter values for a, b and θ are such that the conditions of Proposition 4.5 are satisfied, so that the planar waves are unstable under long-wavelength perturbations. We see in the figure that the small initial perturbations grow into large-amplitude waves with time. The wave front assumes a saw-tooth form as time progresses. We also see a coarsening of the wave, so that, the multiple peaks that were present in earlier times have merged into two peaks by the end of the simulation. The main difference between the cases $\theta/4$ and $3\pi/16$ is that the wave peaks drift in the positive y direction in the case $\theta = 3\pi/16$. This can be seen as a reflection of the fact that α_1 in (4.19) is non-zero when $\theta = 3\pi/16$. The expression of the growing perturbation for long-wavelength perturbations, given in (4.90), can be written as:

$$-\frac{\partial u_{\mathrm{f}}}{\partial \xi} \exp(il\alpha_1 \xi - \alpha_0 l^2 t) \times \exp(il(\alpha_1 c t + \eta). \tag{6.2}$$

If $\alpha_1 \neq 0$, we thus expect to see an initial growing disturbance that travels in a direction perpendicular to the wave front with speed $\alpha_1 c$.

We mention that even the classical Allen-Cahn equation can exhibit fronts with corners in the plane [16, 24, 28]. These fronts, however, are fundamentally different from the fronts discussed here. One such difference is that fronts with corners can never appear in the classical Allen-Cahn equation once periodic boundary conditions are imposed in the direction perpendicular to the direction of propagation. This is because of the fact that the opening angles at the corners of fronts in the classical Allen-Cahn equation are always smaller than π; if one draws a unit circle centered at the corner, the portion of the circle where u is close to 1 is always larger than the portion where u is close to 0. As can be seen in Figure 5, corners of bidomain fronts can have opening angles larger as well as smaller than π.

The instabilities demonstrated above correspond to long-wavelength instabilities studied in Section 4. We have performed some numerical simulations corresponding to intermediate-wavelength instabilities studied in Section 5, and we do indeed observe destabilization of planar fronts. However, the (near) singular nature of the (smoothed) McKean nonlinearity makes it challenging to obtain reliable numerical results, and we cannot confidently distinguish discretization artifacts from genuine effects reflecting behavior of the continuous model. This is a subject for future investigation.

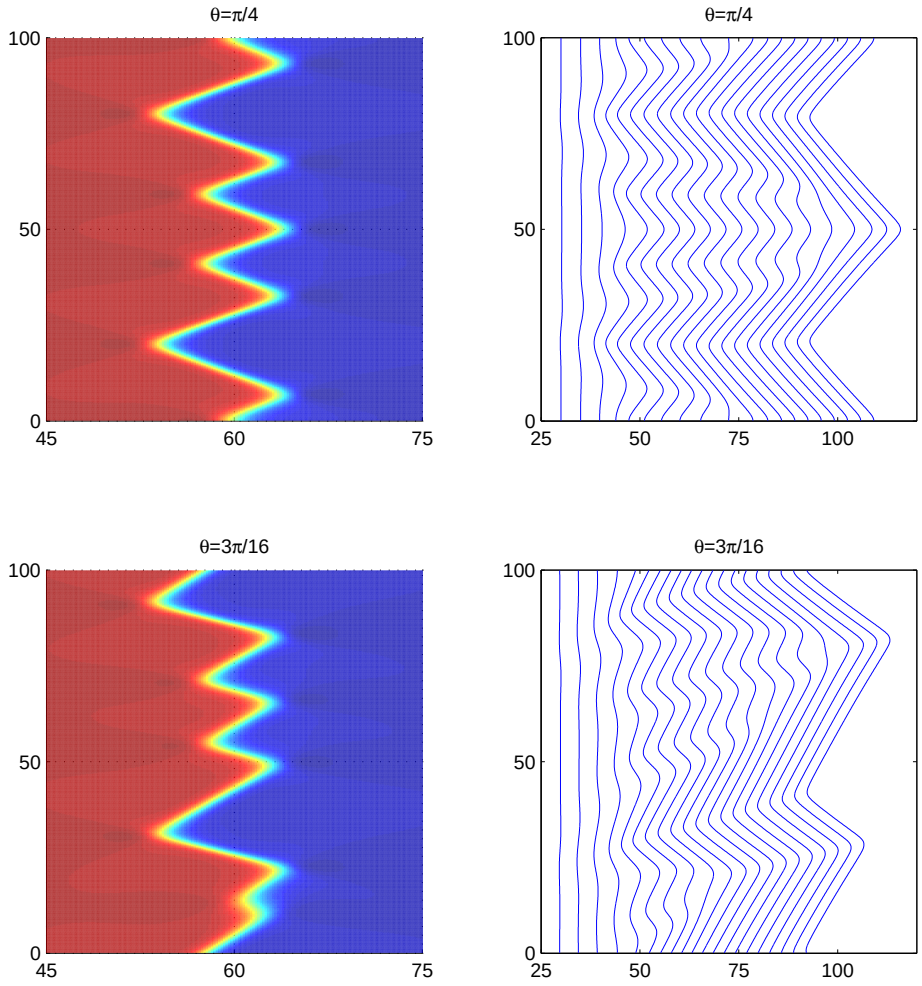

Figure 5: Simulations of the bidomain model. The top two panels correspond to $\theta = \pi/4$ and the bottom two panels $\theta = 3\pi/16$. The wave fronts are traveling in the positive x direction. The left panels show a snapshot of the simulation at time $t = 400$. The solution u is approximately equal to 1 in the red region and 0 in the blue region. The right panels show the position of the wave front (coordinates at which $u = 1/2$) at times $t = 50n, n = 1, 2, \cdots, 20$.

6.2 Spreading Fronts

Fix a nonlinearity f so that the speed c of planar fronts are positive, and let $B(r,0)$ be the ball of radius r centered at the origin. We may consider the solution to the bidomain model with non-negative initial data $u = 1$ in $B(r_1, 0)$ and $u = 0$ for $\mathbb{R}^2 \backslash B(r_2, 0), r_2 > r_1$. If r_1 is sufficiently large, for the classical or anisotropic Allen-Cahn equation, a spreading plateau will develop, and the front (the set on which $u = a$) will propagate outward. For the classical Allen-Cahn equation, it is well-known that the asymptotic shape of the front is an ellipse; with (2.7) and $a = 0$ the asymptotic shape of the front is a propagating circle. For the anisotropic Allen-Cahn equation, the asymptotic shape of the front is the Wulff shape discussed below [11, 12, 5, 1]. Here, we discuss the expected asymptotic behavior of the spreading front for the bidomain Allen-Cahn equation.

Let V be the normal velocity of the spreading front. As the front spreads outward, the front may be locally approximated by a planar front. We thus expect the velocity V in the θ direction to approach

$$V_\infty = c = c_* K(\theta) \tag{6.3}$$

where K is given in (2.12). Define the *Wulff shape*:

$$\mathscr{W} = \bigcap_{0 \le \theta < 2\pi} \{(x,y) \in \mathbb{R}^2 | x\cos\theta + y\sin\theta \le K(\theta)\}. \tag{6.4}$$

Assuming that V approaches V_∞ as the front spreads outward, the asymptotic shape of the spreading front will be given by $\partial\mathscr{W}$, the boundary of the Wulff shape. This is indeed the case for the anisotropic Allen-Cahn equation (with A in (1.7) equal to $Q/2$ as discussed in Section 1) [11, 12, 5, 1]. Examples of Frank diagrams and their corresponding Wulff shapes are given in Figure 6.

Recall that the Frank diagram can be convex or non-convex for the bidomain Allen-Cahn equation. Notice that the Wulff shape, by definition, is always convex. When the Frank diagram is non-convex, the corresponding Wulff shape has corners, and not all values of θ in (6.4) participate in defining the Wulff shape. This is in contrast to the anisotropic Allen-Cahn equation. As discussed in Section 1, in the anisotropic Allen-Cahn equation, the Frank diagram must be convex to ensure well-posedness, and therefore, the corresponding Wulff shape does not have corners.

Consider the convex hull $\widehat{\mathscr{F}}$ of the Frank diagram and let $\partial\widehat{\mathscr{F}}$ be its boundary. Let $P_\theta = (\cos\theta, \sin\theta)/K(\theta) \in \mathscr{F}$. Define

$$\mathcal{S} = \{0 \le \theta < 2\pi | P_\theta \in \partial\widehat{\mathscr{F}}\}. \tag{6.5}$$

It is easily seen that

$$\mathscr{W} = \bigcap_{\theta \in \mathcal{S}} \{(x,y) \in \mathbb{R}^2 | x\cos\theta + y\sin\theta \le K(\theta)\}. \tag{6.6}$$

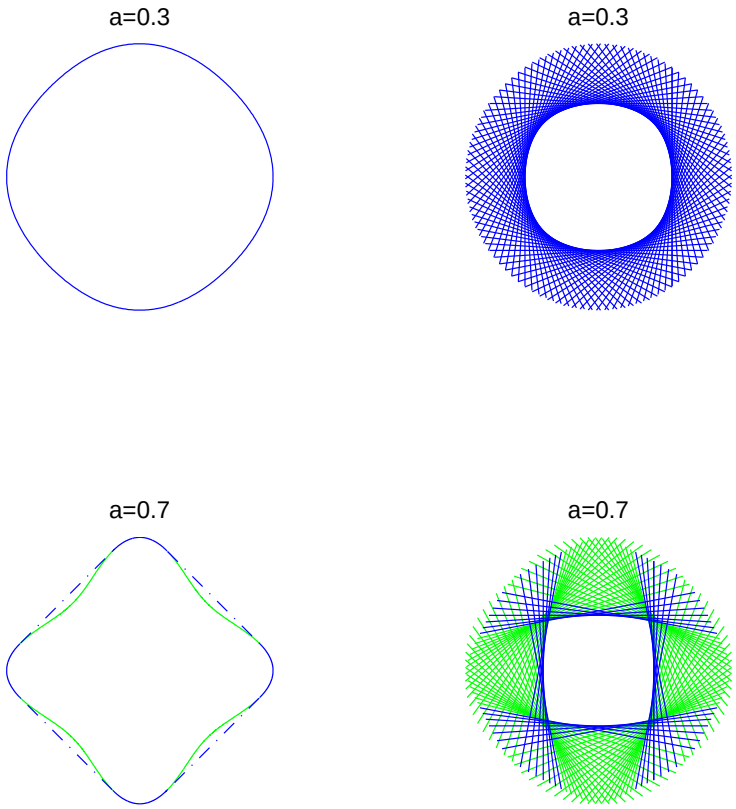

Figure 6: The Frank diagrams and Wulff shapes when $A_{\rm i}$ and $A_{\rm e}$ are as in (2.7) and $b = 0$, $a = 0.3$ and 0.7. When $a = 0.3$, the Frank diagram is convex and the corresponding Wulff shape does not have corners. When $a = 0.7$, the Frank diagram is not convex, and the Wulff shape has corners. The boundary of the convex hull of the Frank plot ($\partial\widehat{\mathscr{F}}$) is given in broken lines, and the portion of the Frank plot that is inside the convex hull is colored in green. The part of the Frank plot that coincides with the boundary of its convex hull is given in blue (these correspond to the θ values that belong to $\mathcal{S}$, see equation (6.5)). In the corresponding Wulff shape, only blue lines (corresponding to angles in the blue region of the Frank plot) contribute in forming the boundary of the Wulff shape.

Thus, only planar fronts propagating in directions $\theta \in \mathcal{S}$ should contribute to the asymptotic shape of the spreading front. We are now ready to state our conjecture.

Conjecture 6.1. *Suppose the normalized traveling front speed $c_* > 0$. Suppose further that, for all $\theta \in \mathcal{S}$, the planar front propagating in the θ direction is spectrally stable. Then, the asymptotic shape of the spreading front for the bidomain Allen-Cahn equation is given by the Wulff shape* (6.4).

Related speculation on the behavior of fronts for the bidomain Allen-Cahn equation is discussed in [5, 4, 6, 3, 13]. What distinguishes our conjecture from previous discussion is the presence of the planar front stability condition. It is certainly possible for the planar front to be unstable in a direction $\theta \in \mathcal{S}$, as was shown in Proposition 5.7 and Corollary 5.8 (it is interesting that this condition *cannot* be violated when $b = 0$ and $c_* = 0$, see Figure 2).

What may happen when the planar front stability condition in the above conjecture is violated? One plausible scenario is that the spreading front will indeed approach the Wulff shape at large length scales, but that at finer length scales the front will be modulated by oscillatory waves of small amplitude corresponding to instabilities at intermediate wavelengths.

A Long Wave Instabilities of Planar Fronts and Energetic Considerations

Here, we provide an energetic interpretation of the long-wavelength instability condition given in Corollary 4.3. The arguments given here are heuristic, and do not constitute an alternate proof of the instability condition.

Consider the energy functional:

$$\mathcal{E}(u) = \int_{\mathbb{R}^2} \left(\frac{1}{2} u(\mathcal{L}u) + W(u) \right) d\mathbf{x}, \; W(u) = -\int_0^u f(s) ds. \tag{A.1}$$

We may view the bidomain equation as the L^2 gradient flow of the above energy functional $\mathcal{E}$. In the monodomain case (the Allen-Cahn case), the first term in the integrand reduces to the familiar Dirichlet integral.

Now let us consider the balanced case, in which $W(1) = 0$. This corresponds to the case when the speed of the planar front is equal to 0. Consider a planar front traveling in the θ direction, and let ξ and η be the coordinate system adapted to the planar front, as was introduced in relation to (2.15). The planar front has infinite extent, and thus infinite energy. To avoid this difficulty, consider only periodic perturbations to the planar front, with period L in the η direction. Then, we may restrict our attention to the strip $-L/2 \le \eta \le L/2$. The dynamics can then be viewed as a gradient flow of the energy function:

$$\mathcal{E}_L(u) = \frac{1}{L} \int_{-L/2}^{L/2} \int_{-\infty}^{\infty} \left(\frac{1}{2} u(\mathcal{L}u) + W(u) \right) d\xi d\eta. \tag{A.2}$$

The energy of the planar front (without perturbations) can be computed as follows:

$$\mathcal{E}_L(u_{\mathrm{f}}) = C_f K(\theta) \tag{A.3}$$

where C_f is a constant that depends only on the nonlinearity f. If there is a small perturbation to the planar wave front that can make this energy less than $C_f K(\theta)$, then the front should be unstable.

Suppose that a small sinusoidal perturbation of wavelength L is given to the wave front, so that the wave front is now located at $\xi = h(\eta) = A\sin(2\pi\eta/L)$, $A \ll L$. Let the perturbed wave front be $\widetilde{u}$. If $L \gg K(\theta)$, the energy associated with this perturbation should be well-approximated by an integral of $C_f K(\theta)$ over the length of the wave front. Thus,

$$\begin{aligned}
\mathcal{E}_L(\widetilde{u}) &\approx \frac{1}{L}\int_{-L/2}^{L/2} C_f K\left(\theta + \arctan\left(\frac{dh}{d\eta}\right)\right)\sqrt{1+\left(\frac{dh}{d\eta}\right)^2}\,d\eta \\
&= \frac{1}{L}\int_{-L/2}^{L/2} C_f K\left(\theta + \frac{dh}{d\eta}\right)\left(1+\frac{1}{2}\left(\frac{dh}{d\eta}\right)^2\right)d\eta + \mathcal{O}(A^3) \\
&= C_f\left(K(\theta) + \left(\frac{\pi A}{L}\right)^2 (K(\theta)+K''(\theta))\right) + \mathcal{O}(A^3),
\end{aligned} \tag{A.4}$$

where $K''(\theta)$ denotes the second derivative of K with respect to θ. If

$$K(\theta) + K''(\theta) < 0, \tag{A.5}$$

the energy of the planar front will decrease under small perturbations ($A \ll L$) of long wavelength ($L \gg K$). Thus, the planar wave should be unstable if (A.5) is satisfied. It can be easily checked that (A.5) is equivalent to the condition that the Frank plot (defined in (4.91)) be non-convex at θ. By Proposition (4.4), (A.5) is equivalent to (4.89).

It should be possible to make the above heuristic argument rigorous. We mention [4] in which the authors study the minimizers of the above energy functional and discuss its relation to the bidomain model. In the above, we only treated the case when the wave speed $c = 0$, but a similar argument may be possible when $c \neq 0$.

B Numerical Method

We discuss the numerical scheme used to study planar waves in Section 6.1. We set A_{i} and A_{e} as in (2.7) and rotate the coordinate system by $-\theta$. This results in the bidomain system:

$$\frac{\partial u}{\partial t} = -\mathcal{L}u + f(u) \tag{B.1}$$

where $\mathcal{L}$ is given in (2.16) (rather than (2.5)). This equation is simulated on a rectangular region $0 \le x \le L_x$ and $0 \le y \le L_y$ with periodic boundary conditions in the y direction and Neumann boundary conditions in the x direction. We solve the above system with initial value $u = u_0$.

To impose Neumann boundary conditions in the x direction, we double the rectangular region in the x direction so that $-L_x \le x \le L_x$. We may then solve equation (B.1) on the $2L_x \times L_y$ rectangle with periodic boundary conditions in the x and y directions, with initial data:

$$u = \begin{cases} u_0(x) & \text{if } x \ge 0, \\ u_0(-x) & \text{if } x \le 0. \end{cases} \tag{B.2}$$

The restriction of the obtained solution to $0 \le x \le L_x$ is equal to the solution of the original problem. We have thus only to solve the bidomain equation (B.1) on a periodic domain of size $2L_x \times L_y$.

Let Δt be the time step size and $2N_x \times N_y$ be the number of spatial grid points in the x and y directions. We let $h_x = L_x/N_x$ and $h_y = L_y/N_y$. Let u_n be the numerical solution at time $n\Delta t$. We use the following operator splitting method to obtain the numerical solution.

Step 1 Given u_n, compute $u_{n,1}$ as follows:

$$u_{n,1*} = u_n + f(u_n)\Delta t/4,\ u_{n,1} = u_n + f(u_{n,1*})\Delta t/2. \tag{B.3}$$

This is essentially a second order Runge-Kutta step (only of the nonlinearity.

Step 2 Given $u_{n,1}$, compute $u_{n,2}$ as follows:

$$u_{n,2} = \mathcal{F}_h^{-1} \exp(-Q_{\theta,h}\Delta t)\mathcal{F}_h u_{n,1}, \tag{B.4}$$

where $\mathcal{F}_h$ and $\mathcal{F}_h^{-1}$ are the discrete Fourier transform and its inverse respectively, and $Q_{\theta,h}$ is the restriction of the Fourier multiplier Q_θ to the discrete wave numbers corresponding to the $2Nx \times N_y$ grid.

Step 3 Given $u_{n,2}$ computer u_{n+1} as follows:

$$u_{n,2*} = u_{n,2} + f(u_{n,2})\Delta t/4,\ u_{n+1} = u_{n,2} + f(u_{n,2*})\Delta t/2. \tag{B.5}$$

This method is of second order accuracy in space and time. In the simulations shown in Figure 5, we set $N_x = 1024$ and $N_y = 512$ with $\Delta t = 0.1$. The initial condition is

$$u_0 = \begin{cases} 1 & \text{if } |y - L_y/2| < L_y/4 \text{ and } x < L_x/8 + \delta, \\ 1 & \text{if } |y - L_y/2| \ge L_y/4 \text{ and } x < L_x/8 - \delta, \\ 0 & \text{otherwise,} \end{cases} \tag{B.6}$$

where $\delta = L_x/N_x$. A grid level disturbance is thus imposed on a planar front.

References

[1] Matthieu Alfaro, Harald Garcke, Danielle Hilhorst, Hiroshi Matano, and Reiner Schätzle. Motion by anisotropic mean curvature as sharp interface limit of an inhomogeneous and anisotropic allen–cahn equation. *Proceedings of the Royal Society of Edinburgh: Section A Mathematics*, 140(04):673–706, 2010.

[2] Rubin R Aliev and Alexander V Panfilov. A simple two-variable model of cardiac excitation. *Chaos, Solitons & Fractals*, 7(3):293–301, 1996.

[3] Stefano Amato, Giovanni Bellettini, and Maurizio Paolini. The nonlinear multidomain model: a new formal asymptotic analysis. In *Geometric Partial Differential Equations proceedings*, pages 33–74. Springer, 2013.

[4] Luigi Ambrosio, P Colli Franzone, and Giuseppe Savaré. On the asymptotic behaviour of anisotropic energies arising in the cardiac biodomain model. *Interfaces and Free Boundaries*, 2(3):213–266, 2000.

[5] Giovanni Bellettini, Piero Colli Franzone, and Maurizio Paolini. Convergence of front propagation for anisotropic bistable reaction–diffusion equations. *Asymptotic Analysis*, 15(3):325–358, 1997.

[6] Giovanni Bellettini, Maurizio Paolini, and Franco Pasquarelli. Nonconvex mean curvature flow as a formal singular limit of the nonlinear bidomain model. *Advances in Differential Equations*, 18(9/10):895–934, 2013.

[7] Eric Bonnetier, Elie Bretin, and Antonin Chambolle. Consistency result for a non monotone scheme for anisotropic mean curvature flow. *Interfaces and Free Boundaries*, 14(1):1–35, 2012.

[8] Yves Bourgault, Yves Coudière, and Charles Pierre. Existence and uniqueness of the solution for the bidomain model used in cardiac electrophysiology. *Nonlinear analysis: Real world applications*, 10(1):458–482, 2009.

[9] P Colli Franzone, LF Pavarino, and B Taccardi. Simulating patterns of excitation, repolarization and action potential duration with cardiac bidomain and monodomain models. *Mathematical biosciences*, 197(1):35–66, 2005.

[10] Robert S Eisenberg and Edward A Johnson. Three-dimensional electrical field problems in physiology. *Progress in biophysics and molecular biology*, 20:1–65, 1970.

[11] Charles M Elliott, Maurizio Paolini, and Reiner Schätzle. Interface estimates for the fully anisotropic allen-cahn equation and anisotropic mean-curvature flow. *Mathematical Models and Methods in Applied Sciences*, 6(08):1103–1118, 1996.

[12] Charles M Elliott and Reiner Schätzle. The limit of the anisotropic double-obstacle allen–cahn equation. *Proceedings of the Royal Society of Edinburgh: Section A Mathematics*, 126(06):1217–1234, 1996.

[13] Piero Colli Franzone, Luca F Pavarino, and Simone Scacchi. *Mathematical cardiac electrophysiology*, volume 13. Springer, 2014.

[14] Piero Colli Franzone and Giuseppe Savaré. Degenerate evolution systems modeling the cardiac electric field at micro-and macroscopic level. In *Evolution equations, semigroups and functional analysis*, pages 49–78. Springer, 2002.

[15] Boyce E Griffith and Charles S Peskin. Electrophysiology. *Communications on Pure and Applied Mathematics*, 66(12):1837–1913, 2013.

[16] François Hamel, Régis Monneau, and Jean-Michel Roquejoffre. Existence and qualitative properties of multidimensional conical bistable fronts. *Discrete and Continuous Dynamical Systems-Series A*, page 1069, 2005.

[17] Craig S Henriquez. Simulating the electrical behavior of cardiac tissue using the bidomain model. *Critical reviews in biomedical engineering*, 21(1):1–77, 1992.

[18] J.P. Keener and J. Sneyd. *Mathematical Physiology*. Springer-Verlag, New York, 1998.

[19] Ryo Kobayashi and Yoshikazu Giga. On anisotropy and curvature effects for growing crystals. *Japan journal of industrial and applied mathematics*, 18(2):207–230, 2001.

[20] Hiroshi Matano, Mitsunori Nara, and Masaharu Taniguchi. Stability of planar waves in the allen–cahn equation. *Communications in Partial Differential Equations*, 34(9):976–1002, 2009.

[21] RT Mathias, JL Rae, and RS Eisenberg. Electrical properties of structural components of the crystalline lens. *Biophysical Journal*, 25(1):181–201, 1979.

[22] HP McKean Jr. Nagumo's equation. *Advances in mathematics*, 4(3):209–223, 1970.

[23] J.C. Neu and W. Krassowska. Homogenization of syncytial tissues. *Critical reviews in biomedical engineering*, 21(2):137–199, 1993.

[24] Hirokazu Ninomiya and Masaharu Taniguchi. Existence and global stability of traveling curved fronts in the allen–cahn equations. *Journal of Differential Equations*, 213(1):204–233, 2005.

[25] Denis Noble and Yoram Rudy. Models of cardiac ventricular action potentials: iterative interaction between experiment and simulation. *Philosophical Transactions of the Royal Society of London. Series A: Mathematical, Physical and Engineering Sciences*, 359(1783):1127–1142, 2001.

[26] Micol Pennacchio, Giuseppe Savaré, and Piero Colli Franzone. Multiscale modeling for the bioelectric activity of the heart. *SIAM Journal on Mathematical Analysis*, 37(4):1333–1370, 2005.

[27] Mark Potse, Bruno Dubé, Jacques Richer, Alain Vinet, and Ramesh M Gulrajani. A comparison of monodomain and bidomain reaction-diffusion models for action potential propagation in the human heart. *Biomedical Engineering, IEEE Transactions on*, 53(12):2425–2435, 2006.

[28] Masaharu Taniguchi. The uniqueness and asymptotic stability of pyramidal traveling fronts in the allen–cahn equations. *Journal of Differential Equations*, 246(5):2103–2130, 2009.

[29] Leslie Tung. *A bi-domain model for describing ischemic myocardial dc potentials.* PhD thesis, Massachusetts Institute of Technology, 1978.

[30] Marco Veneroni. Reaction–diffusion systems for the macroscopic bidomain model of the cardiac electric field. *Nonlinear Analysis: Real World Applications*, 10(2):849–868, 2009.

[31] Aĭzik Isaakovich Volpert, Vitaly A Volpert, and Vladimir A Volpert. *Traveling wave solutions of parabolic systems*, volume 140. American Mathematical Soc., 2000.

[32] James N Weiss, Peng-Sheng Chen, Zhilin Qu, Hrayr S Karagueuzian, and Alan Garfinkel. Ventricular fibrillation how do we stop the waves from breaking? *Circulation Research*, 87(12):1103–1107, 2000.